



UNIVERSITÀ  
DEGLI STUDI  
DI PADOVA



# Optimal reactive power compensation in microgrids

**Laureando**

Federico Cerruti

**Relatore**

prof. Sandro Zampieri

**Correlatore**

Saverio Bolognani

Corso di Laurea Magistrale  
in Ingegneria dell'Automazione

Padova, 25 ottobre 2011



# Abstract

---

This thesis deals with the problem of optimal reactive power compensation for the minimization of power distribution losses in a microgrid.

We first propose a simple nonlinear model for a microgrid and then an approximate linear version of it. It allows to formulate the problem as a convex quadratic, linearly constrained, optimization problem, in which decision variables are the amount of reactive power that compensators inject into the network.

We suppose that agents in the microgrid have a partial knowledge of the problem parameters and state and can only perform local measurements. So, we propose a distribution approach for solving the aforementioned problem: we design a randomized distributed algorithm, whose main idea is the decomposition of the original minimization problem into smaller subproblems, each one related to a specific cluster consisting of agents able to communicate and exchange information.

We provide conditions for convergence of the algorithm and a convenient upper bound of the rate of convergence.

We analyze the rate of convergence for some specific topologies of the grid and for some choices of the agents communication topologies. Our analysis shows that the best performance can be achieved when we command cooperation among agents which are "neighbors" in the microgrid.

As the microgrid is a dynamic system, solving the optimization subproblems makes the grid voltages change: they are subjected to a interval time of transient. The resolution of the following optimization subproblem cannot start before the system attains a new steady state. We face the problem of obtaining an estimate of the time between two consecutive iterations of the proposed algorithm.

We propose a first-order dynamic model, describing the input-output relation between complex power references imposed at compensators and the voltage measurements, and consider its approximate version. It exhibits two interesting features: it is linear and contains explicitly the network parameters and topology. We study the positions of the

eigenvalues of the linear model, being related to the settling time of the system.

Numerical simulations are included to validate the proposed models and confirm the analytical results about the performance of the designed algorithm.

# Contents

---

<b>1</b>	<b>Introduction</b>	<b>1</b>
1.1	Complex power and phasorial notation . . . . .	3
1.1.1	Reactive power . . . . .	5
1.2	Optimal reactive power flow problem in a microgrid . . . . .	6
1.3	Outline . . . . .	7
1.4	Notations . . . . .	8
<b>2</b>	<b>Microgrid model</b>	<b>9</b>
2.1	Matrices $\mathbf{L}$ and $\mathbf{X}$ . . . . .	12
2.2	Approximate model . . . . .	14
2.2.1	Complex gradient . . . . .	14
2.2.2	Approximate solution for currents . . . . .	16
<b>3</b>	<b>Problem formulation</b>	<b>19</b>
3.1	Cost function for power losses minimization . . . . .	19
3.2	Gradient estimation . . . . .	22
<b>4</b>	<b>A randomized distributed algorithm</b>	<b>25</b>
4.1	Optimization problem decomposition . . . . .	26
4.2	Solving optimization subproblems . . . . .	27
4.3	Time between consecutive iterations . . . . .	30
4.3.1	Dynamic network model . . . . .	30
4.3.2	Approximate model . . . . .	32
4.3.3	Eigenvalue analysis . . . . .	33
<b>5</b>	<b>Analysis of the algorithm</b>	<b>35</b>
5.1	Matrix $\Omega_i$ and its properties . . . . .	35
5.2	Convergence results . . . . .	37

5.2.1	Equivalent optimization problem . . . . .	37
5.2.2	Necessary condition for the convergence of the algorithm . . . . .	40
5.3	Bound on the rate of convergence . . . . .	42
<b>6</b>	<b>Optimal strategy</b>	<b>51</b>
6.1	Nearest-neighbor gossip . . . . .	51
6.2	Case studies . . . . .	55
6.2.1	Tree structure . . . . .	55
6.2.2	Circular structure . . . . .	61
<b>7</b>	<b>Simulations and numerical results</b>	<b>69</b>
7.1	Validation of the static model . . . . .	69
7.2	Performance of the proposed algorithm . . . . .	71
7.3	Dynamic model . . . . .	74
7.3.1	Eigenvalue analysis . . . . .	76
<b>8</b>	<b>Conclusions</b>	<b>79</b>
<b>A</b>	<b>Convex optimization problems</b>	<b>81</b>
A.1	Convex optimization problems with equality constraints only . . . . .	82
A.2	Descent methods . . . . .	83
A.2.1	Newton's method for unconstrained problems . . . . .	83
A.2.2	Newton's method for equality constrained problems . . . . .	84
<b>B</b>	<b>Kronecker product</b>	<b>87</b>
B.1	Definition . . . . .	87
B.2	Properties . . . . .	87
<b>C</b>	<b>Generalized inverse</b>	<b>89</b>
C.1	Moore-Penrose generalized inverse . . . . .	90
<b>D</b>	<b>Quadratic forms</b>	<b>91</b>
	<b>References</b>	<b>93</b>

# Introduction

---

This thesis considers the problem of minimizing reactive power flows in distribution power grids (or parts of them). The objective is to define an optimization problem for this purpose and design an algorithm in order to solve it.

The power distribution network is one of the three main subsystems of a traditional electric grid, together with the power generation and transmission subsystems.

Electrical energy is usually generated in a relatively small number of large power plants. They generally take place near the energy resources and then the produced electrical energy is transmitted over long distances to the load centers (*transmission system*). As the energy losses in a transmission line are proportional to the current squared, transmission lines operate at *high* and *extra-high voltages* (above 100 kV). Most of the electrical energy is then transferred to distribution *high* (100 – 300 kV) and *medium voltage* (1 – 100 kV) networks in order to be delivered to large and medium consumers. Finally, power is transformed to a *low voltage* (below 1 kV) and distributed to small customers (domestic, industrial, commercial).

In the industrialized countries, these traditional electric power systems are aging and being stressed by scenarios not imaginable when the majority of them were designed [6], [8].

- *Energy deregulation*: new possibilities of energy trading have implied power flow scenarios and uncertainties the system was not designed to handle.
- *Renewable energy sources*: because of environmental issues such as global warming and sustainability, a great interest is increasing to renewable (but unreliable and intermittent) energy sources, both in large installations and in dispersed micro-generators; their presence in the system increases the uncertainties in supply and adds stress to the existing infrastructures.

- *Power demand*: our society is increasing the amount of power supply and the quality of the service.

Many industries and national governments consider the *smart-grid technology* the answer to these new scenarios.

The objective is to translate the classical electrical power grids into smart-grids, so as to provide a reliable, high-quality electric power in an environmentally friendly and sustainable way.

Smart grids will grow on the existing electric network and should coexist with it at least for a while, adding new functionalities. Part of this process will be done by developing the so called *smart microgrids*.

A microgrid can be defined as a portion of the low-voltage power distribution network which includes electrical loads and distributed power generators. Loads can be residential or industrial consumers; generators may be solar panels, micro wind turbines, or any of alternate power sources. The size of a microgrid can be the size of the whole distribution network, or part of it, like a town or a group of buildings (shopping centers, industrial parks, college campus, etc.). A microgrid is connected to the power transmission network in one point (the point of common coupling or PCC) and it is managed autonomously from the rest of the network to achieve better quality of the service, improve efficiency and pursue specific economic interests.

A smart microgrid can appear deeply different from the traditional power distribution grid, whose unique task is to deliver energy power from the transmission grid to the loads.

A smart microgrid may include a large number of intelligent entities (*agents*), such as micro-generators, able to inject power instead of being supplied with only, electronic loads with their specific dynamic behaviors, "smart" customers which can postpone their demand if financially rewarded, etc.

All the microgenerators are connected to the microgrid via electronic interfaces (inverters), whose main task is to enable the injection of the produced power into the microgrid. However, these devices, if properly commanded and coordinated, can also perform other tasks needed to guarantee a desired quality of the distribution; they are the so called *ancillary services* [9], [12]: reactive power compensation, voltage support and regulation, harmonic compensation, reliability and robustness to faults, etc.

In this thesis we consider the problem of *optimal reactive power compensation*, one of the most important ancillary services.

The solution of such an optimization problem requires the design of a proper algorithm, according to the system features.

A smart microgrid presents some characteristics that allow to include it in the class of complex, large-scale systems; in fact:

- a smart microgrid presents a group of agents, whose number is generally large and



## 1.1 Complex power and phasorial notation

---

may be unknown and time-varying, because of external events or the possibility that some new agents appear, disconnect or are reconfigured;

- agents can have a partial knowledge of the system state and the system structure (*distributed information*), such as the number of agents, their configuration, the communication among them etc.;
- each agent is not usually able to communicate with all the other agents in the system, but it is forced to interact with a smaller subset of neighbors;
- the information exchange among agents is possible not only via a given communication channel, but also via local actuation and measurement performed on an underlying physical system.

Owing to these issues, it might be impossible solving the optimization problem for the minimization of reactive power flows on a global level: it should be preferred a distributed algorithm, like the algorithm we will propose in Chapter 4.

## 1.1 Complex power and phasorial notation

Consider an inverter  $v$  connected to the power distribution network and let be  $u(t)$  and  $i(t)$  the voltage at its point of connection and the injected current respectively.

If the network is operating in steady state, then voltages and currents are sinusoidal signals at the same frequency  $f_0 = \omega_0/2\pi$ , and so:

$$u(t) = U \sin(\omega_0 t + \theta_u), \quad i(t) = I \sin(\omega_0 t + \theta_i). \quad (1.1)$$

The instantaneous power is so defined:

$$\pi(t) = u(t)i(t) = \frac{UI}{2} \cos \phi - \frac{UI}{2} \cos(2\omega_0 t + 2\theta_u - \phi),$$

where  $\phi = \theta_u - \theta_i$ .

The average value in a period of a sinusoidal power is called *active power*:

$$p = \frac{1}{T} \int_T \pi(t) dt = \frac{UI}{2} \cos \phi. \quad (1.2)$$

On the analogy of the active power, the *reactive power* is defined as:

$$q = \frac{UI}{2} \sin \phi. \quad (1.3)$$

The execution of operations among sinusoidal signals may be very burdensome. In order to obviate these difficulties, we will use an alternative representation of signals based on *phasors*.

A one-to-one relation can be defined between each element of the set of sinusoidal signals with the same frequency and each complex number: if  $y(t)$  belongs to the set of sinusoidal signals with the same frequency  $f_0$ , with magnitude  $Y_M$  and phase  $\psi$ , and  $y$  is a complex number, such a relation may be defined:

$$y(t) = Y_M \sin(\omega_0 t + \psi) \quad \Leftrightarrow \quad y = |y| e^{j\angle y}$$

by a couple  $\{K_y, \zeta_F\}$  such that:

$$\begin{cases} |y| = K_y Y_M \\ \angle y = \zeta_F + \psi. \end{cases} \quad (1.4)$$

The complex numbers associated to sinusoidal signals by (1.4) are called *phasors* and are the symbolic representations of sinusoidal signals.

It is frequent using the transformation (1.4) where  $\{K_y = 1/\sqrt{2}, \zeta_F = 0\}$  (*root-mean-square transformation*), so that the phasor  $y$  represents the signal:

$$y(t) = |y| \sqrt{2} \sin(\omega_0 t + \angle y).$$

So, for voltage and current of the inverter  $v$  defined in (1.1), it results:

$$\begin{aligned} u(t) &= U \sin(\omega_0 t + \theta_u) \quad \Leftrightarrow \quad u(v) = \frac{U}{\sqrt{2}} e^{j\theta_u} \\ i(t) &= I \sin(\omega_0 t + \theta_i) \quad \Leftrightarrow \quad i(v) = \frac{I}{\sqrt{2}} e^{j\theta_i}. \end{aligned}$$

By phasors, we can define the *complex power* (a complex operator but not a phasor) of the inverter  $v$ :

$$s(v) = u(v) \bar{i}(v) = \frac{UI}{2} e^{j\phi} = \frac{UI}{2} (\cos \phi + j \sin \phi) = p(v) + jq(v), \quad (1.5)$$

where  $\bar{i}$  denotes the complex conjugate of  $i$ ; therefore, comparing (1.5) with (1.2) and (1.3), active and reactive powers result to be the real and the imaginary part of the complex power respectively:

$$p(v) = \Re[s(v)] \quad q = \Im[s(v)].$$

It is worth noticing that the power terms introduced before can be defined also in the case signals are not sinusoidal; it is possible by defining the *homo-integral* of a generic function  $x(t)$  as:

$$\hat{x}(t) = \omega_0 (X(t) - \tilde{X}(t)),$$

where:

$$X(t) = \int_0^t x(\tau) d\tau, \quad \tilde{X}(t) = \frac{1}{T_0} \int_t^{t+T_0} X(t) dt.$$

By defining the internal product:

$$\langle x, y \rangle = \frac{1}{T_0} \int_t^{t+T_0} x(\tau) y(\tau) d\tau,$$

## 1.1 Complex power and phasorial notation

---

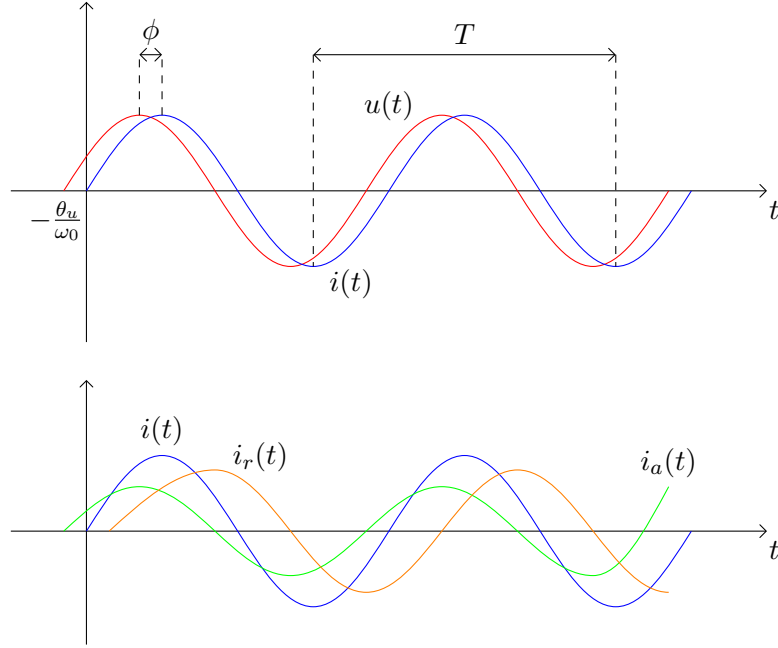


Figure 1.1: Decomposition of  $i(t)$  into two components  $i_a(t)$  and  $i_r(t)$ , in-phase and out-of-phase with  $u(t)$  respectively .

active and reactive powers can be defined as the instantaneous quantities:

$$P(t) = \langle u, i \rangle, \quad Q(t) = \langle \hat{u}, i \rangle.$$

Notice that, if  $u(t)$  and  $i(t)$  are sinusoidal signals, then  $P(t) = p$  and  $Q(t) = q$ .

### 1.1.1 Reactive power

Both residential and industrial users belonging to a microgrid may require a sinusoidal current which is not in phase with voltage.

A convenient description for that consists in saying that they demand active power and reactive power associated with in-phase and out-of-phase components of the current, respectively. Consider the current and voltage sinusoidal signal in (1.1) and suppose  $\phi \neq 0$ . The current  $i(t)$  may be decomposed in two components owing to the properties of sinusoidal functions:

$$\begin{aligned} i(t) &= I \sin(\omega_0 t + \theta_u - \phi) \\ &= (I \cos \phi) \sin(\omega_0 t + \theta_u) + (I \sin \phi) \sin(\omega_0 t + \theta_u - \frac{\pi}{2}) \\ &= i_a(t) + i_r(t), \end{aligned}$$

where  $i_a(t) = I_a \sin(\omega_0 t + \theta_{i_a}) = (I \cos \phi) \sin(\omega_0 t + \theta_u)$  can be defined as the *active current* and it is the component in-phase with the voltage, while  $i_r(t) = I_r \sin(\omega_0 t + \theta_{i_r}) =$

$(I \sin \phi) \sin(\omega_0 t + \theta_u - \frac{\pi}{2})$  can be called *reactive current* and it is the component out-of-phase with  $u(t)$ .

The current  $i_a(t)$  allows to have the following active and reactive powers:

$$\begin{aligned} p^{(a)}(t) &= \frac{VI_a}{2} \cos(\theta_u - \theta_{i_a}) = \frac{VI}{2} \cos \phi = p(t) \\ q^{(a)}(t) &= \frac{VI_a}{2} \sin(\theta_u - \theta_{i_a}) = 0, \end{aligned}$$

being  $\theta_u - \theta_{i_a} = 0$ . It means that we have the same active power with both  $i(t)$  and  $i_a(t)$ .

Differently, having a current  $i_r(t)$ :

$$\begin{aligned} p^{(r)}(t) &= \frac{VI_r}{2} \cos(\theta_u - \theta_{i_r}) = 0 \\ q^{(r)}(t) &= \frac{VI_r}{2} \sin(\theta_u - \theta_{i_r}) = \frac{VI}{2} \sin \phi = q(t), \end{aligned}$$

being  $\theta_u - \theta_{i_r} = \frac{\pi}{2}$ .

Then the concept of reactive power is a convenient way of saying that the current  $i(t)$  has a component ( $i_r(t)$ ) which leads to no active power.

Reactive power is not a real physical power, i.e. it does not involve fuel costs to produce it. Nevertheless, also reactive power flows contribute to power losses on the lines, cause voltage drop, and may lead to grid instability; then it is preferable to minimize reactive power flows by producing it as close as possible to the users that need it [13].

## 1.2 Optimal reactive power flow problem in a micro-grid

Consider a portion of power distribution network (microgrid); let it be described by a graph  $\mathcal{G}$ , whose edges represent the electrical connections among the devices and nodes correspond to agents, each of them injecting an amount  $p(v)$  of active power and a quantity  $q(v)$  of reactive power into the network.

A subset of nodes can be commanded to inject a given amount of reactive power, while they inject a fixed amount of active power (the amount generated by the corresponding micro-generator). The other nodes (users) inject or are supplied with, if negative, a fixed and unknown amount of both active and reactive power.

One possible approach to the problem of distributed reactive power compensation in a smart microgrid has been proposed in [9]. It consists in a centralized controller that measures the reactive power flow at the point where the microgrid connects with the main grid. According to this measurement, the controller produces a reference for the amount of reactive power that has to be produced inside the microgrid. This reference

### 1.3 Outline

---

has to be split by a power sharing unit (PSU) among compensators, which can produce a commanded amount of reactive power, in a way that minimizes reactive power flows in the microgrid.

In [10], it is proposed a decentralized nonlinear controller for reducing system losses by the optimal management of the reactive power supplied by the inverters of photovoltaic units. The control strategy is based on an artificial dynamic system explicitly designed to be stable by the adoption of Lyapunov theory; this dynamic system provides control laws to be sent to local controllers of photovoltaic inverters, acting as references.

Because of the characteristics of a smart microgrid and its agents, we think a distributed approach is preferable. Here, we will propose a distributed algorithm in which the optimization problem is decomposed into smaller subproblems, each one related to a subset of agents able to exchange information. The subproblems are solved one at a time (in a random and possibly repeated order), by using the Newton's method which guarantees a 1-step convergence. Even though this algorithm is not centralized, we will show it to converge to the optimal solution of the problem under a reasonable assumption on the communication constraints among the agents. Moreover we prefer it compared with other possible methods (possibly better from a computational viewpoint) because it keeps information about the network.

## 1.3 Outline

In Chapter 2 we propose a simple nonlinear model for the problem of optimal reactive power flows in a microgrid and present a linearized version of this model, by using the tool of the *complex gradient*. In order to catch the effect of the interconnections among nodes, we express the voltages of nodes as a linear function of the injected currents by all the nodes.

In Chapter 3, we define the optimization problem; by using an approximate expression of the currents, the problem results to be a (quadratic) convex optimization problem. Then we give an approximate expression of the gradient of the cost function, possibly unknown by the agents.

In Chapter 4 we propose a distributed randomized algorithm for this problem. In order to estimate the interval time between two consecutive iterations, we introduce an approximate (linearized) dynamic model of the microgrid.

In Chapter 5 we analyze the performance of the algorithm, by showing a condition for the convergence to the optimal solution of the optimization problem and providing a bound on the rate of convergence.

In Chapter 6 we provide a result on the best achievable behaviour and some study cases, corresponding to specific topologies of the grid.

Finally in Chapter 7 we validate the proposed models and simulate the behaviour of the proposed optimization method.

## 1.4 Notations

In this section we describe the notation we will use throughout this thesis.

We use  $\mathbb{R}$  to denote the set of real numbers,  $\mathbb{R}^+$  to denote the set of positive real numbers and  $\mathbb{C}$  to denote the set of complex numbers. The set of real (complex)  $n$ -vectors is indicated with  $\mathbb{R}^n$  ( $\mathbb{C}^n$ ), while the set of real (complex)  $m \times n$  matrices is indicated with  $\mathbb{R}^{m \times n}$  ( $\mathbb{C}^{m \times n}$ ). We denote vectors and matrices with square brackets.

Sometimes we will use a notation different from standards for vectors and matrices. As we index the PCC node via the integer 0, the first elements of vectors  $u$ ,  $i$  and  $s$  are  $u(0)$ ,  $i(0)$  and  $s(0)$  respectively. Then, we say that the elements of the matrices related to these vectors have the first row (and/or column) of index 0 (because related to the PCC).

For example, the components of a certain  $(m \times n)$ -matrix  $Y$  may be indicated as follows:

$$Y = \begin{bmatrix} y_{00} & y_{01} & \cdots & y_{0n} \\ y_{10} & y_{11} & \cdots & y_{1n} \\ \vdots & & & \\ \vdots & & & \\ y_{m0} & y_{m1} & \cdots & y_{mn} \end{bmatrix}.$$

However, it will be explicitly said when such a notation is used.

A special vector is  $\mathbf{1}_{\mathcal{W}} \in \mathbb{R}^n$ , defined as follows:

$$[\mathbf{1}_{\mathcal{W}}]_i = \begin{cases} 1 & i \in \mathcal{W} \\ 0 & i \notin \mathcal{W} \end{cases}.$$

So, for example, if  $\mathcal{W} = \{w, 1 \leq w \leq n\}$  ( $|\mathcal{W}| = 1$ ), the vector  $\mathbf{1}_{\mathcal{W}}$  is a vector of the canonical basis; if  $\mathcal{W} = \{1, \dots, n\}$ ,  $\mathbf{1}_{\mathcal{W}}$  is a vector whose components are all one and, for the sake of clarity, we denote this vector as  $\mathbf{1}$ .

The real part and the imaginary part of a vector or a variable  $y$  are indicated as  $\operatorname{Re} y$  and  $\operatorname{Im} y$  respectively (analogously for matrices).

We indicate as  $\bar{Y}$  the complex conjugate of a matrix (or vector)  $Y$  and as  $Y^T$  the transpose of  $Y$ ; with  $Y^\sharp$  we denote the Moore-Penrose generalized inverse of  $Y$ .

The kernel of a  $m \times n$  matrix  $Y$  is the set

$$\ker Y = \{y \mid Yy = 0\}$$

while the image of  $Y$  is the set

$$\operatorname{Im} Y = \{Yy, \exists y\}.$$

# Microgrid model

---

In this chapter we introduce an approximate model for the power distribution network (microgrid).

We start by modelling a microgrid as a directed graph  $\mathcal{G} = (\mathcal{V}, \mathcal{E}, \sigma, \tau)$  (Figure 2), where:

- $\mathcal{V} = \{0, 1, \dots, N\}$  is the set of nodes ( $|\mathcal{V}| = N + 1$ ); the node 0 is a special node: the point of connection of the microgrid to the transmission grid (PCC or point of common coupling);
- $\mathcal{E} = \{1, \dots, N_{\mathcal{E}}\}$  is the set of the edges ( $|\mathcal{E}| = N_{\mathcal{E}}$ );
- $\sigma, \tau : \mathcal{E} \rightarrow \mathcal{V}$  are two functions which associate an edge  $e \in \mathcal{E}$  to its source node  $\sigma(e)$  and terminal node  $\tau(e)$  respectively.

Nodes of  $\mathcal{G}$  represent agents (loads and generators connected to the microgrid), while edges represent power lines.

The study of a grid may be decomposed into the analysis of the types of its components (*typology*) and of the way they are interconnected (*topology*).

The typologies are defined by the laws relating currents and voltages at each node of the microgrid. We model the node corresponding to the PCC as a constant voltage generator, i.e.

$$u(0) = u_0 \in \mathbb{C}, \quad (2.1)$$

whereas we assume that all the other nodes inject (or are supplied with, if negative) a constant power into the microgrid:

$$s(v) = u(v) \bar{i}(v) = \hat{s}(v) \in \mathbb{C}, \quad \forall v \in \mathcal{V} \setminus \{0\}, \quad (2.2)$$

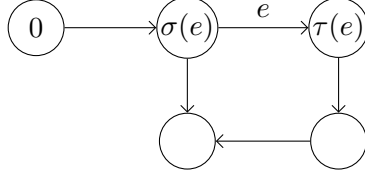


Figure 2.1: Graph describing the adopted microgrid model.

where  $u(v)$  is the voltage at node  $v$ ,  $i(v)$  is the current injected by node  $v$  into the grid,  $s(v)$  is the complex power injected by node  $v$  into the grid and  $\hat{s}(v)$  is a constant reference complex power <sup>1</sup>.

This model choice is a special case of the more general *exponential model* (see for example [18]):

$$p(v) = \hat{p}(v) \left( \frac{|u(v)|}{|u_0|} \right)^{\eta_p}; \quad q(v) = \hat{q}(v) \left( \frac{|u(v)|}{|u_0|} \right)^{\eta_q} \quad (2.3)$$

where  $\hat{p}(v) = \operatorname{Re} \hat{s}(v)$  and  $\hat{q}(v) = \operatorname{Im} \hat{s}(v)$ , while the exponents  $\eta_p$  and  $\eta_q$  are parameters which can take any value; our case is the one in which  $\eta_p = \eta_q = 0$ , so that, by (2.3):

$$s(v) = p(v) + j q(v) = \hat{s}(v),$$

i.e. a constant power model like (2.2) <sup>2</sup>.

The choice of such a model is a good approximation for all the devices connected to the grid via an inverter. The vast majority of microgeneration devices and industrial or residential loads fit in this category.

The topology of the microgrid is studied by *Kirchhoff's laws*:

- Kirchhoff's voltage laws (KVL):

$$u(\sigma(e)) - u(\tau(e)) = \mathbf{z}(e) \xi(e) \quad \forall e \in \mathcal{E} \quad (2.4)$$

where  $\xi(e)$  is the current flowing on the edge  $e$  and  $\mathbf{z}(e)$  is the (complex) impedance of the power line corresponding to the edge  $e$ ;

- Kirchhoff's current laws (KCL):

$$i(v) + \sum_{e \mid \tau(e)=v} \xi(e) - \sum_{e \mid \sigma(e)=v} \xi(e) = 0. \quad (2.5)$$

<sup>1</sup>Our study is limited to the steady state behaviour of the system, so voltages and currents are sinusoidal signals with the same frequency  $f_0$ ; then  $u(v)$  and  $i(v)$  represent the corresponding phasors, according to what described in the Introduction.

<sup>2</sup>Other frequent choices are  $\eta_p = \eta_q = 1$  (constant current model) and  $\eta_p = \eta_q = 2$  (constant impedance model).



---

The topology of a graph can be also described by a matrix  $A \in \{0, \pm 1\}^{N_{\mathcal{E}} \times (N+1)}$  called *incidence matrix*. Each row corresponds to an edge and each column corresponds to a node; the element in position  $(e, v)$  is:

$$[A]_{ev} = \begin{cases} -1 & \text{if } v = \sigma(e) \\ 1 & \text{if } v = \tau(e) \\ 0 & \text{otherwise.} \end{cases} \quad (2.6)$$

As hinted in Section 1.4, we use a notation different from standards for matrix  $A$  (and also for other matrices later): while the rows of  $A$  are indexed via the integers  $1, \dots, N_{\mathcal{E}}$ , the columns are indexed via  $0, \dots, N$ ; this is for the sake of clarity, owing to the notation used for the set  $\mathcal{V} = \{0, \dots, N\}$ . So the element in position  $(h, k)$  of the matrix  $A$  is indicated as  $a_{h,k}$ , with  $1 \leq h \leq N_{\mathcal{E}}$ ,  $0 \leq k \leq N$ .

As each row of  $A$  contains only zeros except one 1 and one  $-1$ , the columns of the matrix  $A$  are not independent.

In the following, we will assume the graph  $\mathcal{G}$  is connected, i.e. there exists a path connecting each couple of its nodes; then it can be shown that the vector  $\mathbf{1}$  is the only vector in  $\ker A$ .

By the matrix  $A$ , the equations (2.4) and (2.5) can be rewritten in a compact way. Let define the vectors:

$$u = \begin{bmatrix} u(0) \\ u(1) \\ \vdots \\ u(N) \end{bmatrix} \quad i = \begin{bmatrix} i(0) \\ i(1) \\ \vdots \\ i(N) \end{bmatrix} \quad \xi = \begin{bmatrix} \xi(1) \\ \xi(2) \\ \vdots \\ \xi(N_{\mathcal{E}}) \end{bmatrix} \quad s = \begin{bmatrix} s(0) \\ s(1) \\ \vdots \\ s(N) \end{bmatrix};$$

then, a microgrid may be modelled by the following system of equations:

$$A^T \xi + i = 0, \quad (2.7a)$$

$$Au + \mathbf{Z}\xi = 0, \quad (2.7b)$$

$$u(v) \bar{i}(v) = s(v), \quad \forall v \in \mathcal{V} \setminus \{0\} \quad (2.7c)$$

$$u(0) = u_0 \quad (2.7d)$$

where  $\mathbf{Z} = \text{diag}(\mathbf{z}(e), e \in \mathcal{E})$ .

It is worth noticing that, by multiplying both the sides of (2.7a) by  $\mathbf{1}^T$ , we deduce a further (redundant) constraint:

$$\mathbf{1}^T (A^T \xi + i) = \mathbf{1}^T i = 0$$

as we are assuming  $\mathcal{G}$  to be connected ( $\mathbf{1} \in \ker A$ ).

Equations in (2.7) provide a nonlinear system of  $2(N+1) + N_{\mathcal{E}}$  equations, whose variables are  $u$ ,  $i$ ,  $\xi$ . Our task is now solving this system in order to obtain the grid voltages and currents, given the network parameters, the injected power at every node and the nominal voltage at the PCC  $u_0$ .

## 2.1 Matrices $\mathbf{L}$ and $\mathbf{X}$

In this paragraph, we introduce two matrices which are useful for giving an expression of  $u$  as a function of  $i$  and vice versa.

The first matrix we present is the *Laplacian matrix*  $\mathbf{L} \in \mathbb{C}^{(N+1) \times (N+1)}$ , defined as:

$$\mathbf{L} = \mathbf{A}^T \mathbf{Z}^{-1} \mathbf{A}$$

Both rows and columns of  $L$  are indicated with indices belonging to the set  $\{0, \dots, N\}$ ; the reason is the same explained before for matrix  $A$ .

From (2.7b):

$$\xi = -\mathbf{Z}^{-1} \mathbf{A} u \quad (2.8)$$

and, by substituting into (2.7a):

$$i = \mathbf{L} u. \quad (2.9)$$

So, we have derived a solution for the current vector of the microgrid which is a linear function of  $u$ .

In order to obtain a similar expression for the voltages, we should find a matrix which allows to express the vector of voltages as a function of the vector of currents. If  $\mathbf{L}$  were a full rank matrix, we would find its inverse. However the matrix  $\mathbf{L}$  is not invertible ( $\mathbf{1} \in \ker \mathbf{L}$ ). A natural approach is to use a generalized inverse (Appendix C) of the Laplacian matrix, defined by the following lemma.

**Lemma 1.** *There exists a unique symmetric matrix  $\mathbf{X} \in \mathbb{C}^{(N+1) \times (N+1)}$  such that:*

$$\begin{cases} \mathbf{X} \mathbf{L} = \mathbf{I} - \mathbf{1} \mathbf{1}_0^T \\ \mathbf{X} \mathbf{1}_0 = 0 \end{cases} \quad (2.10)$$

*Proof.* We have to show the existence, the unicity and the simmetry of the matrix  $\mathbf{X}$ .

- *Existence:* as  $\ker \mathbf{L} = \text{Im } \mathbf{1} = \ker(\mathbf{I} - \mathbf{1} \mathbf{1}_0^T)$ , then there exists  $\tilde{\mathbf{X}}$  such that:  $\tilde{\mathbf{X}} \mathbf{L} = \mathbf{I} - \mathbf{1} \mathbf{1}_0^T$ . Let be:  $\mathbf{X} = \tilde{\mathbf{X}} (\mathbf{I} - \mathbf{1}_0 \mathbf{1}^T)$ . Then:

$$\begin{aligned} \mathbf{X} \mathbf{L} &= \tilde{\mathbf{X}} (\mathbf{I} - \mathbf{1}_0 \mathbf{1}^T) \mathbf{L} = \tilde{\mathbf{X}} \mathbf{L} = \mathbf{I} - \mathbf{1} \mathbf{1}_0^T \\ \mathbf{X} \mathbf{1}_0 &= \tilde{\mathbf{X}} (\mathbf{I} - \mathbf{1}_0 \mathbf{1}^T) \mathbf{1}_0 = 0, \end{aligned}$$

so there exists a matrix  $\mathbf{X}$  satisfying (2.10).

- *Uniqueness:* as

$$\begin{bmatrix} \mathbf{X} & \mathbf{1} \\ \mathbf{1}^T & \mathbf{0} \end{bmatrix} \begin{bmatrix} \mathbf{L} & \mathbf{1}_0 \\ \mathbf{1}_0^T & \mathbf{0} \end{bmatrix} = \begin{bmatrix} \mathbf{X} \mathbf{L} + \mathbf{1} \mathbf{1}_0^T & \mathbf{X} \mathbf{1}_0 \\ \mathbf{1}^T \mathbf{L} & \mathbf{1}^T \mathbf{1}_0 \end{bmatrix} = \begin{bmatrix} \mathbf{I} & \mathbf{0} \\ \mathbf{0} & \mathbf{1} \end{bmatrix}$$

it results:

$$\begin{bmatrix} \mathbf{X} & \mathbf{1} \\ \mathbf{1}^T & \mathbf{0} \end{bmatrix} = \begin{bmatrix} \mathbf{L} & \mathbf{1}_0 \\ \mathbf{1}_0^T & \mathbf{0} \end{bmatrix}^{-1}.$$

Owing to the uniqueness of the inverse of a matrix,  $\mathbf{X}$  is unique.

## 2.1 Matrices $\mathbf{L}$ and $\mathbf{X}$

---

- *Simmetry*: as  $\mathbf{L} = \mathbf{L}^T$ :

$$\begin{bmatrix} \mathbf{X} & \mathbf{1} \\ \mathbf{1}^T & \mathbf{0} \end{bmatrix}^T = \begin{bmatrix} \mathbf{X}^T & \mathbf{1} \\ \mathbf{1}^T & \mathbf{0} \end{bmatrix} = \left( \begin{bmatrix} \mathbf{L} & \mathbf{1}_0 \\ \mathbf{1}_0^T & \mathbf{0} \end{bmatrix}^{-1} \right)^T = \begin{bmatrix} \mathbf{L} & \mathbf{1}_0 \\ \mathbf{1}_0^T & \mathbf{0} \end{bmatrix}^{-1} = \begin{bmatrix} \mathbf{X} & \mathbf{1} \\ \mathbf{1}^T & \mathbf{0} \end{bmatrix}$$

and so  $\mathbf{X} = \mathbf{X}^T$ .

□

In order to satisfy these properties, the matrix  $\mathbf{X}$  must have the first row and the first column (indexed with 0: for  $\mathbf{X}$  we use the same notation of  $\mathbf{L}$ ) equal to zero.

The matrix  $\mathbf{X}$  is positive semidefinite, it has only one eigenvalue in zero and  $\ker(\mathbf{X}) = \{\mathbf{1}_0\}$ .

By  $\mathbf{X}$  it is possible to express  $u$  as a linear function of  $i$ : by multiplying both sides of (2.9) by  $\mathbf{X}$ , it results  $\mathbf{X}\mathbf{L}u = \mathbf{X}i$  and, by (2.10):

$$u = \mathbf{X}i + u_0 \mathbf{1}. \quad (2.11)$$

Then:

$$u(v) = \mathbf{1}_v^T \mathbf{X}i + u_0, \quad (2.12)$$

for each node  $v \in \mathcal{V}$ , included the node 0 representing the PCC, being:

$$u(0) = \mathbf{1}_0^T \mathbf{X}i + u_0 = u_0$$

owing to the properties of the matrix  $\mathbf{X}$ .

Finally, the *effective impedance* between two nodes is expressed as a function of  $\mathbf{X}$ , as stated by the following lemma.

**Lemma 2.** *Let consider two nodes  $v$  and  $w$  of the graph  $\mathcal{G}$ . The effective impedance between  $v$  and  $w$  is  $\mathbf{z}_{\text{eff}}(v, w): \mathcal{V} \times \mathcal{V} \rightarrow \mathbb{C}$  and can be expressed as:*

$$\mathbf{z}_{\text{eff}}(v, w) = (\mathbf{1}_v - \mathbf{1}_w)^T \mathbf{X}(\mathbf{1}_v - \mathbf{1}_w). \quad (2.13)$$

*Proof.* The effective impedance measured across nodes  $v$  and  $w$  is the difference of potentials that appears across terminals  $v$  and  $w$  when a unit current source is applied between them. Consider the specific case when  $i = \mathbf{1}_v - \mathbf{1}_w$ , corresponding to a unit current source connected from the node  $v$  to the node  $w$ . Then:

$$\begin{aligned} \mathbf{z}_{\text{eff}}(v, w) &= u(v) - u(w) = (\mathbf{1}_v - \mathbf{1}_w)^T u \\ &= (\mathbf{1}_v - \mathbf{1}_w)^T [\mathbf{X}i + u_0 \mathbf{1}] \\ &= (\mathbf{1}_v - \mathbf{1}_w)^T \mathbf{X}(\mathbf{1}_v - \mathbf{1}_w). \end{aligned}$$

□

## 2.2 Approximate model

In this section we derive an approximate model for a microgrid, by linearization of the nonlinear system (2.7) obtained in the previous section.

By substituting (2.9) into (2.7c), the system (2.7) can be rewritten as:

$$\begin{cases} u(v)\mathbf{1}_v^T \bar{\mathbf{L}} \bar{u} = s(v) & \forall v \in \mathcal{V} \setminus \{0\} \\ u(0) = u_0 \end{cases}$$

Let be:  $\mu = u - u_0\mathbf{1}$  and  $\epsilon = 1/u_0$ .

A microgrid can be described by the system  $\mathbf{g}(\mu, \epsilon) = 0$ , with:  $\mathbf{g}: \mathbb{C}^N \rightarrow \mathbb{C}^N$  such that:

$$\begin{cases} g_0 = \mu(0) \\ g_v = \epsilon \left[ \mu(v) + \frac{1}{\epsilon} \mathbf{1}_v^T \bar{\mathbf{L}} \bar{\mu} - s(v) \right] & \forall v \in \mathcal{V} \setminus \{0\} \end{cases} \quad (2.14)$$

In order to make this system linear, we use the linear Taylor polynomial. Nevertheless,  $\mathbf{g}(\mu, \epsilon)$  is a complex function of complex variables and this can create some problems.

A complex function can be thought as:  $\mathbf{g} = \mathbf{g}^r + j\mathbf{g}^i$  and the linearization of  $\mathbf{g}$  can be made through the linearization of  $\mathbf{g}^r$  and  $\mathbf{g}^i$  and composing  $\mathbf{g}$  at the end.

Typically, the linearizations of  $\mathbf{g}^r$  and  $\mathbf{g}^i$  are done with respect to the real and imaginary parts of their complex variables, so the gradient concerned is real. In [17], an alternative approach based on the definition of *complex gradient* is proposed. It will be briefly explained in the next paragraph.

### 2.2.1 Complex gradient

Let define the vector  $\mathbf{w} \in \mathbb{R}^{2n \times 1}$  as

$$\mathbf{w} = \begin{bmatrix} x_1 \\ y_1 \\ \vdots \\ x_n \\ y_n \end{bmatrix}$$

and  $f: \mathbb{R}^{2n} \rightarrow \mathbb{R}$  a smooth function of elements of the vector  $\mathbf{w}$ .

The linear Taylor polynomial of  $f$  about the point  $\mathbf{w} = \mathbf{0}$  is:

$$f(\mathbf{w}) \approx f(\mathbf{0}) + \left. \frac{\partial f}{\partial \mathbf{w}^T} \right|_{\mathbf{w}=\mathbf{0}} \mathbf{w} \quad (2.15)$$

where  $\frac{\partial f}{\partial \mathbf{w}^T} \in \mathbb{R}^{1 \times 2n}$  is the row-vector of first-order derivatives of  $f$  with respect to the elements of  $\mathbf{w}$  and its transpose is called *real gradient*.

## 2.2 Approximate model

Let consider a complex vector  $z \in \mathbb{C}^n$ , whose components are  $z_i = x_i + jy_i$ :

$$\begin{bmatrix} z_i \\ \bar{z}_i \end{bmatrix} = \hat{J} \begin{bmatrix} x_i \\ y_i \end{bmatrix} \quad \text{with} \quad \hat{J} = \begin{bmatrix} 1 & j \\ 1 & -j \end{bmatrix} \quad (2.16)$$

$$\begin{bmatrix} x_i \\ y_i \end{bmatrix} = \hat{J}^{-1} \begin{bmatrix} z_i \\ \bar{z}_i \end{bmatrix} \quad \text{with} \quad \hat{J}^{-1} = \frac{1}{2} \bar{\hat{J}}^T. \quad (2.17)$$

Defining:

$$\mathbf{v} = \begin{bmatrix} z_1 \\ \bar{z}_1 \\ \vdots \\ z_n \\ \bar{z}_n \end{bmatrix}$$

it results:

$$\mathbf{v} = J\mathbf{w} \quad \text{with} \quad J = \text{diag}[\hat{J}, \dots, \hat{J}] \in \mathbb{C}^{2n \times 2n}$$

and

$$\mathbf{w} = J^{-1}\mathbf{v} = \frac{1}{2} \bar{J}^T \mathbf{v}. \quad (2.18)$$

As:

$$\frac{\partial f}{\partial v_i} = \sum_{j=1}^{2n} \frac{\partial f}{\partial w_j} \frac{\partial w_j}{\partial v_i}$$

it follows:

$$\frac{\partial f}{\partial \mathbf{v}} = \frac{1}{2} \bar{J} \frac{\partial f}{\partial \mathbf{w}}, \quad \frac{\partial f}{\partial \mathbf{v}^T} = \left( \frac{\partial f}{\partial \mathbf{v}} \right)^T = \frac{1}{2} \left( \frac{\partial f}{\partial \mathbf{w}} \right)^T \bar{J}^T = \frac{1}{2} \left( \frac{\partial f}{\partial \mathbf{w}^T} \right) \bar{J}^T \quad (2.19)$$

by keeping in mind that  $\frac{\partial f}{\partial \mathbf{v}}$  and  $\frac{\partial f}{\partial \mathbf{w}}$  are the transpose of  $\frac{\partial f}{\partial \mathbf{v}^T}$  and  $\frac{\partial f}{\partial \mathbf{w}^T}$  respectively.

The vector  $\frac{\partial f}{\partial \mathbf{v}} \in \mathbb{C}^{2n \times 1}$  is defined as the *complex gradient* on the real function  $f$  with respect to complex variable  $\mathbf{v}$ .

From equations (2.18) and (2.19) it results:

$$\frac{\partial f}{\partial \mathbf{w}^T} \mathbf{w} = \frac{1}{2} \frac{\partial f}{\partial \mathbf{w}^T} \bar{J}^T \mathbf{v} = \frac{\partial f}{\partial \mathbf{v}^T} \mathbf{v}. \quad (2.20)$$

Equations (2.19) and (2.20) show that the real gradient  $\frac{\partial f}{\partial \mathbf{w}}$  and the complex gradient  $\frac{\partial f}{\partial \mathbf{v}}$  are related by a simple linear transformation.

By substituting (2.20) in (2.15):

$$f(\mathbf{v}) \approx f(\mathbf{0}) + \left. \frac{\partial f}{\partial \mathbf{v}^T} \right|_{\mathbf{v}=\mathbf{0}} \mathbf{v}. \quad (2.21)$$

It is easy the extension to functions  $f_c: \mathbb{C}^n \rightarrow \mathbb{C}$ : we can follow the same procedure seen before for the real functions  $\Re f_c$  and  $\Im f_c$  (which we assume both smooth functions) and then compose  $f_c = \Re f_c + j \Im f_c$  at the end: by (2.21)

$$f_c(\mathbf{v}) = f_c(\mathbf{0}) + \sum_{i=1}^n \left. \frac{\partial f_c}{\partial z_i} \right|_{\mathbf{v}=\mathbf{0}} z_i + \sum_{i=1}^n \left. \frac{\partial f_c}{\partial \bar{z}_i} \right|_{\mathbf{v}=\mathbf{0}} \bar{z}_i + o(|\mathbf{v}|^2), \quad (2.22)$$

where  $|\mathbf{v}|$  denotes the vector containing the absolute values of the components of  $\mathbf{v}$ .

It is worth noticing that, if  $\mathbf{v} = \hat{\mathbf{v}}$  is the solution of

$$f_c(\mathbf{0}) + \sum_{i=1}^n \left. \frac{\partial f_c}{\partial z_i} \right|_{\mathbf{v}=\mathbf{0}} z_i + \sum_{i=1}^n \left. \frac{\partial f_c}{\partial \bar{z}_i} \right|_{\mathbf{v}=\mathbf{0}} \bar{z}_i = 0,$$

then, by (2.22),  $f_c(\hat{\mathbf{v}}) \in o(|\mathbf{v}|^2)$ .

## 2.2.2 Approximate solution for currents

Let consider the system described by the equations  $\mathbf{g}(\mu, \epsilon) = 0$ , where  $\mathbf{g} = \mathbf{g}^r + j\mathbf{g}^i$  is the one of equation (2.14) with:

$$g_v^r = \frac{g_v + \bar{g}_v}{2} = \begin{cases} \frac{\mu_0 + \bar{\mu}_0}{2} & v = 0 \\ \frac{\chi_v + \bar{\chi}_v}{2} & v \neq 0 \end{cases} \quad g_v^i = \frac{g_v - \bar{g}_v}{2j} = \begin{cases} \frac{\mu_0 - \bar{\mu}_0}{2j} & v = 0 \\ \frac{\chi_v - \bar{\chi}_v}{2j} & v \neq 0 \end{cases} \quad (2.23)$$

where  $\chi_v = (\epsilon \mu(v) + 1) \mathbf{1}_v^T \bar{\mathbf{L}} \bar{\mu} - \epsilon s(v)$ .

We want to write  $\mathbf{g}^r$  and  $\mathbf{g}^i$  by using the linear Taylor polynomial, as described in the previous paragraph; by equation (2.21), it results:

$$\mathbf{g}^r(\mu, \epsilon) \approx \mathbf{g}^r(0, 0) + \left. \frac{\partial \mathbf{g}^r}{\partial \mu} \right|_{(0,0)} \mu + \left. \frac{\partial \mathbf{g}^r}{\partial \bar{\mu}} \right|_{(0,0)} \bar{\mu} + \left. \frac{\partial \mathbf{g}^r}{\partial \epsilon} \right|_{(0,0)} \epsilon + \left. \frac{\partial \mathbf{g}^r}{\partial \bar{\epsilon}} \right|_{(0,0)} \bar{\epsilon} \quad (2.24)$$

where:  $\mathbf{g}^r(0, 0) = 0$ ,

$$\left. \frac{\partial g_v^r}{\partial \epsilon} \right|_{(0,0)} = \left. \frac{\partial \bar{g}_v^r}{\partial \epsilon} \right|_{(0,0)} = \begin{cases} 0 & v = 0 \\ \left. \frac{\mu(v) \mathbf{1}_v^T \bar{\mathbf{L}} \bar{\mu} - s(v)}{2} \right|_{(0,0)} = -\frac{s(v)}{2} & v \neq 0 \end{cases}$$

$$\frac{\partial g_v^r}{\partial \mu(w)} = \frac{\partial \bar{g}_v^r}{\partial \bar{\mu}(w)} = \begin{cases} \frac{1}{2} & v = w = 0 \\ 0 & v = 0, w \neq 0 \\ \frac{(\bar{\epsilon} \bar{\mu}(v) + 1) \mathbf{1}_v^T \mathbf{L} \mathbf{1}_v + \epsilon \mathbf{1}_v^T \bar{\mathbf{L}} \bar{\mu}}{2} & v = w \neq 0 \\ \frac{(\bar{\epsilon} \bar{\mu}(v) + 1) \mathbf{1}_v^T \mathbf{L} \mathbf{1}_w}{2} & \text{otherwise} \end{cases}$$

and so:

$$\left. \frac{\partial g_v^r}{\partial \mu(w)} \right|_{(0,0)} = \frac{\mathbf{1}_v^T \mathbf{L} \mathbf{1}_w}{2} \quad v \neq 0.$$

As to the imaginary part of  $\mathbf{g}$ :

$$\mathbf{g}^i(\mu, \epsilon) \approx \mathbf{g}^i(0, 0) + \left. \frac{\partial \mathbf{g}^i}{\partial \mu} \right|_{(0,0)} \mu + \left. \frac{\partial \mathbf{g}^i}{\partial \bar{\mu}} \right|_{(0,0)} \bar{\mu} + \left. \frac{\partial \mathbf{g}^i}{\partial \epsilon} \right|_{(0,0)} \epsilon + \left. \frac{\partial \mathbf{g}^i}{\partial \bar{\epsilon}} \right|_{(0,0)} \bar{\epsilon} \quad (2.25)$$

## 2.2 Approximate model

where:  $\mathbf{g}^i(0, 0) = 0$ ,

$$\begin{aligned} \left. \frac{\partial g_v^i}{\partial \epsilon} \right|_{(0,0)} &= \left. \frac{\partial \overline{g_v^i}}{\partial \epsilon} \right|_{(0,0)} = \begin{cases} 0 & v = 0 \\ \left. \frac{\mu(v) \mathbf{1}_v^T \bar{\mathbf{L}} \bar{\mu} - s(v)}{2j} \right|_{(0,0)} = -\frac{s(v)}{2j} & v \neq 0. \end{cases} \\ \frac{\partial g_v^i}{\partial \mu(w)} = \frac{\partial \overline{g_v^i}}{\partial \bar{\mu}(w)} &= \begin{cases} \frac{1}{2j} & v = w = 0 \\ 0 & v = 0, w \neq 0 \\ \frac{-(\bar{\epsilon} \bar{\mu}(v) + 1) \mathbf{1}_v^T \mathbf{L} \mathbf{1}_v + \epsilon \mathbf{1}_v^T \bar{\mathbf{L}} \bar{\mu}}{2j} & v = w \neq 0 \\ \frac{-(\bar{\epsilon} \bar{\mu}(v) + 1) \mathbf{1}_v^T \mathbf{L} \mathbf{1}_w}{2j} & \text{otherwise} \end{cases} \end{aligned} \quad (2.26)$$

and so:

$$\left. \frac{\partial g_v^i}{\partial \mu(w)} \right|_{(0,0)} = -\frac{\mathbf{1}_v^T \mathbf{L} \mathbf{1}_w^T}{2j} \quad v \neq 0.$$

From (2.22), by replacing these derivatives in (2.24) and (2.25), it results:

$$\begin{aligned} \mathbf{g}(\mu, \epsilon) = \mathbf{g}^r + j \mathbf{g}^i &\approx -\frac{1}{2} \begin{bmatrix} \mathbf{0} \\ s_M \end{bmatrix} \epsilon - \frac{1}{2} \begin{bmatrix} \mathbf{0} \\ \bar{s}_M \end{bmatrix} \bar{\epsilon} + \frac{1}{2} \begin{bmatrix} \mathbf{1}_0^T \\ \mathbf{L}_M \end{bmatrix} \mu + \frac{1}{2} \begin{bmatrix} \mathbf{1}_0^T \\ \bar{\mathbf{L}}_M \end{bmatrix} \bar{\mu} + \\ &j \left( -\frac{1}{2j} \begin{bmatrix} \mathbf{0} \\ s_M \end{bmatrix} \epsilon + \frac{1}{2j} \begin{bmatrix} \mathbf{0} \\ \bar{s}_M \end{bmatrix} \bar{\epsilon} - \frac{1}{2j} \begin{bmatrix} -\mathbf{1}_0^T \\ \mathbf{L}_M \end{bmatrix} \mu + \frac{1}{2j} \begin{bmatrix} -\mathbf{1}_0^T \\ \bar{\mathbf{L}}_M \end{bmatrix} \bar{\mu} \right) \end{aligned}$$

where  $s_M$  is the  $N$ -vector obtained from  $s$  by eliminating its first element  $s(0)$ , while  $\mathbf{L}_M$  is the  $N \times (N + 1)$  matrix obtained from  $\mathbf{L}$  by eliminating its first row (indexed with 0 according to our notation).

So, the system described by equations  $\mathbf{g}(\mu, \epsilon) = 0$  is approximated by:

$$\begin{cases} \mu^r(0) + j \mu^i(0) = 0 \\ \bar{\mathbf{L}}_M \bar{\mu} - s_M \epsilon = 0 \end{cases}$$

which is equivalent to:

$$\begin{cases} u(0) = u_0 \\ \mathbf{L}_M(u - u_0 \mathbf{1}) = \mathbf{L}_M, u = \bar{\epsilon} \bar{s}_M \end{cases} \quad (2.27)$$

The system (2.27) is linear, with  $N + 1$  equations and the couple  $(u, s)$  as variables.

From (2.9) and (2.27) we can conclude (indicating with  $\mathbf{l}_0$  the first row of  $\mathbf{L}$ , indexed with 0):

$$i = \mathbf{L}u = \begin{bmatrix} \mathbf{l}_0 u \\ \mathbf{L}_M u \end{bmatrix} \approx \frac{1}{\bar{u}_0} \bar{s} \quad (2.28)$$

with the constraint  $s(0) = -\sum_{v \in \mathcal{V} \setminus \{0\}} s(v)$ , according to (2.7a)

In particular, by the considerations in the previous paragraph, it results:

$$i = \frac{1}{\bar{u}_0} \bar{s} + o\left(\frac{1}{|u_0|^2}\right) :$$

the solution of (2.27) in (2.28) is a good approximation for large values of the voltage at the PCC  $u_0$  and values of voltages of nodes which are about  $u_0$ .

A numerical validation of the approximate model proposed in this section will be presented in Section 7.1.



# Problem formulation

---

This chapter and the following one represent the core of this thesis. Here we will define the optimization problem, then we will propose an algorithm to solve it.

As described in the previous chapter, we will choose of optimizing the power losses minimization, and in particular the losses related to the reactive power. Thanks to the proposed model of a microgrid, we will be able to define an approximate but quadratic cost function and so we will have the advantage of working with a convex optimization problem.

Moreover, an estimation of the gradient of the cost function will be proposed: it will depend only on local measurements, as it is necessary owing to the characteristics of the agents, which usually have a partial knowledge of the grid.

## 3.1 Cost function for power losses minimization

In this section we define the optimization problem for the optimal reactive power compensation.

Our choice is to minimize the total active power losses on the edge:

$$\sum_{e \in \mathcal{E}} \mathbb{R}e \, l(e) = \sum_{e \in \mathcal{E}} \mathbb{R}e[\mathbf{z}(e) |\xi(e)|^2] = \mathbb{R}e[\bar{\xi}^T \mathbf{Z} \xi].$$

By (2.8):

$$\begin{aligned}
 \mathbb{R}e \, l(e) &= \mathbb{R}e[\bar{\xi}^T \mathbf{Z} \xi] = \mathbb{R}e[\bar{u}^T A^T \bar{\mathbf{Z}}^{-1} A u] \\
 &= \mathbb{R}e[(\bar{\mathbf{X}} \bar{i} + u_0 \mathbf{1})^T \bar{\mathbf{L}} (\mathbf{X} i + u_0 \mathbf{1})] \\
 &= \mathbb{R}e[\bar{i}^T \bar{\mathbf{X}} \bar{\mathbf{L}} \mathbf{X} i] \\
 &= \mathbb{R}e[\bar{i}^T (I - \mathbf{1} \mathbf{1}_0^T) \mathbf{X} i] \\
 &= \mathbb{R}e[\bar{i}^T \mathbf{X} i]
 \end{aligned}$$

where we have used (2.11) and the properties of the matrices  $\mathbf{L}$  and  $\mathbf{X}$ .

By using the approximate solution for the variable  $i$  obtained in (2.28):

$$\begin{aligned}
 \sum_{e \in \mathcal{E}} \mathbb{R}e \, l(e) &= \mathbb{R}e[\bar{i}^T \mathbf{X} i] \approx \frac{1}{|u_0|^2} \mathbb{R}e[s^T \mathbf{X} \bar{s}] \\
 &= \frac{1}{|u_0|^2} \mathbb{R}e[\bar{s}^T \mathbf{X} s] \\
 &= \frac{1}{|u_0|^2} \mathbb{R}e[(p^T - jq^T)(\mathbb{R}e[\mathbf{X}] + j \mathbb{I}m[\mathbf{X}])(p + jq)] \\
 &= \frac{1}{|u_0|^2} (p^T \mathbb{R}e[\mathbf{X}] p + q^T \mathbb{R}e[\mathbf{X}] q)
 \end{aligned} \tag{3.1}$$

where  $p = \mathbb{R}e \, s$  is the injected active power, while  $q = \mathbb{I}m \, s$  is the injected reactive power. So the problem of optimal power flows has been decomposed into the problem of optimal active and reactive power compensation.

For the formulation of the minimization problem, it is reasonable to command only a subset  $\mathcal{C} \subseteq \mathcal{V}$ : this is the set of compensators, whose cardinality is indicated as  $|\mathcal{C}| = N_{\mathcal{C}}$ .

Moreover, according to what said in Section 1.1.1, we assume we are allowed to command only the amount of reactive power injected into the grid by the nodes of  $\mathcal{C}$ , as the decision on the amount of active power follows imperative economic criteria (for example, in the case of renewable energy sources, any available active power is generally injected into the grid to replace generation from traditional plants which are more expensive and exhibit a worse environmental impact).

According to these assumptions, we introduce, without loss of generality<sup>1</sup>, the following block-form for  $q$  and  $\mathbf{X}$ :

$$q = \begin{bmatrix} q_{\bar{\mathcal{C}}} \\ q_{\mathcal{C}} \end{bmatrix} \quad \mathbf{X} = \begin{bmatrix} \mathbf{X}_{\bar{\mathcal{C}}\bar{\mathcal{C}}} & \mathbf{X}_{\bar{\mathcal{C}}\mathcal{C}} \\ \mathbf{X}_{\mathcal{C}\bar{\mathcal{C}}} & \mathbf{X}_{\mathcal{C}\mathcal{C}} \end{bmatrix}. \tag{3.2}$$

Then, the cost function (3.1) is equivalent to:

---

<sup>1</sup>If nodes are not ordered according to this notation, it is sufficient to introduce a proper reordering of nodes' indices.

### 3.1 Cost function for power losses minimization

---

$$\begin{aligned}
J'(q_C) &= \frac{1}{|u_0|^2} q_C^T \mathbb{R}e[\mathbf{X}] q_C \\
&= \frac{1}{|u_0|^2} \begin{bmatrix} q_{\bar{C}}^T & q_C^T \end{bmatrix} \mathbb{R}e \begin{bmatrix} \mathbf{X}_{\bar{C}\bar{C}} & \mathbf{X}_{\bar{C}C} \\ \mathbf{X}_{C\bar{C}} & \mathbf{X}_{CC} \end{bmatrix} \begin{bmatrix} q_{\bar{C}} \\ q_C \end{bmatrix} \\
&= \frac{1}{|u_0|^2} (q_{\bar{C}}^T \mathbb{R}e[\mathbf{X}_{CC}] q_C + 2q_{\bar{C}}^T \mathbb{R}e[\mathbf{X}_{\bar{C}C}] q_C + q_{\bar{C}}^T \mathbb{R}e[\mathbf{X}_{\bar{C}\bar{C}}] q_{\bar{C}}),
\end{aligned} \tag{3.3}$$

where we have exploited the symmetry of the matrix  $\mathbf{X}$ .

The optimization problem may be formulated as follows:

$$\begin{aligned}
&\min_{q_C} J(q_C) \\
&\text{subject to } \mathbf{1}^T q_C = -\mathbf{1}^T q_{\bar{C}}
\end{aligned} \tag{3.4}$$

where

$$J(q_C) = \frac{1}{|u_0|^2} (q_{\bar{C}}^T \mathbb{R}e[\mathbf{X}_{CC}] q_C + 2q_{\bar{C}}^T \mathbb{R}e[\mathbf{X}_{\bar{C}C}] q_C) \tag{3.5}$$

is the objective function of the problem, obtained from (3.3) exploiting the fact that the minimization is with respect to  $q_C$ ; thanks to the approximation (2.28), (3.5) is a (quadratic) convex function and the problem of optimal reactive injection at the compensators, defined by (3.4), is a quadratic, linearly constrained problem.

We now introduce an assumption on the impedances of the edges (power lines) of the microgrid.

**Assumption 3.** *The inductance-resistance ratio is fixed for each edges, i.e.:*

$$\mathbf{z}(e) = z(e) e^{j\theta_e} \quad \text{with } \theta_e = \theta \quad \forall e \in \mathcal{E},$$

where  $z(e) = |\mathbf{z}(e)|$ .

By Assumption 3:

$$\mathbf{Z} = e^{j\theta} Z \quad \mathbf{L} = A^T \mathbf{Z}^{-1} A = e^{-j\theta} A^T Z^{-1} A = e^{-j\theta} L \quad \mathbf{X} = e^{j\theta} X, \tag{3.6}$$

where  $Z$ ,  $L$ ,  $X$  are real valued matrices.

Moreover, the cost function (3.5), can be rewritten as:

$$J(q_C) = \frac{\cos \theta}{|u_0|^2} (q_{\bar{C}}^T X_{CC} q_C + 2q_{\bar{C}}^T X_{\bar{C}C} q_C). \tag{3.7}$$

The matrix  $X_{CC}$  (together with  $\mathbf{X}_{CC}$ ) is, in general, positive semidefinite. However, under the following assumption, we will show that  $X_{CC} > 0$ .

**Assumption 4.** *The set of compensators does not contain the PCC node, i.e.:  $0 \notin \mathcal{C}$ .*

We suppose Assumption 4 holds in the following chapters, because it simplify our analysis: in fact, the result in the following proposition is guaranteed.

**Proposition 5.** *Let Assumption 4 hold. Then  $X_{CC} > 0$ .*

*Proof.* We have to show that  $y^T X_{CC} y > 0$  for each  $y \neq 0$ .

If there exist a  $\hat{y} \neq 0$  such that  $\hat{y}^T X_{CC} \hat{y} = 0$ , then there would exist also a vector  $\tilde{y}$  such that:

$$\tilde{y}^T X \tilde{y} = \begin{bmatrix} 0 & \hat{y}^T \end{bmatrix} \begin{bmatrix} X_{\bar{C}\bar{C}} & X_{\bar{C}C} \\ X_{C\bar{C}} & X_{CC} \end{bmatrix} \begin{bmatrix} 0 \\ \hat{y} \end{bmatrix} = \hat{y}^T X_{CC} \hat{y} = 0.$$

This implies that  $\tilde{y} \in \ker X$ , according to Proposition 32 in Appendix D.

But this is absurd, because we have obtained a vector  $\tilde{y} \neq \mathbf{1}_0$  in  $\ker X$  ( $\mathbf{1}_0$  is the only vector in  $\ker X$  according to the definition of the matrix  $X$ ).

Notice that if the node 0 were a compensator, then the absurd could not occur.  $\square$

It is worth noticing that the results we will present in the following chapters hold also in absence of the Assumption 4, provided that the inverse matrices of  $X_{CC}$  are replaced with the corresponding generalized inverse matrices. In fact we can state, with abuse of language, that  $X_{CC}$  is actually positive definite "in the subspace defined by the constraint", because, if  $0 \in \mathcal{C}$ , then  $q_0$  could be removed from the set of decision variables thanks to the constraint  $\mathbf{1}^T q = 0$  and the optimization problem be expressed as:

$$\min_{\mathbf{1}^T q_{C'} = -\mathbf{1}^T q_{\bar{C}} - q_0} \frac{\cos \theta}{|u_0|^2} (q_{C'}^T X_{CC}^M q_{C'} + 2q_{\bar{C}}^T X_{CC}^M q_{C'}),$$

where  $X_{CC}^M$  and  $X_{CC}^M > 0$  are obtained from the matrix  $X_{CC}$  after eliminating the column and the row and the column corresponding to node 0 respectively, whereas  $\mathcal{C}' = \mathcal{C} \setminus \{0\}$ .

In Chapters 6 and 7 these considerations will be confirmed, as simulations will be presented including the PCC node among the compensators.

## 3.2 Gradient estimation

In the following chapter, we will present an algorithm to solve the quadratic optimization problem (3.4), which requires the knowledge of the gradient of the cost function (3.7):

$$\begin{aligned} \nabla J(qc) &= \frac{2 \cos \theta}{|u_0|^2} (X_{CC} qc + X_{C\bar{C}} q_{\bar{C}}) \\ &= \frac{2 \cos \theta}{|u_0|^2} \begin{bmatrix} \mathbf{0} & I \end{bmatrix} \begin{bmatrix} X_{\bar{C}\bar{C}} & X_{\bar{C}C} \\ X_{C\bar{C}} & X_{CC} \end{bmatrix} \begin{bmatrix} q_{\bar{C}} \\ qc \end{bmatrix} \\ &= \frac{2 \cos \theta}{|u_0|^2} \text{Im} \left( \hat{X} s \right), \end{aligned} \tag{3.8}$$

where we have defined  $\hat{X} = \begin{bmatrix} X_{\bar{C}\bar{C}} & X_{\bar{C}C} \end{bmatrix} X$ .

### 3.2 Gradient estimation

---

The cost function  $J(q_C)$  and its gradient  $\nabla J(q_C)$  depend on the grid parameters (matrix  $X$  or parts of it) and the power demand (vector  $q_C$ ) of the whole compensators of the microgrid. As described in Section 1, the agents of a smart microgrid (nodes of the graph  $\mathcal{G}$ ) usually have only a partial knowledge of this information and so we exclude that agents are able to retrieve all these data or there exists a centralized agent capable to collect all the necessary information.

In this section we try to calculate an estimate of the gradient (3.8), depending only on the information of a subset of agents  $\mathcal{C}' \subseteq \mathcal{C}$ .

By (2.11) and (2.28):

$$\begin{aligned} u_C &= e^{j\theta} \hat{X} i + u_0 \mathbf{1} \\ &\approx e^{j\theta} \frac{\hat{X} \bar{s}}{\bar{u}_0} + u_0 \mathbf{1}, \end{aligned}$$

where  $u_C$  denotes the vector of voltages of the nodes belonging to the set  $\mathcal{C}$ .

It follows that:

$$\hat{X} \bar{s} \approx e^{-j\theta} \bar{u}_0 (u_C - u_0 \mathbf{1})$$

and:

$$\mathbb{Im}[\hat{X} \bar{s}] \approx \mathbb{Im}(e^{-j\theta} \bar{u}_0 u_C - e^{-j\theta} |u_0|^2 \mathbf{1}).$$

It is unlikely that the value of  $u_0$  is known and so it must be estimated. A possible choice is to replace it with the average voltage of the nodes belonging to  $\mathcal{C}'$ , so that:

$$\begin{aligned} \mathbb{Im}[\hat{X} s] &= -\mathbb{Im}[\hat{X} \bar{s}] \approx -\mathbb{Im}(e^{-j\theta} \frac{\bar{u}_C^T \mathbf{1}_{\mathcal{C}'}}{|\mathcal{C}'|} u_C) + \mathbb{Im}(e^{-j\theta} |u_0|^2 \mathbf{1}) \\ &= -\nu + \kappa \mathbf{1}, \end{aligned} \tag{3.9}$$

where:

$$\nu = \mathbb{Im} \left[ e^{-j\theta} \frac{\bar{u}_C^T \mathbf{1}_{\mathcal{C}'}}{|\mathcal{C}'|} u_C \right]. \tag{3.10}$$

By substituting (3.9) into (3.8):

$$\nabla J \approx -\frac{2 \cos \theta}{|u_0|^2} \nu + \kappa' \mathbf{1}, \tag{3.11}$$

where  $\kappa'$  is a constant but unknown term.

We suppose nodes in  $\mathcal{C}'$  to be allowed to measure the voltages of the nodes of the same subset ( $u_{C'}$ ) and the inductance-resistance ratio  $\theta$  (local measurements), so that they are able to compute the quantity  $\nu_{C'}$ .

Then, these nodes can obtain an estimate of their corresponding components of the gradient ( $\nabla J_{C'}$ ), up to a common but unknown constant.

However, the term  $\kappa' \mathbf{1}$  is orthogonal to the subspace of feasible solutions and it is not harmful for our analysis, as it will be shown in the next chapter.

The quality of the gradient estimation (3.11) via voltage measurements will be validated via simulations in Section 7.1.



# A randomized distributed algorithm

---

In this chapter we will propose an algorithm in order to solve the optimization problem (3.4), whose cost function is given by (3.7).

Owing to the characteristics of a smart microgrid and its agents, we will design a distributed algorithm.

As described in Chapter 1, the agents of the microgrid generally have only a partial knowledge of the system. So they have to make estimates from local measurements and the information they gather in their neighborhood.

For this purpose, the optimization algorithm will have to alternate operations of sensing, processing and actuating the system. This aspect of the problem is one of the most important facts that differentiate the application of distributed optimization methods in this framework from the ones available in literature, mainly derived for the problem of dispatching part of a large scale optimization algorithm to different processing units [1], [11].

The main idea of the proposed algorithm is the clustering of agents able to exchange information, together with the decomposition of the original large minimization problem into smaller subproblems (each one related to a specific cluster of agents). These subproblem are solved iteratively and randomly, by using the Newton's method because of its good convergence features.

We think that a distributed approach is the right way of solving the problem (3.4). However, it guarantees the convergence to the optimal solution under a reasonable assumption on the communication graph among the nodes, as shown in the following chapter. Moreover, compared with other possible approaches, the solutions of the optimization subproblems explicitly contain the matrix  $X_{CC}$  (or parts of it), so that we

keep information on the topology of the network.

In the second part of this chapter, we will try to obtain an estimate of the minimum time between two consecutive iterations of the algorithm. For this purpose, we will introduce a dynamic model of the microgrid. The linearity of the considered model will allow us to calculate the settling time of the system (and so the time needed to attain a new steady state and the analysis of the previous and the following chapters still holds), which is a function of the eigenvalues, the eigenvectors and the initial state of the system.

## 4.1 Optimization problem decomposition

Let the compensators be divided into  $\ell$  possibly overlapping sets  $\mathcal{C}_1, \dots, \mathcal{C}_\ell$ , with

$$\bigcup_{i=1}^{\ell} \mathcal{C}_i = \mathcal{C}, \quad |\mathcal{C}_i| = N_{\mathcal{C}_i} \quad 1 \leq i \leq \ell.$$

We assume that nodes belonging to the same set are able to communicate each other, i.e. they can coordinate their actions and sharing their measurements.

The proposed algorithm minimizes the optimization problem (3.4) by solving a sequence of optimization *subproblems* (one at a time), each one related to a specific cluster  $\mathcal{C}_i$ . In particular, at a certain instant  $t$ , one of the clusters, say  $\mathcal{C}_i$ , is randomly "activated": by using the information that the nodes belonging to the same set  $\mathcal{C}_i$  share, they update their states according the solution of the optimization subproblem:

$$\arg \min_{\Delta q_{\mathcal{C}} \in \mathcal{S}_i} J(q_{\mathcal{C}} + \Delta q_{\mathcal{C}}), \quad (4.1)$$

where

$$\mathcal{S}_i = \left\{ q \in \mathbb{R}^{N_{\mathcal{C}}} : \sum_{j \in \mathcal{C}_i} q_j = 0 ; q_j = 0, \forall j \notin \mathcal{C}_i \right\}.$$

That means that nodes belonging to  $\mathcal{C}_i$  update their state, while the others (belonging to  $\bar{\mathcal{C}}_i = \mathcal{C} \setminus \mathcal{C}_i$ ) keep their state constant, at the value solution of the previous minimization subproblem (notice that it is uninfluent if the previous subproblem was related to the same cluster or to another one).

When the subproblem related to the cluster  $\mathcal{C}_i$  has been solved, a new cluster  $\mathcal{C}_j$  is (randomly) chosen and a new subproblem (related to the cluster  $\mathcal{C}_j$ ) has to be solved.

The goal is attaining the minimizer of the original problem (3.4): the existence of such a minimizer is guaranteed, being the problem quadratic; the convergence to this point will be demonstrated in the next chapter.



## 4.2 Solving optimization subproblems

In this paragraph we define and solve the optimization subproblems faced by the nodes belonging to the cluster  $\mathcal{C}_i$ .

For the sake of simplicity, we introduce a block-form for  $X_{\bar{\mathcal{C}}\mathcal{C}}$  and for  $X_{\mathcal{C}\mathcal{C}}$  and  $q_{\mathcal{C}}$ , similarly to what done in (3.2):

$$q_{\mathcal{C}} = \begin{bmatrix} q_{\bar{\mathcal{C}}_i} \\ q_{\mathcal{C}_i} \end{bmatrix} \quad X_{\mathcal{C}\mathcal{C}} = \begin{bmatrix} X_{\bar{\mathcal{C}}_i\bar{\mathcal{C}}_i} & X_{\bar{\mathcal{C}}_i\mathcal{C}_i} \\ X_{\mathcal{C}_i\bar{\mathcal{C}}_i} & X_{\mathcal{C}_i\mathcal{C}_i} \end{bmatrix} \quad X_{\bar{\mathcal{C}}\mathcal{C}} = \begin{bmatrix} \bar{Y}_i & Y_i \end{bmatrix}$$

From (3.7)

$$\begin{aligned} J &= \frac{\cos \theta}{|u_0|^2} \left( \begin{bmatrix} q_{\bar{\mathcal{C}}_i}^T & q_{\mathcal{C}_i}^T \end{bmatrix} \begin{bmatrix} X_{\bar{\mathcal{C}}_i\bar{\mathcal{C}}_i} & X_{\bar{\mathcal{C}}_i\mathcal{C}_i} \\ X_{\mathcal{C}_i\bar{\mathcal{C}}_i} & X_{\mathcal{C}_i\mathcal{C}_i} \end{bmatrix} \begin{bmatrix} q_{\bar{\mathcal{C}}_i} \\ q_{\mathcal{C}_i} \end{bmatrix} + 2q_{\bar{\mathcal{C}}}^T \begin{bmatrix} \bar{Y}_i & Y_i \end{bmatrix} \begin{bmatrix} q_{\bar{\mathcal{C}}_i} \\ q_{\mathcal{C}_i} \end{bmatrix} \right) \\ &= \frac{\cos \theta}{|u_0|^2} \left[ q_{\bar{\mathcal{C}}_i}^T X_{\mathcal{C}_i\mathcal{C}_i} q_{\mathcal{C}_i} + 2q_{\bar{\mathcal{C}}_i}^T X_{\bar{\mathcal{C}}_i\mathcal{C}_i} q_{\mathcal{C}_i} + q_{\bar{\mathcal{C}}_i}^T X_{\bar{\mathcal{C}}_i\bar{\mathcal{C}}_i} q_{\bar{\mathcal{C}}_i} + 2(m_{\bar{\mathcal{C}}_i}^T q_{\mathcal{C}_i} + m_{\mathcal{C}_i}^T q_{\bar{\mathcal{C}}_i}) \right]. \end{aligned} \quad (4.2)$$

where:  $m_{\bar{\mathcal{C}}_i}^T = q_{\bar{\mathcal{C}}}^T Y_i$  and  $m_{\mathcal{C}_i}^T = q_{\bar{\mathcal{C}}}^T \bar{Y}_i$  and we have exploited the symmetry of matrix  $X$ .

The optimization subproblem faced by the nodes in  $\mathcal{C}_i$  can be formulated as:

$$\begin{aligned} \min_{q_{\mathcal{C}_i}} \quad & J(q_{\mathcal{C}_i}) = \frac{\cos \theta}{|u_0|^2} \left[ q_{\bar{\mathcal{C}}_i}^T X_{\mathcal{C}_i\mathcal{C}_i} q_{\mathcal{C}_i} + 2(q_{\bar{\mathcal{C}}_i}^T X_{\bar{\mathcal{C}}_i\mathcal{C}_i} q_{\mathcal{C}_i} + m_{\mathcal{C}_i}^T q_{\mathcal{C}_i}) \right] \\ \text{subject to} \quad & \mathbf{1}^T q_{\mathcal{C}_i} = c. \end{aligned} \quad (4.3)$$

where the cost function has been obtained by (4.2), keeping in mind that the minimization is with respect to  $q_{\mathcal{C}_i}$  and  $c = -\mathbf{1}^T q_{\bar{\mathcal{C}}} - \mathbf{1}^T q_{\bar{\mathcal{C}}_i}$ .

In order to solve the minimization problem (4.3), we use a classical tool in convex optimization. It is a class of algorithms (called *descent algorithms*), which produce a minimizing sequence  $\{q_{\mathcal{C}_i}(t)\}$ , where:

$$q_{\mathcal{C}_i}(t+1) = q_{\mathcal{C}_i}(t) + \Delta q_{\mathcal{C}_i}(t). \quad (4.4)$$

In this way, agents in  $\mathcal{C}_i$  can attain the optimal solution by adding the step  $\Delta q_{\mathcal{C}_i}$  to  $q_{\mathcal{C}_i}$ .

Descent algorithms include many methods which differ for the choice of the step  $\Delta q_{\mathcal{C}_i}$ ; here we will choose the *Newton's method*: supposing that the Hessian matrix of the cost function in (4.3) is completely known, it allows to obtain the fastest (1-step) convergence (being the problem quadratic)<sup>1</sup>.

<sup>1</sup>If the Hessian matrix is not fully known, other descent methods can be used. For example, if a minimal knowledge is available (diagonal of the matrix), then the Steepest Descent method can be used, but it may require a large number of iterations to converge. Otherwise, it is possible to use a Quasi-Newton Method, which build an estimate of the inverse of the Hessian from the previous step of the algorithm: it requires a minimal knowledge of the problem and allows a faster convergence compared to Steepest Descent Method [2].

According to this method (see Section A.2.2 for details):

$$\Delta q_{\mathcal{C}_i} = -(\nabla^2 J(q_{\mathcal{C}_i}))^{-1} [\nabla J(q_{\mathcal{C}_i}) + \mathbf{1}\gamma],$$

where:

$$\nabla J(q_{\mathcal{C}_i}) = \frac{2 \cos \theta}{|u_0|^2} [X_{\mathcal{C}_i \mathcal{C}_i} q_{\mathcal{C}_i} + X_{\bar{\mathcal{C}}_i \mathcal{C}_i} q_{\bar{\mathcal{C}}_i} + m_{\mathcal{C}_i}] \quad \nabla^2 J_{\mathcal{C}_i}(q_{\mathcal{C}_i}) = \frac{2 \cos \theta}{|u_0|^2} X_{\mathcal{C}_i \mathcal{C}_i}.$$

Then the following proposition holds.

**Proposition 6.** *The solution of the constrained optimization problem (4.3) is given by (4.4) where:*

$$\Delta q_{\mathcal{C}_i} = \frac{|u_0|^2}{\cos \theta} \left[ -\frac{X_{\mathcal{C}_i \mathcal{C}_i}^{-1}}{2} \nabla J_{\mathcal{C}_i} + \frac{\mathbf{1}^T X_{\mathcal{C}_i \mathcal{C}_i}^{-1} \nabla J_{\mathcal{C}_i}}{\mathbf{1}^T X_{\mathcal{C}_i \mathcal{C}_i}^{-1} \mathbf{1}} \frac{X_{\mathcal{C}_i \mathcal{C}_i}^{-1}}{2} \mathbf{1} \right],$$

assuming the matrix  $X_{\mathcal{C}_i \mathcal{C}_i}$  fully known.

*Proof.* We have to show (see Section A.1):

- $q_{\mathcal{C}_i}(t+1)$  is feasible:

$$\begin{aligned} \mathbf{1}^T q_{\mathcal{C}_i}(t+1) &= \mathbf{1}^T q_{\mathcal{C}_i}(t) + \frac{|u_0|^2}{\cos \theta} \left[ -\mathbf{1}^T \frac{X_{\mathcal{C}_i \mathcal{C}_i}^{-1}}{2} \nabla J_{\mathcal{C}_i} + \frac{\mathbf{1}^T X_{\mathcal{C}_i \mathcal{C}_i}^{-1} \nabla J_{\mathcal{C}_i}}{\mathbf{1}^T X_{\mathcal{C}_i \mathcal{C}_i}^{-1} \mathbf{1}} \frac{\mathbf{1}^T X_{\mathcal{C}_i \mathcal{C}_i}^{-1}}{2} \mathbf{1} \right] \\ &= c + \frac{|u_0|^2}{\cos \theta} \mathbf{1}^T \frac{X_{\mathcal{C}_i \mathcal{C}_i}^{-1}}{2} \nabla J_{\mathcal{C}_i} \left[ \frac{\mathbf{1}^T X_{\mathcal{C}_i \mathcal{C}_i}^{-1} \mathbf{1}}{\mathbf{1}^T X_{\mathcal{C}_i \mathcal{C}_i}^{-1} \mathbf{1}} - 1 \right] = c \end{aligned} \quad (4.5)$$

- the gradient  $\nabla J_{\mathcal{C}_i}$  is orthogonal to the constraint:

$$\begin{aligned} \nabla J_{\mathcal{C}_i}(q_{\mathcal{C}_i}(t+1)) &= 2 \frac{\cos \theta}{|u_0|^2} [X_{\mathcal{C}_i \mathcal{C}_i}(q_{\mathcal{C}_i}(t) + \Delta q_{\mathcal{C}_i}(t)) + X_{\bar{\mathcal{C}}_i \mathcal{C}_i} q_{\bar{\mathcal{C}}_i}(t) + m_{\mathcal{C}_i}(t)] \\ &= \nabla J_{\mathcal{C}_i} + 2 X_{\mathcal{C}_i \mathcal{C}_i} \left[ -\frac{X_{\mathcal{C}_i \mathcal{C}_i}^{-1}}{2} \nabla J_{\mathcal{C}_i} + \frac{\mathbf{1}^T X_{\mathcal{C}_i \mathcal{C}_i}^{-1} \nabla J_{\mathcal{C}_i}}{\mathbf{1}^T X_{\mathcal{C}_i \mathcal{C}_i}^{-1} \mathbf{1}} \frac{X_{\mathcal{C}_i \mathcal{C}_i}^{-1}}{2} \mathbf{1} \right] \\ &= \nabla J_{\mathcal{C}_i} - \nabla J_{\mathcal{C}_i} + \frac{\mathbf{1}^T X_{\mathcal{C}_i \mathcal{C}_i}^{-1} \nabla J_{\mathcal{C}_i}}{\mathbf{1}^T X_{\mathcal{C}_i \mathcal{C}_i}^{-1} \mathbf{1}} \mathbf{1} \\ &= \frac{\mathbf{1}^T X_{\mathcal{C}_i \mathcal{C}_i}^{-1} \nabla J_{\mathcal{C}_i}}{\mathbf{1}^T X_{\mathcal{C}_i \mathcal{C}_i}^{-1} \mathbf{1}} \mathbf{1} \in \text{Im } \mathbf{1}. \end{aligned} \quad (4.6)$$

□

As said before, nodes usually have a partial knowledge of the system, and so the gradient of the cost function may be unknown.

By sensing the network voltages and calculating the quantity  $\nu_{\mathcal{C}_i}$ , the nodes of the cluster  $\mathcal{C}_i$  can estimate  $\nabla J_{\mathcal{C}_i}$  according to (3.11).

## 4.2 Solving optimization subproblems

---

Nodes in  $\mathcal{C}_i$  can therefore solve their corresponding optimization subproblem by performing the update

$$\begin{aligned}
\Delta q_{\mathcal{C}_i} &= q_{\mathcal{C}_i}(t+1) - q_{\mathcal{C}_i}(t) \\
&= \frac{|u_0|^2}{\cos \theta} \left[ -\frac{X_{\mathcal{C}_i\mathcal{C}_i}^{-1}}{2} \nabla J_{\mathcal{C}_i} + \frac{\mathbf{1}^T X_{\mathcal{C}_i\mathcal{C}_i}^{-1} \nabla J_{\mathcal{C}_i}}{\mathbf{1}^T X_{\mathcal{C}_i\mathcal{C}_i}^{-1} \mathbf{1}} \frac{X_{\mathcal{C}_i\mathcal{C}_i}^{-1}}{2} \mathbf{1} \right] \\
&= \frac{|u_0|^2}{\cos \theta} \left[ -\frac{X_{\mathcal{C}_i\mathcal{C}_i}^{-1}}{2} \left( -\frac{2 \cos \theta}{|u_0|^2} \nu_{\mathcal{C}_i} + \kappa' \mathbf{1} \right) + \frac{\mathbf{1}^T X_{\mathcal{C}_i\mathcal{C}_i}^{-1}}{\mathbf{1}^T X_{\mathcal{C}_i\mathcal{C}_i}^{-1} \mathbf{1}} \left( -\frac{2 \cos \theta}{|u_0|^2} \nu_{\mathcal{C}_i} + \kappa' \mathbf{1} \right) \frac{X_{\mathcal{C}_i\mathcal{C}_i}^{-1}}{2} \mathbf{1} \right] \\
&= X_{\mathcal{C}_i\mathcal{C}_i}^{-1} \nu_{\mathcal{C}_i} + \frac{|u_0|^2}{\cos \theta} \kappa' \frac{X_{\mathcal{C}_i\mathcal{C}_i}^{-1}}{2} \mathbf{1} - \frac{\mathbf{1}^T X_{\mathcal{C}_i\mathcal{C}_i}^{-1} \nu_{\mathcal{C}_i} X_{\mathcal{C}_i\mathcal{C}_i}^{-1} \mathbf{1}}{\mathbf{1}^T X_{\mathcal{C}_i\mathcal{C}_i}^{-1} \mathbf{1}} + \frac{|u_0|^2}{\cos \theta} \kappa' \frac{\mathbf{1}^T X_{\mathcal{C}_i\mathcal{C}_i}^{-1} \mathbf{1} X_{\mathcal{C}_i\mathcal{C}_i}^{-1} \mathbf{1}}{\mathbf{1}^T X_{\mathcal{C}_i\mathcal{C}_i}^{-1} \mathbf{1}} \\
&= X_{\mathcal{C}_i\mathcal{C}_i}^{-1} \nu_{\mathcal{C}_i} - \frac{\mathbf{1}^T X_{\mathcal{C}_i\mathcal{C}_i}^{-1} \nu_{\mathcal{C}_i}}{\mathbf{1}^T X_{\mathcal{C}_i\mathcal{C}_i}^{-1} \mathbf{1}} X_{\mathcal{C}_i\mathcal{C}_i}^{-1} \mathbf{1}
\end{aligned}$$

It can be noticed that now the update law depends only on the matrix  $X_{\mathcal{C}_i\mathcal{C}_i}$  together with the inductance-resistance ratio  $\theta$  and the voltage measurements of the nodes belonging to a same subset  $\mathcal{C}_i$  (according to (3.10)).

As said in Section 3.2, the term  $\kappa' \mathbf{1}$ , depending on the possibly unknown voltage  $u_0$ , is canceled from the expression of  $\Delta q_{\mathcal{C}_i}$ .

We conclude this section summarizing the operations of the proposed algorithm. It consists of the following, repeated steps:

1. a set  $\mathcal{C}_i$  is randomly chosen according to a sequence of symbols  $\eta(t) \in \{1, \dots, \ell\}$ ;
2. agents in  $\mathcal{C}_i$  sense the network and obtain an estimate of the gradient;
3. agents in  $\mathcal{C}_i$  determine a feasible update step that minimizes the given cost function, coordinating their actions and communicating;
4. they actuate the system by updating their state (the injected reactive power).

The iterated algorithm will then results in the following discrete time system for  $q$

$$q_{\mathcal{C}}(t+1) = T_{\eta(t)}[q_{\mathcal{C}}(t)] := \arg \min_{\Delta q_{\mathcal{C}} \in \mathcal{S}_{\eta(t)}} J(q_{\mathcal{C}}(t) + \Delta q_{\mathcal{C}}), \quad (4.7)$$

with initial conditions  $q(0)$  such that  $\mathbf{1}^T q_{\mathcal{C}}(0) = -\mathbf{1}^T q_{\bar{\mathcal{C}}}(0)$ .

In the following chapter we will show that the proposed algorithm exhibits good characteristics: it converges to the optimal solution of the optimization problem under an assumption on the communication constraints of the compensators; moreover we will say something about the speed of convergence, at least for specific topologies of the grid.

Before, we consider another question, related to the time between two consecutive iterations of the proposed algorithm.

### 4.3 Time between consecutive iterations

In this section, we want to say something about the interval time between consecutive iterations of the distributed algorithm proposed in 4.2.

When a subproblem is solved, the amount of reactive power injected by the compensators (the state of the system) is updated. It affects the grid voltages, which are subject to a transient period. We need to understand how long after changing the vector  $q$ , the grid voltages reach a new steady state value: the following iteration of the algorithm cannot start before it occurs.

We aim at obtaining a model capable of describing the dynamic behaviour of the measured voltages as a function of the injected complex power.

A static model, such as the one introduced in Chapter 2, is unlikely for such a task. Thus, in the following paragraphs, we will introduce a dynamic network model. Instead of using a simulative tool, we will derive it analytically: in this way, we will be able to have a model in which the effects of the network topologies and parameters are recognizable.

The approximate version of the aforementioned model will allow us to use the classical tools of the linear systems; in particular, it will be possible to estimate the settling time of the system, being also related to the largest of its eigenvalues, and then to bound the interval time between consecutive iterations of the algorithm.

Also in this section we will use a phasorial notation, even though the phasors should rigorously be used for steady state behavior only. This is however acceptable if the typical transient duration that we are considering is longer than the fundamental period of the signals [19].

#### 4.3.1 Dynamic network model

In this paragraph we deduce a dynamic model for a microgrid. Simplifying the scenario, we can say that the dynamics of a microgrid are mainly due to:

- the power lines;
- the inverters, related to compensators or loads.

The dynamics due to the power lines are generally considered negligible after a fundamental period of the signals, because the lines' characteristic resistance and inductance have usually values so that the time constant  $L/R$  is small.

As to the nodes, we build a model which keeps into account the assumptions on the typologies of the microgrid introduced in Section 2.

We still model the node 0, corresponding to the PCC, as a constant voltage generator; for the other nodes (loads and compensators) we now adopt the following dynamic model:

$$\tau_v \frac{di(v)}{dt} = -i(v) + \frac{\bar{s}(v)}{\bar{u}(v)}, \quad v = 1, \dots, N, \quad (4.8)$$

### 4.3 Time between consecutive iterations

---

where  $\tau_v$  is the characteristic time constant, and  $s(v)$  is the constant reference complex power.

The choice of such a model comes from the fact that the steady state of (4.8) is

$$i(v) = \frac{\bar{s}(v)}{\bar{u}(v)},$$

i.e. a static constant power model, like in Section 2.

In this way, we assume that loads and compensators behave as constant power loads with a first-order dynamic.

The model (4.8) corresponds to the widely adopted model introduced in [21], [22], [23] on the basis of experimental data. According to the literature, it describes quite well the behavior of the vast majority of microgeneration devices [24], [25], and is also a good approximation for many industrial and residential loads.

The time constant  $\tau_v$  can differ a lot from node to node: it is generally large for loads and small for compensators. This is because the dynamics of compensators are fast compared to the ones of loads, so we could neglect them and consider the steady state relation (2.2) for compensators and the dynamic model (4.8) for loads. As said before, we instead use the dynamic model (4.8) for all the nodes (loads and compensators); this choice does not affect our results because, setting the time constants very small for compensators ( $\tau_v \approx 0$ ), then:

$$\tau_v \frac{di(v)}{dt} = -i(v) + \frac{\bar{s}(v)}{\bar{u}(v)} \approx 0 \quad \Rightarrow \quad i(v) \approx \frac{\bar{s}(v)}{\bar{u}(v)},$$

which is an approximation of the steady state relation (2.2).

So, the dynamic model proposed for the microgrid is the following:

$$\begin{cases} Lu = i, & \mathbf{1}^T i = 0 \\ u(0) = u_0 \\ \tau_v \frac{di(v)}{dt} = -i(v) + \frac{\bar{s}(v)}{\bar{u}(v)}, & v \in \mathcal{V} \setminus \{0\} \end{cases} \quad (4.9)$$

As the voltages and the currents of the PCC are trivially defined by:

$$u(0) = u_0 \quad i(0) = -\sum_{v \neq 0} i(v),$$

we continue the analysis only for the other nodes.

Let us define the  $N$ -vectors  $U$ ,  $J$  and  $S$ , obtained from  $u$ ,  $i$  and  $s$  respectively, after eliminating the first element (indexed by 0):

$$U = \begin{bmatrix} u(1) \\ \vdots \\ u(N) \end{bmatrix}, \quad J = \begin{bmatrix} i(1) \\ \vdots \\ i(N) \end{bmatrix}, \quad S = \begin{bmatrix} s(1) \\ \vdots \\ s(N) \end{bmatrix}$$

and the matrix  $\mathbf{X}_M$  as the matrix obtained from  $\mathbf{X}$  after eliminating the first row and the first column.

Let be  $\epsilon = \frac{1}{u_0}$ ; by (2.12), the dynamics described by (4.8) can be written as:

$$\tau_v \frac{di(v)}{dt} = h_v(J; \epsilon), \quad v \in \mathcal{V} \setminus \{0\} \quad (4.10)$$

where:

$$h_v(J; \epsilon) = -i(v) + \frac{\bar{s}(v)}{\bar{u}(v)} = -i(v) + \frac{\bar{s}(v)\epsilon}{\epsilon \mathbf{1}_v^T \bar{\mathbf{X}}_M \bar{J} + 1}, \quad v \in \mathcal{V} \setminus \{0\}. \quad (4.11)$$

The model (4.10) is a  $N$ -dimensional nonlinear dynamic system, in which the state of the system corresponds to the currents injected by the nodes, and the coupling between the individual nodes is due to the matrix  $\mathbf{X}_M$  in the denominator. It is a nonlinear input-output relation between power references  $s(v)$  and node voltages  $u(v)$ .

### 4.3.2 Approximate model

The model introduced in the previous paragraph is nonlinear: as it can be very hard working with nonlinear models, we now derive an approximate model by linearization of (4.11).

By using the quadratic Taylor expansion of  $h_v$ 's about the point  $\epsilon = 0$ :

$$h_v(J; \epsilon) \approx h_v(J; 0) + \left. \frac{\partial h_v(J; \epsilon)}{\partial \epsilon} \right|_{\epsilon=0} \epsilon + \frac{1}{2} \left. \frac{\partial^2 h_v(J; \epsilon)}{\partial \epsilon^2} \right|_{\epsilon=0} \epsilon^2 \quad (4.12)$$

where:

$$\begin{aligned} h_v(J; \epsilon)|_{\epsilon=0} &= -i(v) \\ \left. \frac{\partial h_v(J; \epsilon)}{\partial \epsilon} \right|_{\epsilon=0} &= \frac{\bar{s}(v) [\epsilon \mathbf{1}_v^T \bar{\mathbf{X}}_M \bar{J} + 1] - \epsilon \bar{s}(v) \mathbf{1}_v^T \bar{\mathbf{X}}_M \bar{J}}{(\epsilon \mathbf{1}_v^T \bar{\mathbf{X}}_M \bar{J} + 1)^2} \Big|_{\epsilon=0} = \bar{s}(v) \\ \left. \frac{\partial^2 h_v(J; \epsilon)}{\partial \epsilon^2} \right|_{\epsilon=0} &= \frac{-2 \bar{s}(v) (\epsilon \mathbf{1}_v^T \bar{\mathbf{X}}_M \bar{J} + 1) \mathbf{1}_v^T \bar{\mathbf{X}}_M \bar{J}}{(\epsilon \mathbf{1}_v^T \bar{\mathbf{X}}_M \bar{J} + 1)^4} \Big|_{\epsilon=0} \\ &= -2 \bar{s}(v) \mathbf{1}_v^T \bar{\mathbf{X}}_M \bar{J} \end{aligned}$$

Then, by (4.12), the dynamics of each node are approximated with:

$$\tau_v \frac{di(v)}{dt} \approx -i(v) + \epsilon \bar{s}(v) - \epsilon^2 \bar{s}(v) \mathbf{1}_v^T \bar{\mathbf{X}}_M \bar{J}.$$

While the first and the second term depend only on the current and power reference of each node, the third term models the coupling between all the grid nodes via the matrix  $\mathbf{X}_M$ .

Then, the approximate system is the following:

$$T \frac{dJ}{dt} = -J + \epsilon \bar{S} - \epsilon^2 \text{diag}(\bar{S}) \bar{\mathbf{X}}_M \bar{J}$$

### 4.3 Time between consecutive iterations

---

where:

$$T = \begin{bmatrix} \tau_1 & 0 & \cdots & \cdots & 0 \\ 0 & \tau_2 & 0 & \cdots & 0 \\ \vdots & \ddots & \ddots & \ddots & \vdots \\ \vdots & \ddots & \ddots & \ddots & \vdots \\ 0 & \cdots & \cdots & 0 & \tau_N \end{bmatrix}.$$

In order to obtain a linear system in a state-space form, we augment the state and the input, obtaining a  $2N$ -dimensional system:

$$\begin{bmatrix} T & 0 \\ 0 & T \end{bmatrix} \frac{d}{dt} \begin{bmatrix} J \\ \bar{J} \end{bmatrix} = \Gamma \begin{bmatrix} J \\ \bar{J} \end{bmatrix} + \Phi \begin{bmatrix} S \\ \bar{S} \end{bmatrix} \quad (4.13)$$

where

$$\Gamma = \begin{bmatrix} -I & -\epsilon^2 \text{diag}(\bar{S}) \bar{\mathbf{X}}_M \\ -\bar{\epsilon}^2 \text{diag}(S) \mathbf{X}_M & -I \end{bmatrix} \quad \text{and} \quad \Phi = \begin{bmatrix} 0 & \epsilon I \\ \bar{\epsilon} I & 0 \end{bmatrix}.$$

This system is a linear, time-varying system, as the input  $S$  is also present in the state update matrix  $\Gamma$ . However, if we assume that power references change slowly compared to the transient of the system, then we can assume that  $\text{diag}(\bar{S})$  is a constant matrix and (4.13) becomes a linear, time-invariant system.

It is worth noticing that the proposed approximate model (4.13) explicitly presents the network topology (matrix  $\mathbf{X}_M$ ) and the power demands (vector  $S$ ): it allows to understand how these parameters affect the dynamic behaviour of the model.

#### 4.3.3 Eigenvalue analysis

In the previous paragraph we have built the dynamic model described by (4.13): it is an approximate version of the exact model (4.9).

In Section 7.3, we will show how the model (4.13) approximates well the behaviour of the original nonlinear system.

Owing to this characteristic, we will use the approximate model: being a linear system, we are able to study its dynamic behaviour by using the classical tools of linear systems, for example the eigenvalue analysis.

It can be shown that the eigenvalues of the state update matrix  $\Gamma$  can be approximated, for small values of  $\epsilon$  as:

$$\Lambda(\Gamma) = \left\{ -\frac{1}{\tau_v} \pm \frac{|\epsilon| |s(v)| |\mathbf{X}_M]_{vv}|}{\tau_v} \right\}. \quad (4.14)$$

Expression (4.14) shows that eigenvalues of the system depend on the time constant of each node  $v$ , its power demand and the element of the matrix  $\mathbf{X}_M$  in position  $(v, v)$ .

If the dominant eigenvalue of the system were much larger than all the others, than a simple expression for the settling time could be given by:

$$t_s \approx -\frac{3}{p},$$

where  $p$  is the position of the dominant eigenvalue.

Nevertheless, this expression for the settling time does not hold in general. What we can say is that the settling time of a system of large order is a function of the dominant eigenvalue, together with other many factors (eigenvalues, eigenvectors and initial state).

A possible approach to obtain a formula for the settling time could be the use of reduced-order system.

However, by the positions of the dominant eigenvalues, we can have an idea of the possible settling time of the system (see simulations in Chapter 7).

Then, when we know the settling time of the system (i.e. the time  $\Delta t$  in order that the system reaches a new steady state value after changing the commanded reactive power at the compensators), we can conclude that the interval time between consecutive iterations of the algorithm must be larger than the settling time  $\Delta t$ .



# Analysis of the algorithm

---

In this chapter we will show that the algorithm introduced in the previous chapter has good convergence characteristics: we will give a sufficient and necessary condition (related to the communication constraints among the compensators) for the convergence to the optimal solution of the minimization problem (3.4).

Then, we will study the speed of convergence of the algorithm, obtaining a convenient upper bound for the rate of convergence.

Before discussing about the convergence results, a new set of matrices is introduced; it will be useful in the rest of the thesis.

## 5.1 Matrix $\Omega_i$ and its properties

Define the  $N_C \times N_C$  matrices

$$\Omega_i = I_{\mathcal{C}_i} - \frac{1}{|\mathcal{C}_i|} \mathbf{1}_{\mathcal{C}_i} \mathbf{1}_{\mathcal{C}_i}^T \quad 1 \leq i \leq \ell, \quad (5.1)$$

where  $|\mathcal{C}_i|$  is the cardinality of the set  $\mathcal{C}_i$  and  $I_{\mathcal{C}_i}$  is the diagonal matrix having diagonal entries 1 in positions belonging to  $\mathcal{C}_i$  and zero elsewhere.

It is easy to verify that the set of matrices  $\Omega_i$ , defined in (5.1) can be also expressed as:

$$\Omega_i = \frac{1}{2|\mathcal{C}_i|} \sum_{h,k \in \mathcal{C}_i} (\mathbf{1}_h - \mathbf{1}_k)(\mathbf{1}_h - \mathbf{1}_k)^T \quad (5.2)$$

**Proposition 7.** *The matrix  $\Omega_i$  is a symmetric projector, i.e. it satisfies the following properties:*

1. *simmetry:*  $\Omega_i = \Omega_i^T$ ;

2. *idempotency*:  $\Omega_i = \Omega_i^2$

The two previous properties are easily proved by applying the definition (5.1).

It is possible to state another property of  $\Omega_i$ , related to its Moore-Penrose generalized inverse (Section C.1 in Appendix C):

$$\Omega_i = \Omega_i^\sharp.$$

In fact, by using the properties of the matrix  $\Omega_i$  and the properties of the generalized inverse of a matrix (Definition 30), we can state that:

$$\begin{aligned} \Omega_i^\sharp &= \Omega_i^\sharp \Omega_i \Omega_i^\sharp \\ &= \left( \Omega_i^\sharp \Omega_i \right) \Omega_i \left( \Omega_i \Omega_i^\sharp \right) \\ &= \left( \Omega_i^\sharp \Omega_i \right)^T \Omega_i \left( \Omega_i \Omega_i^\sharp \right)^T \\ &= \Omega_i \left( \Omega_i^\sharp \Omega_i \Omega_i^\sharp \right) \Omega_i \\ &= \Omega_i \Omega_i^\sharp \Omega_i = \Omega_i \end{aligned}$$

where we have used also the fact that:  $\left( \Omega_i^\sharp \right)^T = \left( \Omega_i^T \right)^\sharp$ .

The following proposition state some properties of the matrix  $(\Omega_i M \Omega_i)$  and its pseudoinverse, which will appear in the following.

**Proposition 8.** *Let be  $\Omega_i$  the matrix defined in (5.1) and  $M \in \mathbb{R}^{N_c \times N_c}$  a symmetric positive definite matrix; it holds:*

1.  $\ker(\Omega_i M \Omega_i)^\sharp = \ker(\Omega_i M \Omega_i)$        $\text{Im}(\Omega_i M \Omega_i)^\sharp = \text{Im}(\Omega_i M \Omega_i)$
2.  $\ker(\Omega_i M \Omega_i) = \ker \Omega_i$
3.  $(\Omega_i M \Omega_i)^\sharp = (\Omega_i M \Omega_i)^\sharp \Omega_i = \Omega_i (\Omega_i M \Omega_i)^\sharp$

*Proof.* Let show separately the three properties:

1. From Proposition (C.2), it results that:

$$\ker(K^\sharp) = \ker(K^T) \quad \text{Im}(K^\sharp) = \text{Im } K \quad \forall K. \quad (5.3)$$

In particular, (5.3) holds for  $K = (\Omega_i M \Omega_i) = (\Omega_i M \Omega_i)^T$ .

2. It easy to show that if  $y \in \ker \Omega_i$ , then it also holds:  $y \in \ker(\Omega_i M \Omega_i)$ .

Vice versa, if  $y \in \ker(\Omega_i M \Omega_i)$ , then:  $y^T (\Omega_i M \Omega_i y) = 0$ .

By defining:  $\tilde{y} = \Omega_i y$ , as  $M > 0$ , it results:

$$\tilde{y}^T M \tilde{y} = 0 \quad \Leftrightarrow \quad \tilde{y} = \Omega_i y = 0.$$

## 5.2 Convergence results

---

3. We will show that:

$$(\Omega_i M \Omega_i)^\sharp y = (\Omega_i M \Omega_i)^\sharp \Omega_i y \quad \forall y \in \mathbb{C}^{N_c}$$

The vector  $y$  can be written as the sum of a vector in the subspace  $\ker \Omega_i$  of  $\mathbb{C}^{N_c}$  and a vector in its orthogonal complement  $\ker \Omega_i^\perp = \text{Im } \Omega_i$ :

$$y = \alpha \mathbf{1}_{\mathcal{C}_i} + \Omega_i y;$$

so:

$$\begin{aligned} (\Omega_i M \Omega_i)^\sharp y &= (\Omega_i M \Omega_i)^\sharp (\alpha \mathbf{1}_{\mathcal{C}_i} + \Omega_i y) \\ &= (\Omega_i M \Omega_i)^\sharp \Omega_i y \end{aligned}$$

where we have exploited the fact that, according to the previous properties:

$$\mathbf{1}_{\mathcal{C}_i} \in \ker \Omega_i = \ker(\Omega_i M \Omega_i) = \ker(\Omega_i M \Omega_i)^\sharp$$

□

## 5.2 Convergence results

In this section we analyze the algorithm proposed in Section 4.1.

We give a condition for the convergence of the algorithm to the optimal solution of the convex problem (3.4), whose existence is guaranteed by the fact that the problem is quadratic.

We also show that the condition for the convergence corresponds to a requirement on the clusters  $\mathcal{C}_i$ ,  $i = 1, \dots, \ell$ .

For this purpose we give a more general definition of graph.

**Definition 9.** An hypergraph  $\mathcal{H}$  is a pair  $(\mathcal{V}, \mathcal{E})$  in which edges (*hyperedges*) are subsets of  $\mathcal{V}$  of arbitrary cardinality.

By Definition 9, the subset  $\mathcal{C}_i$ ,  $i = 1, \dots, \ell$  introduced in Section 4.1 can be interpreted as the edges of a hypergraph defined over the set of nodes  $\mathcal{C}$ .

### 5.2.1 Equivalent optimization problem

In this paragraph we introduce an equivalent optimization problem which allows to express the solution of the subproblems as a linear system.

Let define a variable  $x = q_{\mathcal{C}} - q_{\mathcal{C}}^{\text{opt}} \in \mathbb{R}^{N_c}$ , where  $q_{\mathcal{C}}^{\text{opt}}$  is the solution of the optimization problem (3.4).

**Proposition 10.** *The optimization problem (3.4) with cost function (3.7) is equivalent to:*

$$\begin{aligned} \min_x \quad & V(x) = x^T M x \\ \text{subject to} \quad & \mathbf{1}^T x = 0, \end{aligned} \quad (5.4)$$

where  $M = \frac{\cos \theta}{|u_0|^2} X_{CC} > 0$ .

*Proof.* Consider the problem (3.4). As to the constraint, by substituting  $q_C = x + q_C^{\text{opt}}$ :

$$\begin{aligned} \mathbf{1}^T q_C &= \mathbf{1}^T (x + q_C^{\text{opt}}) \\ &= \mathbf{1}^T x - \mathbf{1}^T q_{\bar{C}}, \end{aligned} \quad (5.5)$$

where we have used the fact that the constraint is satisfied by the optimal solution.

Comparing (5.5) and the constraint in (3.4), it results:

$$\mathbf{1}^T x = 0. \quad (5.6)$$

Then, by expressing the cost function (3.7) as a function of  $x$  and defining  $m = \frac{2 \cos \theta}{|u_0|^2} X_{C\bar{C}} q_{\bar{C}}$ :

$$\begin{aligned} J(q_C) &= q_C^T M q_C + m^T q_C \\ &= (x + q_C^{\text{opt}})^T M (x + q_C^{\text{opt}}) + m^T (x + q_C^{\text{opt}}) \\ &= x^T M x + (q_C^{\text{opt}})^T M q_C^{\text{opt}} + x^T M q_C^{\text{opt}} + (q_C^{\text{opt}})^T M x + m^T x + m^T q_C^{\text{opt}}. \end{aligned}$$

As the cost function has to be minimize with respect to  $x$ , we neglect the terms independent by  $x$ ; it means that minimizing  $J(q_C)$  is equivalent to minimize:

$$\begin{aligned} V(x) &= x^T M x + x^T (2M q_C^{\text{opt}} + m) \\ &= x^T M x + x^T \nabla J(q_C^{\text{opt}}) \\ &= x^T M x + \gamma x^T \mathbf{1} = x^T M x \end{aligned} \quad (5.7)$$

where we have used (5.6) and the fact that  $\nabla J(q_C^{\text{opt}}) = \gamma \mathbf{1}$  according to (4.6).

From (5.7) and (5.6), we can conclude that the optimization problem (3.4) with cost function (3.7) is equivalent to (5.4).  $\square$

The formulation (5.4) of the optimization problem implies that the subproblems described in the Section 4.1 are equivalent to the subproblems:

$$\begin{aligned} \min_{\Delta x} \quad & V(x + \Delta x) \\ \text{subject to} \quad & \Delta x \in \text{Im } \Omega_i. \end{aligned} \quad (5.8)$$

being:  $\mathcal{S}_i = \text{Im } \Omega_i$ .

## 5.2 Convergence results

---

**Proposition 11.** *Consider the optimization subproblem (5.8). It is possible to express its solution as a linear time-varying system (corresponding to the system (4.7)), described by:*

$$x(t+1) = F_{\eta(t)}x(t), \quad F_{\eta(t)} = I - (\Omega_{\eta(t)}M\Omega_{\eta(t)})^\sharp M \in \mathbb{R}^{N_c \times N_c}. \quad (5.9)$$

*Proof.* For the sake of clarity, let assume that at the instant  $t$  we are considering  $\eta(t) = i$ , i.e. the cluster we are considering is  $\mathcal{C}_i$ .

In order to show that  $x(t+1) = F_i x(t)$  is a solution of the subproblem (5.8) (i.e. it is a constrained optimal point for the subproblem), we have to verify two properties, similarly to what done in the proof of Proposition 6:

- the constraint is satisfied:

$$\begin{aligned} \mathbf{1}^T x(t+1) &= \mathbf{1}^T \left[ I - (\Omega_i M \Omega_i)^\sharp M \right] x(t) \\ &= \mathbf{1}^T x(t) - \mathbf{1}^T (\Omega_i M \Omega_i)^\sharp M x(t) \\ &= \mathbf{1}^T x(t) - \mathbf{1}^T \Omega_i (\Omega_i M \Omega_i)^\sharp M x(t) = 0 \end{aligned}$$

where we have used the third property in Proposition 8, the constraint (5.6) (holding for  $x(t)$ ) and the fact that  $\mathbf{1} \in \ker \Omega_i$ .

- the gradient is orthogonal to the constraint:

$$\begin{aligned} \Omega_i [2Mx(t+1)] &= 2\Omega_i M F_i x(t) \\ &= 2\Omega_i M \left[ I - (\Omega_i M \Omega_i)^\sharp M \right] x(t) \\ &= 2\Omega_i M x(t) - 2\Omega_i M \Omega_i (\Omega_i M \Omega_i)^\sharp \Omega_i M x(t) \end{aligned} \quad (5.10)$$

where the results in Proposition 8 have been used.

As:

$$\Omega_i M x(t) \in \text{Im } \Omega_i = \text{Im}(\Omega_i M \Omega_i) \quad \Rightarrow \quad \exists w \mid \Omega_i M x(t) = \Omega_i M \Omega_i w$$

then:

$$\begin{aligned} \Omega_i M \Omega_i (\Omega_i M \Omega_i)^\sharp \Omega_i M x(t) &= \Omega_i M \Omega_i (\Omega_i M \Omega_i)^\sharp (\Omega_i M \Omega_i w) \\ &= \Omega_i M \Omega_i w = \Omega_i M x(t) \end{aligned} \quad (5.11)$$

where we have used the properties of the generalized inverse in Definition 30.

By substituting (5.11) into (5.10), it results:

$$\Omega_i [2Mx(t+1)] = 0.$$

□

The matrices  $F_i$ ,  $i = 1, \dots, \ell$  satisfy the following properties:

- they are projection operators:

$$\begin{aligned}
 F_i^2 &= \left[ I - (\Omega_i M \Omega_i)^\# M \right] \left[ I - (\Omega_i M \Omega_i)^\# M \right] \\
 &= I - 2(\Omega_i M \Omega_i)^\# M + (\Omega_i M \Omega_i)^\# M (\Omega_i M \Omega_i)^\# M \\
 &= I - 2(\Omega_i M \Omega_i)^\# M + (\Omega_i M \Omega_i)^\# \Omega_i M \Omega_i (\Omega_i M \Omega_i)^\# M \\
 &= I - 2(\Omega_i M \Omega_i)^\# M + (\Omega_i M \Omega_i)^\# M \\
 &= I - (\Omega_i M \Omega_i)^\# M = F_i
 \end{aligned}$$

where we have used the properties of the generalized inverse in Definition 30.

- they are orthogonal projections with respect to the inner product  $\langle \cdot, \cdot \rangle_M$  defined as  $\langle x, y \rangle_M := x^T M y$ ; in other words:

$$\begin{aligned}
 \langle F_i x, F_i x - x \rangle_M &= x^T F_i^T M (F_i x - x) \\
 &= -x^T M (\Omega_i M \Omega_i)^\# M x + x^T M (\Omega_i M \Omega_i)^\# \Omega_i M \Omega_i (\Omega_i M \Omega_i)^\# M x \\
 &= -x^T M (\Omega_i M \Omega_i)^\# M x + x^T M (\Omega_i M \Omega_i)^\# M x = 0
 \end{aligned}$$

- they are self-adjoint matrices with respect to the inner product  $\langle \cdot, \cdot \rangle_M$ , i.e.:

$$u^T F_i^T M v = u^T M F_i v \quad \forall u, v;$$

owing to:  $F_i^T M = M F_i$ ; it follows that  $F_i$ 's have real eigenvalues.

## 5.2.2 Necessary condition for the convergence of the algorithm

The following result characterizes the uniqueness of the equilibrium for all maps  $F_i x$ .

**Lemma 12.** *Consider the family of linear transformations  $\{F_i\}$  as described in (5.9). Consider the set of the points in  $\ker \mathbf{1}^T$ , which are invariant for all  $F_i$ 's:*

$$\mathcal{W} = \{x \in \ker \mathbf{1}^T \mid F_i x = x, \forall i = 1, \dots, \ell\}.$$

Then:

$$\mathcal{W} = \{\bar{x} = \mathbf{0}\} \Leftrightarrow \text{Im}[\Omega_1 \dots \Omega_\ell] = \ker \mathbf{1}^T.$$

*Proof.* Let us prove the reverse implication first. Let consider an arbitrary point  $x \in \mathcal{W}$ ; as  $\mathcal{W}$  is a subset of  $\ker \mathbf{1}^T$ :

$$\text{Im}[\Omega_1 \dots \Omega_\ell] = \ker \mathbf{1}^T \Rightarrow x = \sum_i \Omega_i y_i. \quad (5.12)$$

Moreover, as in  $\mathcal{W}$  it holds:  $F_i x = x$  for all  $i$ , then:

$$\begin{aligned}
 \Omega_i M x &= \Omega_i M F_i x \\
 &= \Omega_i M \left[ I - (\Omega_i M \Omega_i)^\# M \right] x \\
 &= \Omega_i M x - \Omega_i M \Omega_i (\Omega_i M \Omega_i)^\# \Omega_i M x = 0
 \end{aligned} \quad (5.13)$$

## 5.2 Convergence results

---

where, in the last equation, we have done similarly to (5.11); so it results:  $Mx \in \ker \Omega_i$ . Since  $M$  is positive definite, we can conclude:

$$x^T Mx = \sum_i y_i^T \Omega_i Mx = 0 \quad \Leftrightarrow \quad x = \bar{x} = \mathbf{0}.$$

Suppose conversely that

$$\ker H^T = \{\bar{x} = \mathbf{0}\} \quad \text{with} \quad H^T = \begin{bmatrix} \mathbf{1}^T \\ I - F_1 \\ \vdots \\ I - F_\ell \end{bmatrix}. \quad (5.14)$$

From equation (5.14), it results that  $\ker H^T$  contains only the vector  $\mathbf{0}$  and it implies that  $H^T$  is a full rank matrix. By a theorem from Linear Algebra,  $H$  is a full rank matrix if and only if the linear system  $Hy = b$  has one and only solution  $y$ , for any given  $b$ .

In particular, choosing  $b = M\bar{x}$ , there exists a vector  $y$  such that:

$$\begin{aligned} b &= M\bar{x} = Hy \\ &= \mathbf{1}y_0 + \sum_{i=1}^{\ell} (I - F_i)^T y_i \\ &= \mathbf{1}y_0 + \sum_{i=1}^{\ell} M(\Omega_i M \Omega_i)^{\sharp} y_i \end{aligned}$$

Then:

$$\bar{x} = M^{-1} \mathbf{1}y_0 + \sum_{i=1}^{\ell} (\Omega_i M \Omega_i)^{\sharp} y_i$$

As  $\mathbf{1}^T \bar{x} = y_0 \mathbf{1}^T M^{-1} \mathbf{1}$  and  $M^{-1}$  is positive definite, then  $y_0 = 0$  and so  $\bar{x} \in \text{Im}[\Omega_1 \dots \Omega_\ell]$ . The converse inclusion is trivial: if  $\bar{x} \in \text{Im}[\Omega_1 \dots \Omega_\ell]$ , (5.12) holds. Then:

$$\mathbf{1}^T \bar{x} = \sum_i \mathbf{1}^T \Omega_i y_i = 0 \quad \Rightarrow \quad \bar{x} \in \ker \mathbf{1}^T.$$

□

The condition expressed in Lemma 12 corresponds to a necessary condition for the convergence of the algorithm, and can be also expressed as a connectivity requirement on the hypergraph  $\mathcal{H}$ .

**Proposition 13.** *The condition  $\text{Im}[\Omega_1 \dots \Omega_\ell] = \ker \mathbf{1}^T$ , which is a necessary condition for the convergence of algorithm (4.7) to the solution  $q_{\mathcal{C}}^{\text{opt}}$  of the optimization problem (3.4), holds if and only if the hypergraph  $\mathcal{H}$  is connected.*

*Proof.* Consider the undirected graph  $\mathcal{G}_{\mathcal{H}}$ , defined as a weighted graph having the compensators (nodes of set  $\mathcal{C}$ ) as nodes and weights on the edge  $\{h, k\}$  equal to the number of the sets  $\mathcal{C}_i$  which contain both  $h$  and  $k$ .

It is quite easy to see that the hypergraph  $\mathcal{H}$  with edges  $\mathcal{C}_i$  is connected if and only if  $\mathcal{G}_{\mathcal{H}}$  is a connected graph.

Let us define  $\delta_{\mathcal{C}_i} : \mathcal{C} \rightarrow \{0, 1\}$  as the characteristic function of the set  $\mathcal{C}_i$ , namely a function of the nodes that is 1 when the node belongs to  $\mathcal{C}_i$  and is zero otherwise. Consider then the Laplacian matrix  $L_{\mathcal{H}}$  of  $\mathcal{G}_{\mathcal{H}}$ :

$$\begin{aligned} L_{\mathcal{H}} &= \sum_{h,k \in \mathcal{C}_i} (\mathbf{1}_h - \mathbf{1}_k)(\mathbf{1}_h - \mathbf{1}_k)^T \sum_{i=1}^{\ell} \delta_{\mathcal{C}_i}(h) \delta_{\mathcal{C}_i}(k) \\ &= \sum_{i=1}^{\ell} \sum_{h,k \in \mathcal{C}_i} (\mathbf{1}_h - \mathbf{1}_k)(\mathbf{1}_h - \mathbf{1}_k)^T = \sum_i 2|\mathcal{C}_i| \Omega_i \\ &= [\Omega_1 \dots \Omega_{\ell}] \text{diag}\{2|\mathcal{C}_1|I, \dots, 2|\mathcal{C}_{\ell}|I\} [\Omega_1 \dots \Omega_{\ell}]^T. \end{aligned}$$

The condition  $\text{Im}[\Omega_1 \dots \Omega_{\ell}] = \ker \mathbf{1}^T$  is equivalent to the fact that  $L_{\mathcal{H}} + \mathbf{1}\mathbf{1}^T$  is positive definite; this is a characterization of connectivity of  $\mathcal{G}_{\mathcal{H}}$ , i.e.:

$$\begin{cases} L_{\mathcal{H}} \mathbf{1} = 0 \\ L_{\mathcal{H}} y \neq 0 \quad \forall y = \alpha \mathbf{1} + y_{\perp} \end{cases}$$

In fact:

- $L_{\mathcal{H}} + \mathbf{1}\mathbf{1}^T > 0 \quad \Rightarrow \quad y^T (L_{\mathcal{H}} + \mathbf{1}\mathbf{1}^T) y > 0, \quad \forall y.$

In particular, it holds for:  $y = \alpha \mathbf{1} + y_{\perp}$ ; so:

$$\begin{aligned} y^T (L_{\mathcal{H}} + \mathbf{1}\mathbf{1}^T) y &= y^T L_{\mathcal{H}} y + (\alpha \mathbf{1}^T + y_{\perp}^T) \mathbf{1} \mathbf{1}^T (\alpha \mathbf{1} + y_{\perp}) \\ &= y^T L_{\mathcal{H}} y + \alpha^2 N^2 > 0 \end{aligned}$$

As  $L_{\mathcal{H}} \geq 0$ , this relationship holds if and only if  $L_{\mathcal{H}} y \neq 0$  (Proposition 32).

- Vice versa:  $L_{\mathcal{H}} y \neq 0 \quad \forall y = \alpha \mathbf{1} + y_{\perp} \quad \Rightarrow \quad y^T L_{\mathcal{H}} y > 0.$

The hypothesis  $L_{\mathcal{H}} y \neq 0$  implies that also:

$$y^T L_{\mathcal{H}} y + y^T \mathbf{1} \mathbf{1}^T y = y^T (L_{\mathcal{H}} + \mathbf{1}\mathbf{1}^T) y > 0.$$

□

## 5.3 Bound on the rate of convergence

For the study of the rate of convergence of the proposed algorithm, we introduce the following assumption of the random sequence  $\eta(t)$ .



### 5.3 Bound on the rate of convergence

---

**Assumption 14.** *The sequence  $\eta(t)$  is a sequence of independently, uniformly distributed symbols in  $\{1, \dots, \ell\}$ .*

We consider the following performance metric:

$$R = \sup_{x(0) \in \ker \mathbf{1}^T} \limsup v(t)^{1/t}$$

where  $v(t) = \mathbb{E} [V(x(t))]$ .  $R$  describes the exponential rate of convergence to zero of  $v(t)$  and so also the exponential rate of convergence of  $q_C(t)$  to the optimal solution  $q_C^{\text{opt}}$ .

Let define the matrix

$$\Omega = I - \frac{\mathbf{1}\mathbf{1}^T}{N}; \quad (5.15)$$

observing that  $\Omega x(t) = x(t)$  and using (5.9):

$$\begin{aligned} v(t) &= \mathbb{E} [x(t)^T M x(t)] \\ &= \mathbb{E} [x(t)^T \Omega M \Omega x(t)] \\ &= \mathbb{E} [x(t-1)^T F_{\eta(t-1)}^T \Omega M \Omega F_{\eta(t-1)} x(t-1)] \\ &= x(0)^T \mathbb{E} [F_{\eta(0)}^T \cdots F_{\eta(t-1)}^T \Omega M \Omega F_{\eta(t-1)} \cdots F_{\eta(0)}] x(0). \end{aligned}$$

Let us then define

$$\Delta(\tau) = \mathbb{E} [F_{\eta(t-\tau)}^T \cdots F_{\eta(t-1)}^T \Omega M \Omega F_{\eta(t-1)} \cdots F_{\eta(t-\tau)}].$$

Via Assumption 14, the sequence  $\eta(\tau)$  is a sequence of independent symbols and so we can derive the following linear system:

$$\begin{aligned} \Delta(\tau+1) &= \mathbb{E} [F^T \Delta(\tau) F] = \mathcal{L}(\Delta(\tau)), & \Delta(0) &= \Omega M \Omega \\ \Xi(\tau) &= \Omega \Delta(\tau) \Omega. \end{aligned} \quad (5.16)$$

whose state is the matrix  $\Delta$ .

It is worth noticing that the expected cost function can now be expressed as

$$v(t) = \mathbb{E} [V(x(t))] = \mathbb{E} [x(t)^T \Omega M \Omega x(t)] = x(0)^T \Xi(t) x(0). \quad (5.17)$$

Being a linear system, the analysis of convergence of the system (5.16) (and so, by (5.17), also of the algorithm (5.9)) is studied by eigenvalues and eigenvectors.

We define the function

$$\lambda_{\mathcal{L}}(i) : \{1, \dots, N_C^2\} \rightarrow \mathbb{R}$$

that returns the  $i$ -th eigenvalue of  $\mathcal{L}$ ; we assume that it is monotonically non increasing.

We can represent this map as a  $N_C^2$ -vector

$$\Lambda(\mathcal{L}) = [\lambda_{\mathcal{L}}(1) \cdots \lambda_{\mathcal{L}}(N_C^2)]^T \quad \text{with} \quad \lambda_{\mathcal{L}}(i) \geq \lambda_{\mathcal{L}}(i+1) \quad \forall i$$

where repetitions are possible.

Moreover, let be  $\Delta_{\mathcal{L}}(i)$  an eigenvector (but it is a matrix) associated with the eigenvalue  $\lambda_{\mathcal{L}}(i)$ :

$$\mathcal{L}(\Delta_{\mathcal{L}}(i)) = \lambda_{\mathcal{L}}(i)\Delta_{\mathcal{L}}(i).$$

In order to simplify the study of the system (5.16), we translate it into a classical system whose state is a vector. It is possible by introducing a vector  $\delta(\tau) = \text{vec}(\Delta(\tau))$  and a  $(N_{\mathcal{C}}^2 \times N_{\mathcal{C}}^2)$ -matrix  $\mathbf{F}$  associated with the linear transformation  $\mathcal{L}$ :

$$\mathbf{F} = \mathbb{E} [F^T \otimes F^T]$$

where symbol  $\otimes$  denotes the *Kronecker product* (see Appendix B for definition and properties of this operator).

Then, the system (5.16) is equivalent to the following:

$$\delta(\tau + 1) = \mathbf{F}\delta(\tau). \quad (5.18)$$

By using the properties of the Kronecker product (Proposition 27) and the fact that  $F_i M^{-1} = M^{-1} F_i^T$ , it results:

$$\begin{aligned} \mathbf{F}^T(M^{-1} \otimes M^{-1}) &= \mathbb{E} [(F \otimes F)(M^{-1} \otimes M^{-1})] \\ &= \mathbb{E} [(FM^{-1}) \otimes (FM^{-1})] \\ &= \mathbb{E} [(M^{-1}F^T) \otimes (M^{-1}F^T)] \\ &= \mathbb{E} [(M^{-1} \otimes M^{-1})(F^T \otimes F^T)] \\ &= (M^{-1} \otimes M^{-1})\mathbf{F} \end{aligned}$$

and it allows to say that  $\mathbf{F}$  is self-adjoint with respect to the inner product  $\langle \cdot, \cdot \rangle_{M^{-1} \otimes M^{-1}}$ , and therefore it has real eigenvalues.

Moreover:

$$\mathbf{F} \delta_{\mathbf{F}}(i) = \lambda_{\mathbf{F}}(i) \delta_{\mathbf{F}}(i),$$

where  $\lambda_{\mathbf{F}}(i) = \lambda_{\mathcal{L}}(i) \in \mathbb{R}$  and  $\delta_{\mathbf{F}}(i) = \text{vec}(\Delta_{\mathcal{L}}(i))$ ,  $i = 1, \dots, N_{\mathcal{C}}^2$ .

By decomposing  $\Omega M \Omega$  into  $\sum_i \alpha_i \Delta_{\mathcal{L}}(i)$ , we can then express the convergence rate  $R$  as:

$$R = \max \{ |\lambda_{\mathcal{L}}(i)| \mid \alpha_i \neq 0, \Delta_{\mathcal{L}}(i) \notin \mathcal{O} \}, \quad (5.19)$$

i.e. the largest eigenvalue of  $\mathbf{F}$ , which is reachable from  $\Delta(0)$  and whose related eigenvector is observable, being the *non-observable space* for the system (5.16)

$$\mathcal{O} = \{ \Delta \in \mathbb{R}^{N_{\mathcal{C}} \times N_{\mathcal{C}}} \mid \Omega \Delta \Omega = 0 \}. \quad (5.20)$$

The following proposition proves a result which guarantees the convergence of the algorithm (5.9).

**Proposition 15.** *Let  $\text{Im}[\Omega_1 \cdots \Omega_{\ell}] = \ker \mathbf{1}^T$ . Then  $R < 1$ .*

### 5.3 Bound on the rate of convergence

*Proof.* Let define the linear transformation  $\mathcal{L}_i(\Delta) = F_i^T \Delta F_i$ . The  $N_{\mathcal{L}}^2$  eigenvalues of  $\mathcal{L}_i$  are the eigenvalues of  $F_i^T \otimes F_i^T$  and they belong to set  $\{0, 1\}$ , as follows from the property about the eigenvalues of the Kronecker product (Proposition 28).

As, for the 2-norm of each matrix equals its largest eigenvalue:

$$\max\{\lambda_{\mathcal{L}}(i)\} = \|\mathbf{F}\| = \|\mathbb{E}[F^T \otimes F^T]\| \leq \mathbb{E}[\|F^T \otimes F^T\|] = 1, \quad (5.21)$$

being  $\|F_i^T \otimes F_i^T\| = \max\{\lambda_{F_i^T \otimes F_i^T}\} = 1$ .

Consider the eigenvalue  $\lambda_{\mathcal{L}}(i)$  such that  $|\lambda_{\mathcal{L}}(i)| = 1$  and let be  $y = \delta_{\mathbf{F}}(i)$  the corresponding eigenvector of  $\mathbf{F}$ ; we have:

$$\|y\| = \|\mathbf{F}y\| \leq \|\mathbf{F}\| \cdot \|y\| = \|\mathbb{E}[F^T \otimes F^T]\| \cdot \|y\| \leq \mathbb{E}[\|F^T \otimes F^T\|] \cdot \|y\| = \|y\|, \quad (5.22)$$

where we have exploited (5.21) in the last passage.

It follows that the relations in (5.22) must hold as equalities and so:

$$\|y\| = \|\mathbf{F}y\| = \mathbb{E}[\|F^T \otimes F^T\|] \cdot \|y\| = \|F_i^T \otimes F_i^T\| \cdot \|y\|, \quad \forall i.$$

The matrix  $F_i^T \otimes F_i^T$  is a projector and so:

$$\|F_i^T \otimes F_i^T\| \Rightarrow F_i^T \otimes F_i^T, \quad \forall i.$$

As said before,  $F_i^T \otimes F_i^T$  has only 0 and 1 as eigenvalues and  $v_h^{(i)} \otimes v_k^{(i)}$  as eigenvectors ( $v_h^{(i)}$  and  $v_k^{(i)}$  are right eigenvectors of  $F_i^T$ ). Therefore:

$$y = v_h \otimes v_k \quad \text{with} \quad \Omega_i^T v_h = \Omega_i^T v_k = 0, \quad \forall i.$$

As:

$$\text{Im}[\Omega_1 \cdots \Omega_\ell] = \ker \mathbf{1}^T \Rightarrow \bigcap_i \ker \Omega_i^T = \text{Im} \mathbf{1},$$

we have  $v_h = v_k = \mathbf{1}$  and therefore the only eigenvector of  $\mathcal{L}$  corresponding to an eigenvalue of norm 1 is  $\Delta_{\mathcal{L}}(1) = \mathbf{1} \otimes \mathbf{1} = \mathbf{1}\mathbf{1}^T$ . As  $\Omega\mathbf{1}\mathbf{1}^T\Omega = 0$ , the eigenvector  $\mathbf{1}\mathbf{1}^T$  is not observable and, according to definition of  $R$  in (5.19), we can conclude that  $R < 1$ .  $\square$

Proposition 15 states that all the eigenvalues of interest (the reachable and observable ones) of  $\mathcal{L}$  are inside the unitary circle. This guarantees the asymptotic stability (and, in particular, the convergence) of the dynamics of (5.16). Then, by (5.17):

$$\mathbb{E}[V(x(t))] = \mathbb{E}[x(t)^T M x(t)] \rightarrow 0$$

and, as  $M > 0$ , it results the convergence in variance of  $x(t)$  to zero.

By Proposition 13, Lemma 12 and Proposition 15, we can conclude that the proposed algorithm (4.7) is guaranteed to converge to the optimal solution  $q_{\mathcal{C}}^{\text{opt}}$  of the optimization problem (3.4), under the (reasonable) assumption that each clusters has (at least) a node in common with another cluster.

Computing  $R$  as defined in (5.19) is in general not simple.

In the following, we will derive an upper bound for  $R$  that can be computed from  $\bar{F} = \mathbb{E}[F]$ . In order to prove them, we state three lemmas.

**Lemma 16.** *Let  $P, Q \in \mathbb{R}^{N_C \times N_C}$  and  $P \geq Q$ . Then  $\mathcal{L}^k(P) \geq \mathcal{L}^k(Q)$  for all  $k \in \mathbb{N} \cup \{0\}$ .*

*Proof.* From the definition of  $\mathcal{L}$  in (5.16), we have

$$\begin{aligned} x^T [\mathcal{L}(P) - \mathcal{L}(Q)] x &= x^T [\mathbb{E}[F^T P F] - \mathbb{E}[F^T Q F]] x \\ &= \mathbb{E}[x^T F^T (P - Q) F x] \geq 0. \end{aligned}$$

By iterating these steps  $k$  times we then obtain  $\mathcal{L}^k(M) \geq \mathcal{L}^k(N)$ .  $\square$

**Lemma 17.**

$$\Omega \mathcal{L}^t(\Omega \Delta \Omega) \Omega = \Omega \mathcal{L}^t(\Delta) \Omega, \quad \forall \Delta.$$

*Proof.* Proof is by induction:

- *Base case:* we have to show that the statement holds for  $t = 0$ :

$$\Omega \mathcal{L}^0(\Omega \Delta \Omega) \Omega = \Omega^2 = \Omega.$$

- *Inductive step:* we have to show that, if the statement holds for some  $t$  (*inductive hypothesis*), then the statement also holds when  $t + 1$  is substituted for  $t$ :

$$\begin{aligned} \Omega \mathcal{L}^{t+1}(\Delta) \Omega &= \Omega \mathcal{L}(\mathcal{L}^t(\Delta)) \Omega \\ &= \Omega \mathcal{L}(\Omega \mathcal{L}^t(\Delta) \Omega) \Omega \\ &= \Omega \mathcal{L}(\Omega \mathcal{L}^t(\Omega \Delta \Omega) \Omega) \Omega \\ &= \Omega \mathcal{L}(\mathcal{L}^t(\Omega \Delta \Omega)) \Omega \\ &= \Omega \mathcal{L}^{t+1}(\Omega \Delta \Omega) \Omega. \end{aligned}$$

$\square$

**Lemma 18.** *Let  $\bar{F} = \mathbb{E}[F]$ . If  $\text{Im}[\Omega_1 \cdots \Omega_\ell] = \ker \mathbf{1}^T$ , then all the eigenvalues of  $\bar{F}$  have absolute value not larger than 1, and its only eigenvalue on the unitary circle is  $\lambda = 1$ , with associated left eigenvector  $\mathbf{1}$  and right eigenvector  $M^{-1} \mathbf{1}$ .*

*Proof.* The fact that all eigenvalues lie inside or on the unit circle follows from:

$$|\lambda_j(\bar{F})| \leq |\lambda_{\max}(\bar{F})| = \|\bar{F}\| = \|\mathbb{E}[F]\| \leq \mathbb{E}[\|F_i\|] = 1, \quad \forall j = 1, \dots, N_C,$$

being  $\|F_i\|_2 = 1$  for all  $i$ 's.

Consider then an eigenvector  $y$  such that  $\|y\| = \|\bar{F}y\|$ . We have

$$\|\bar{F}y\| \leq \|\bar{F}\| \cdot \|y\| = \|\mathbb{E}[F]\| \cdot \|y\| \leq \mathbb{E}[\|F_i\|] \cdot \|y\| = \|y\|,$$

### 5.3 Bound on the rate of convergence

---

and therefore  $\|F_i y\| = \|y\|$  for all  $i$ 's.

As  $F_i$  are projection matrices, it means that  $F_i y = y$  and then  $My \in \ker \Omega_i^T, \forall i$  as shown in (5.13). Similarly to what done in Proposition 15:

$$\text{Im}[\Omega_1 \cdots \Omega_\ell] = \ker \mathbf{1}^T \quad \Rightarrow \quad \bigcap_i \ker \Omega_i^T = \text{Im } \mathbf{1},$$

and so:  $My \in \ker \Omega_i^T = \text{Im } \mathbf{1}$ . It implies that the eigenvector of  $\bar{F}$ , related to the eigenvalue 1, is  $y = M^{-1} \mathbf{1}$ .

By inspection we can verify that the left eigenvector corresponding to the same eigenvalue is  $\mathbf{1}^T$ .  $\square$

The following theorem provides an upper bound for  $R$ , defined by:

$$\beta = \max\{|\lambda| \mid \lambda \in \Lambda(\bar{F}), \lambda \neq 1\}. \quad (5.23)$$

**Theorem 19.** *Let be  $\text{Im}[\Omega_1 \cdots \Omega_\ell] = \ker \mathbf{1}^T$ . Consider the linear system (5.16) and the rate of convergence  $R$  defined in (5.19). Then  $R \leq \beta$ .*

*Proof.* Let us first prove that  $\Omega \mathcal{L}(\Omega M \Omega) \Omega \leq \beta \Omega M \Omega$ . Indeed, we have, for all  $y$ :

$$\begin{aligned} y^T \Omega \mathcal{L}(\Omega M \Omega) \Omega y &= \mathbb{E} [y^T \Omega F^T \Omega M \Omega F \Omega y] \\ &= \mathbb{E} [y^T \Omega F^T M F \Omega y] \\ &= y^T \Omega M^{1/2} \mathbb{E} [M^{1/2} F M^{-1/2}] M^{1/2} \Omega y, \end{aligned}$$

where we use the fact that  $\Omega F_i \Omega = F_i \Omega$  and that  $F_i^T M F_i = M F_i$ .

The matrix  $\mathbb{E} [M^{1/2} F M^{-1/2}]$  is real and symmetric, in fact:

$$\begin{aligned} \left( \mathbb{E} [M^{1/2} F M^{-1/2}] \right)^T &= \mathbb{E} [M^{-1/2} F^T M^{1/2}] \\ &= \sum_{i=1}^{\ell} p_i M^{-1/2} \left[ I - M(\Omega_i M \Omega_i)^\sharp \right] M^{1/2} \\ &= \sum_{i=1}^{\ell} p_i M^{1/2} \left[ I - (\Omega_i M \Omega_i)^\sharp M \right] M^{-1/2} \\ &= \mathbb{E} [M^{1/2} F M^{-1/2}] \end{aligned}$$

where we have used the definition of  $F_i$ 's in (5.9).

Moreover, by Lemma 18, the matrix  $\mathbb{E} [M^{1/2} F M^{-1/2}] = M^{1/2} \bar{F} M^{-1/2}$  has only one eigenvalue on the unit circle (precisely in 1), with eigenvector  $M^{-1/2} \mathbf{1}$ , being:

$$\begin{aligned} (M^{1/2} \bar{F} M^{-1/2})(M^{-1/2} \mathbf{1}) &= (M^{1/2} \bar{F} M^{-1/2}) M^{1/2} M^{-1} \mathbf{1} \\ &= M^{1/2} \bar{F} M^{-1} \mathbf{1} \\ &= M^{1/2} M^{-1} \mathbf{1} \\ &= M^{-1/2} \mathbf{1}. \end{aligned}$$

As the matrix  $M^{1/2}\bar{F}M^{-1/2}$  is self-adjoint, then its eigenvalues are real and its eigenvectors are linearly independent and each vector can be written as a linear combination of these eigenvectors:

$$z = \sum_{j=1}^{N_c} \alpha_j z_j = \alpha_1 M^{-1/2} \mathbf{1} + \sum_{j=2}^{N_c} \alpha_j z_j, \quad \forall z$$

where  $z_j$ 's denote the eigenvectors of  $M^{1/2}\bar{F}M^{-1/2}$ .

Then, an upper bound of the *Rayleigh quotient*  $\rho$  can be found:

$$\begin{aligned} \rho &= \frac{z^T (M^{1/2}\bar{F}M^{-1/2}) z}{z^T z} = \frac{z^T (M^{1/2}\bar{F}M^{-1/2}) (\alpha_1 M^{-1/2} \mathbf{1} + \sum_{j=2}^{N_c} \alpha_j z_j)}{z^T z} \\ &= \frac{z^T (\alpha_1 \lambda_{\max} M^{-1/2} \mathbf{1} + \sum_{j=2}^{N_c} \lambda_j \alpha_j z_j)}{z^T z} \\ &\leq \lambda_{\max} \frac{z^T (\alpha_1 M^{-1/2} \mathbf{1} + \sum_{j=2}^{N_c} \alpha_j z_j)}{z^T z} = 1, \end{aligned} \quad (5.24)$$

being  $\lambda_{\max} = \lambda_{\max}(M^{1/2}\bar{F}M^{-1/2}) = 1$ .

As (5.24) holds for all  $z$ , in particular it holds for  $z = M^{1/2}\Omega y$ ; moreover, as  $M^{1/2}\bar{F}M^{-1/2}$  has only one eigenvalue in 1 and the others are smaller:

$$y^T \Omega \mathcal{L}(\Omega M \Omega) \Omega y = y^T \Omega M^{1/2} \mathbb{E} \left[ M^{1/2} F M^{-1/2} \right] M^{1/2} \Omega y \leq \beta y^T \Omega M \Omega y.$$

From this result, using Lemmas 16 and 17, we can say that:

$$\begin{aligned} \Omega \mathcal{L}^t(\Omega M \Omega) \Omega &= \Omega \mathcal{L}^{t-1}(\mathcal{L}(\Omega M \Omega)) \Omega \\ &= \Omega \mathcal{L}^{t-1}(\Omega \mathcal{L}(\Omega M \Omega) \Omega) \Omega \\ &\leq \Omega \mathcal{L}^{t-1}(\beta \Omega M \Omega) \Omega \\ &= \beta \Omega \mathcal{L}^{t-1}(\Omega M \Omega) \Omega \\ &\leq \dots \leq \beta^t \Omega M \Omega \end{aligned} \quad (5.25)$$

and therefore  $R \leq \beta$ .  $\square$

We now state a result that allows us to compute  $R$  when the spectra of  $\mathcal{L}$  and  $\bar{F}$  are available.

Before we show that the convergence rate  $R$  equals the rate:

$$R_{\mathcal{O}} = \max\{|\lambda_{\mathcal{L}(i)}| : \Delta_{\mathcal{L}}(i) \notin \mathcal{O}\}. \quad (5.26)$$

**Proposition 20.** *Let  $R$  and  $R_{\mathcal{O}}$  be defined by (5.19) and (5.26) respectively. Then  $R = R_{\mathcal{O}}$ .*

*Proof.* For any eigenvector  $\Delta_{\mathcal{L}}(i)$  and  $M > 0$ , there exists a  $\gamma > 0$  such that  $\Delta_{\mathcal{L}}(i) \leq \gamma M$ . Then we have  $\Omega \mathcal{L}^t(\Delta_{\mathcal{L}}(i)) \Omega \leq \gamma \Omega \mathcal{L}^t(M) \Omega$  and therefore  $\lambda_{\mathcal{L}}(i) \Omega \Delta_{\mathcal{L}}(i) \Omega \leq \gamma \Omega \mathcal{L}^t(M) \Omega$ .

If  $\Delta_{\mathcal{L}}(i) \notin \mathcal{O}$ , then we must have  $\lambda_{\mathcal{L}}(i) \leq R$ , therefore  $R_{\mathcal{O}} \leq R$ . As of course  $R_{\mathcal{O}} \geq R$ , we conclude that  $R_{\mathcal{O}} = R$ .  $\square$

### 5.3 Bound on the rate of convergence

---

Let be  $\Lambda(\mathcal{L}) \in \mathbb{R}^{N_c^2}$  and  $\Lambda(\bar{F}) \in \mathbb{R}^{N_c}$  the ordered vectors of possibly repeated eigenvalues of  $\mathcal{L}$  and  $\bar{F}$ ; we can then state the following result.

**Theorem 21.** *Let be  $\text{Im}[\Omega_1 \cdots \Omega_\ell] = \ker \mathbf{1}^T$ .*

*The eigenvalues of  $\mathcal{L}$  are the eigenvalues of  $\bar{F}$ , each one taken twice (except for the first one  $\lambda_{\mathcal{L}}(1) = \lambda_{\bar{F}}(1) = 1$ , which appears only once in the vector  $\Lambda(\mathcal{L})$ ).*

*The convergence rate  $R$  is the  $(N_c + 1)$ -th element of the vector  $\Lambda(\mathcal{L})$ , i.e. the largest of the elements in the vector  $\Lambda(\mathcal{L})$ , after eliminating a number of elements equals to the cardinality of the set  $\Lambda(\bar{F})$ .*

*Proof.* Via Lemma 17 it is possible to show that the non-observable space  $\mathcal{O}$  defined in (5.20) is an invariant set:

$$\Omega \mathcal{L}(\Delta) \Omega = \Omega \mathcal{L}(\Omega \Delta \Omega) \Omega \quad \forall \Delta \in \mathcal{O}.$$

By exploiting the properties of the Kronecker product (see Appendix B):

$$\text{rank}(\Omega \otimes \Omega) = (\text{rank} \Omega)(\text{rank} \Omega) = (N_c^2 - 1)^2 \quad \dim(\ker[\Omega \otimes \Omega]) = 2N_c - 1.$$

So the dimension of  $\mathcal{O}$  is  $2N_c - 1$ , thus there must exist  $2N_c - 1$  eigenvectors of  $\mathcal{L}$  in  $\mathcal{O}$ . These eigenvectors can be constructed from the eigenvectors of  $\bar{F}^T$ . Indeed, consider  $N_c$  linearly independent eigenvectors  $y_1, \dots, y_{N_c}$  such that:

$$\bar{F}^T y_i = \mu_i y_i \quad \text{with} \quad 1 = \mu_1 > \mu_2 \geq \dots \geq \mu_{N_c}$$

where we have used the results from Lemma 18 and the fact that eigenvalues of  $\bar{F}$  are real, being  $\bar{F}$  a self-adjoint matrix.

For all  $i$ , it results:

$$\begin{aligned} \mathcal{L}(\mathbf{1} y_i^T) &= \mathbb{E} [F^T \mathbf{1} y_i^T F] = \mathbf{1} y_i^T \bar{F} = \mu_i \mathbf{1} y_i^T \\ \mathcal{L}(y_i \mathbf{1}^T) &= \mathbb{E} [F^T y_i \mathbf{1}^T F] = \bar{F}^T y_i \mathbf{1}^T = \mu_i y_i \mathbf{1}^T, \end{aligned}$$

i.e.  $\mathbf{1} y_i^T$  and  $y_i \mathbf{1}^T$  are eigenvectors of  $\mathcal{L}$  related to the eigenvalue  $\mu_i$ . For these eigenvectors, it results:

$$\begin{aligned} \Omega \mathcal{L}(\mathbf{1} y_i^T) \Omega &= \mu_i \Omega \mathbf{1} y_i^T \Omega = 0 \\ \Omega \mathcal{L}(y_i \mathbf{1}^T) \Omega &= \mu_i \Omega y_i \mathbf{1}^T \Omega = 0, \end{aligned}$$

being  $\mathbf{1} \in \ker \Omega$ .

We therefore constructed a basis of  $2N_c - 1$  linearly independent eigenvectors of  $\mathcal{L}$  in  $\mathcal{O}$ . One of them,  $\Delta_{\mathcal{L}}(1) = \mathbf{1} \mathbf{1}^T$ , corresponds to the eigenvalue  $\lambda_{\mathcal{L}}(1) = 1$ . The remaining  $(2N_c - 2)$  eigenvectors correspond to the eigenvalues  $\lambda_{\bar{F}}(2), \dots, \lambda_{\bar{F}}(N_c)$  taken twice.

According to Proposition 20, then  $R$  is the largest among the eigenvalues left when removing (twice)  $[\lambda_{\bar{F}}(2) \dots \lambda_{\bar{F}}(N_c)]^T$  from  $[\lambda_{\mathcal{L}}(2) \dots \lambda_{\mathcal{L}}(N_c^2)]^T$ .  $\square$





# Optimal strategy

---

In this chapter we will show that the best performance of the proposed algorithm can be achieved when the graph representing a microgrid is a tree and a nearest-neighbor clustering strategy has chosen.

We will confirm this result, computing analytically the bound  $\beta$  (which will be shown to be a tight bound of the rate of convergence  $R$ ) for the same and other topologies of the network, and we will express it as a function of the number of compensators of the grid.

In the following chapter the rate of convergence will be studied numerically and compared with simulations for more general cases (as to the topology of the network or decomposition choices).

## 6.1 Nearest-neighbor gossip

Consider the case in which the compensators are divided into  $\ell$  clusters  $\mathcal{C}_1, \dots, \mathcal{C}_\ell$ , each one containing exactly two nodes, i.e.:

$$\mathcal{C}_i = \{h, k \mid h, k \in \mathcal{C}\}, \quad 1 \leq i \leq \ell. \quad (6.1)$$

Owing to this structure, we will refer to these subsets also with  $\mathcal{C}_{h,k}$  ( $h, k \in \mathcal{C}$ ), where the indices explicitly show the nodes they contain. Thus we will denote the set containing the compensators  $h$  and  $k$  with  $\mathcal{C}_i$  or  $\mathcal{C}_{h,k}$  indifferently. The same for the matrices related to the clusters; for example we will indicate the projector related to the cluster  $\mathcal{C}_i$  indifferently with  $F_i$  or  $F_{h,k}$ .

**Theorem 22.** *Consider the hypergraph  $\mathcal{H}$  defined over the set of nodes  $\mathcal{C}$  and suppose  $\mathcal{H}$  to be a connected graph. Let assume an arbitrary value for the triggering probabilities*

$p_i$ 's associated to the related clusters  $\mathcal{C}_i = \mathcal{C}_{h,k}$  (according to the notation introduced before).

Then the bound  $\beta$  on the convergence rate of the algorithm satisfies:

$$\beta \geq 1 - \frac{1}{N_{\mathcal{C}} - 1}. \quad (6.2)$$

*Proof.* Let consider the matrix  $\bar{F} = \mathbb{E}[F]$ ; it can be expressed as:

$$\bar{F} = [I - (\Omega_i M \Omega_i)^\sharp M] = I - \bar{E} \quad (6.3)$$

where  $\bar{E} = \mathbb{E}[(\Omega_i M \Omega_i)^\sharp M]$ . It follows that:

$$\lambda_j(\bar{F}) = 1 - \lambda_{N_{\mathcal{C}}-j+1}(\bar{E}), \quad 1 \leq j \leq N_{\mathcal{C}}. \quad (6.4)$$

In this case in which all the clusters have cardinality 2, the matrix  $\Omega_i$  (related to the cluster  $\mathcal{C}_i = \mathcal{C}_{h,k}$ ) can be expressed in the following simple way, according to (5.2):

$$\Omega_i = \frac{(\mathbf{1}_h - \mathbf{1}_k)(\mathbf{1}_h - \mathbf{1}_k)^T}{2}. \quad (6.5)$$

Expression (6.5) is useful to calculate the trace of  $\bar{E}$ :

$$\begin{aligned} \sum_{j=1}^{N_{\mathcal{C}}} \lambda_j(\bar{E}) &= \text{Tr}(\bar{E}) = \text{Tr} \left[ \sum_{i=1}^{\ell} p_i (\Omega_i M \Omega_i)^\sharp M \right] \\ &= \text{Tr} \left[ \sum_{i=1}^{\ell} p_i \left( \frac{(\mathbf{1}_h - \mathbf{1}_k)(\mathbf{1}_h - \mathbf{1}_k)^T}{2} M \frac{(\mathbf{1}_h - \mathbf{1}_k)(\mathbf{1}_h - \mathbf{1}_k)^T}{2} \right)^\sharp M \right] \\ &= \text{Tr} \left[ \sum_{i=1}^{\ell} p_i \left( \frac{1}{2} (\mathbf{1}_h - \mathbf{1}_k) \frac{(\mathbf{1}_h - \mathbf{1}_k)^T M (\mathbf{1}_h - \mathbf{1}_k)}{2} (\mathbf{1}_h - \mathbf{1}_k)^T \right)^\sharp M \right] \\ &= \text{Tr} \left[ \sum_{i=1}^{\ell} p_i \frac{2}{(\mathbf{1}_h - \mathbf{1}_k)^T M (\mathbf{1}_h - \mathbf{1}_k)} \left( \frac{(\mathbf{1}_h - \mathbf{1}_k)(\mathbf{1}_h - \mathbf{1}_k)^T}{2} \right)^\sharp M \right]. \end{aligned} \quad (6.6)$$

Using (6.5) and the facts:  $\Omega_i^\sharp = \Omega_i$  and  $\text{Tr}(ABC) = \text{Tr}(CAB) = \text{Tr}(BCA)$ :

$$\begin{aligned}
 \sum_{j=1}^{N_C} \lambda_j(\bar{E}) &= \text{Tr} \left[ \sum_{i=1}^{\ell} p_i \frac{2}{(\mathbf{1}_h - \mathbf{1}_k)^T M (\mathbf{1}_h - \mathbf{1}_k)} \Omega_i \right] \\
 &= \sum_{i=1}^{\ell} p_i \frac{2}{(\mathbf{1}_h - \mathbf{1}_k)^T M (\mathbf{1}_h - \mathbf{1}_k)} \text{Tr} \left[ \frac{(\mathbf{1}_h - \mathbf{1}_k)(\mathbf{1}_h - \mathbf{1}_k)^T}{2} M \right] \\
 &= \sum_{i=1}^{\ell} p_i \frac{1}{(\mathbf{1}_h - \mathbf{1}_k)^T M (\mathbf{1}_h - \mathbf{1}_k)} \text{Tr} [(\mathbf{1}_h - \mathbf{1}_k) M (\mathbf{1}_h - \mathbf{1}_k)^T] \quad (6.7) \\
 &= \sum_{i=1}^{\ell} p_i \frac{1}{(\mathbf{1}_h - \mathbf{1}_k)^T M (\mathbf{1}_h - \mathbf{1}_k)} (\mathbf{1}_h - \mathbf{1}_k) M (\mathbf{1}_h - \mathbf{1}_k)^T \\
 &= \sum_{i=1}^{\ell} p_i = 1.
 \end{aligned}$$

As the hypergraph  $\mathcal{H}$  is connected, then  $\text{Im} [\Omega_1 \cdots \Omega_{\ell}] = \ker \mathbf{1}^T$  (Proposition 13). Then, the hypothesis of Lemma 18 is satisfied and we can state:

$$\Lambda(\bar{F}) = [\lambda_1(\bar{F}) \cdots \lambda_{N_C}(\bar{F})]^T \quad \text{with} \quad 1 = \lambda_1(\bar{F}) > \lambda_2(\bar{F}) \geq \cdots \geq \lambda_{N_C}(\bar{F}).$$

Then, by (6.4):

$$\Lambda(\bar{E}) = [\lambda_1(\bar{E}) \cdots \lambda_{N_C}(\bar{E})]^T \quad \text{with} \quad 0 = \lambda_{N_C}(\bar{E}) < \lambda_{N_C-1}(\bar{E}) \leq \cdots \leq \lambda_1(\bar{E}). \quad (6.8)$$

By (6.7) and (6.8)

$$1 = \sum_{j=1}^{N_C} \lambda_j(\bar{E}) \geq \sum_{j=1}^{N_C} \lambda_{N_C-1}(\bar{E}) = \lambda_{N_C}(\bar{E}) + \sum_{j=1}^{N_C-1} \lambda_{N_C-1}(\bar{E}) = (N_C - 1) \lambda_{N_C-1}(\bar{E})$$

and by (5.23) and (6.4):

$$\beta = \lambda_2(\bar{F}) = 1 - \lambda_{N_C-1}(\bar{E}) \geq 1 - \frac{1}{N_C - 1}.$$

□

In the following proposition we will present the case in which  $\beta$  assumes the smallest possible value (equation (6.2) in Theorem 22 holds as equality). This optimal performance is achieved by a *nearest-neighbor clustering choice*, i.e. each cluster has the form  $\mathcal{C}_e = \mathcal{C}_{h,k} = \{h, k \mid (h, k) = e \in \mathcal{E}\}$ .

We assume that the graph  $\mathcal{G}$  which represents the microgrid is a tree and  $\mathcal{C} = \mathcal{V}$ <sup>1</sup>: the latter assumption simplifies the definition of neighbors among compensators but does affect the results: it is possible to add passive nodes among compensators, without affecting the convergence rate analysis  $R$ , depending only on  $X_{CC}$ .

<sup>1</sup>From now on, we remove Assumption 4; as said in Section 3.1, it only simplifies the analysis, allowing the use of the inverse matrix of  $X_{CC}$  instead of the corresponding generalized inverse, but does not affect the results obtained before.

**Proposition 23.** *Let the graph  $\mathcal{G}$  be a tree and the set of compensators coincide with the entire set of nodes ( $\mathcal{C} = \mathcal{V}$ ). Assume a nearest-neighbor clustering choice.*

*Suppose that each cluster  $\mathcal{C}_e$  has the same triggering probability  $p_e = 1/N_{\mathcal{E}}$ . Then:*

$$\beta = 1 - \frac{1}{N_{\mathcal{C}} - 1}. \quad (6.9)$$

*Proof.* As before, we can define the matrix:

$$\bar{E} = \mathbb{E} \left[ (\Omega_e M \Omega_e)^\# M \right] = \mathbb{E} \left[ (\Omega_e X \Omega_e)^\# X \right],$$

where we have exploited the hypothesis of this proposition. By (6.5):

$$\Omega_e = \frac{[\mathbf{1}_{\sigma(e)} - \mathbf{1}_{\tau(e)}] [\mathbf{1}_{\sigma(e)} - \mathbf{1}_{\tau(e)}]^T}{2}$$

and, by (2.13):

$$[\mathbf{1}_{\sigma(e)} - \mathbf{1}_{\tau(e)}]^T X [\mathbf{1}_{\sigma(e)} - \mathbf{1}_{\tau(e)}] = e^{-j\theta} \mathbf{z}(e) = |\mathbf{z}_{\text{eff}}(e)| = z(e),$$

where  $z(e) = |\mathbf{z}(e)|$  and we have exploited the fact that  $\mathcal{G}$  is a tree.

As:

$$\begin{aligned} (\Omega_e X \Omega_e)^\# &= \left( \frac{[\mathbf{1}_{\sigma(e)} - \mathbf{1}_{\tau(e)}] [\mathbf{1}_{\sigma(e)} - \mathbf{1}_{\tau(e)}]^T}{2} X \frac{[\mathbf{1}_{\sigma(e)} - \mathbf{1}_{\tau(e)}] [\mathbf{1}_{\sigma(e)} - \mathbf{1}_{\tau(e)}]^T}{2} \right)^\# \\ &= \left( \frac{\mathbf{1}_{\sigma(e)} - \mathbf{1}_{\tau(e)}}{2} z(e) \frac{\mathbf{1}_{\sigma(e)} - \mathbf{1}_{\tau(e)}}{2} \right)^\# \\ &= \frac{2}{z(e)} \left( \frac{[\mathbf{1}_{\sigma(e)} - \mathbf{1}_{\tau(e)}] [\mathbf{1}_{\sigma(e)} - \mathbf{1}_{\tau(e)}]^T}{2} \right)^\# \\ &= \frac{2}{z(e)} \Omega_e^\# = \frac{2}{z(e)} \Omega_e \end{aligned}$$

and the triggering probability  $p_e = \frac{1}{N_{\mathcal{E}}} = \frac{1}{N_{\mathcal{C}} - 1}, \forall e \in \mathcal{E}$ , then:

$$\begin{aligned} \bar{E} &= \mathbb{E} \left[ (\Omega_e X \Omega_e)^\# X \right] = \sum_{e \in \mathcal{E}} p_e (\Omega_e X \Omega_e)^\# X \\ &= \frac{1}{N_{\mathcal{C}} - 1} \sum_{e \in \mathcal{E}} \frac{2}{z(e)} \Omega_e X \\ &= \frac{1}{N_{\mathcal{C}} - 1} \sum_{e \in \mathcal{E}} \frac{1}{z(e)} [\mathbf{1}_{\sigma(e)} - \mathbf{1}_{\tau(e)}] [\mathbf{1}_{\sigma(e)} - \mathbf{1}_{\tau(e)}]^T X \quad (6.10) \\ &= \frac{1}{N_{\mathcal{C}} - 1} A^T Z^{-1} A X = \frac{1}{N_{\mathcal{C}} - 1} L X \\ &= \frac{1}{N_{\mathcal{C}} - 1} (I - \mathbf{1}\mathbf{1}_0^T). \end{aligned}$$

By (6.10) and definition of  $\beta$ :

$$\beta = 1 - \lambda_{N_{\mathcal{C}} - 1}(\bar{E}) = 1 - \lambda_{N_{\mathcal{C}} - 1} \left( \frac{I - \mathbf{1}\mathbf{1}_0^T}{N_{\mathcal{C}} - 1} \right) = 1 - \frac{1}{N_{\mathcal{C}} - 1}.$$

□

## 6.2 Case studies

In this section we will derive the parameter  $\beta$ , used as a reliable metric for the evaluation of the algorithm performance, for some simple topologies of electrical networks (i.e. different structures of graphs).

We will see that the first step is giving an analytical expression to the matrix  $X$ , necessary in order to obtain the matrices  $F_i$ 's,  $\bar{F}$  and its eigenvalues. This is a not easy step, because it does not exist a general procedure, but it is strictly related to the structure of the graph.

In particular, we will consider the case in which  $\mathcal{G}$  is a line: we will confirmed the statement of Proposition 23 and we will be able to say something more.

Then, we will consider the case in which the edges of the graph  $\mathcal{G}$  form a circular path. We will show that the result in Proposition 23 can be extended also to this configuration, under a proper assumption.

### 6.2.1 Tree structure

As hinted before, the starting-point for the calculus of  $\beta$  is to find an analytical expression for the matrix  $X$ . Here we exploit the characteristics of the tree structure of the network. Before starting, a definition of *tree* is recalled; it is given from the definition of graph.

**Definition 24.** Consider a graph  $\mathcal{G} = (\mathcal{V}, \mathcal{E})$ . Then  $\mathcal{G}$  is a *tree* if:

1. there exists the following relationship between the number of nodes and the number of edges of  $\mathcal{G}$ :  $|\mathcal{E}| = |\mathcal{V}| - 1$ ;
2.  $\mathcal{G}$  is connected, i.e. for each pair of nodes  $v, w \in \mathcal{V}$  there exists exactly one path connecting them.

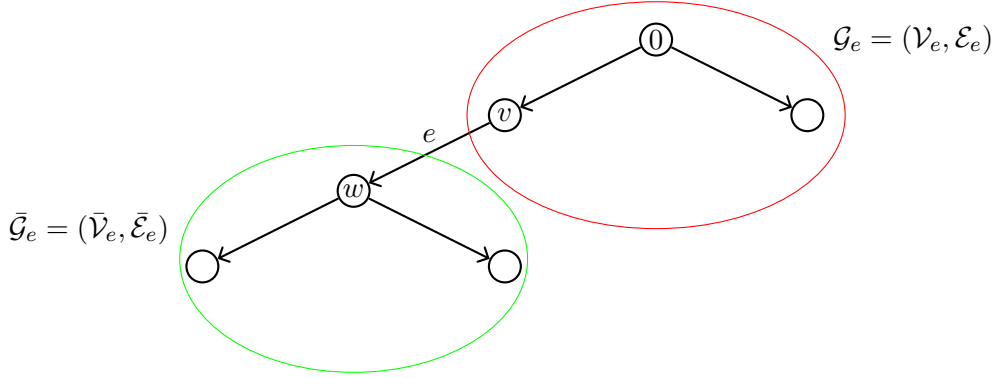
From definition 24, it follows that no cycles can be possible.

Let consider the tree  $\mathcal{G} = (\mathcal{V}, \mathcal{E})$ , with  $|\mathcal{V}| = N + 1$  and  $|\mathcal{E}| = N_{\mathcal{E}} = N$ . Consider an edge  $e = (v, w) \in \mathcal{E}$  and suppose to remove it from  $\mathcal{G}$ . From definition 24,  $\mathcal{G}$  results divided into two subgraphs (see Figure 6.1):  $\bar{\mathcal{G}}_e = (\bar{\mathcal{V}}_e, \bar{\mathcal{E}}_e)$ , the subtree whose root is the node  $w$ , and  $\mathcal{G}_e = (\mathcal{V}_e, \mathcal{E}_e)$ , the subtree whose root is the node 0, with  $\mathcal{V}_e = \mathcal{V} \setminus \bar{\mathcal{V}}_e$  and  $\mathcal{E}_e = \mathcal{E} \setminus \bar{\mathcal{E}}_e \setminus \{e\}$ ; so:

$$\mathcal{V}_e \cup \bar{\mathcal{V}}_e = \mathcal{V} \quad \mathcal{V}_e \cap \bar{\mathcal{V}}_e = \emptyset.$$

Let define the matrix  $B \in \mathbb{R}^{N \times (N+1)}$  as follows:

$$[B]_{ev} = \begin{cases} -1 & \text{if } v \in \bar{\mathcal{V}}_e \\ 0 & \text{if } v \in \mathcal{V}_e. \end{cases}$$


 Figure 6.1: Subtrees  $\mathcal{G}_e$  and  $\bar{\mathcal{G}}_e$  of  $\mathcal{G}$ .

For any  $\tilde{e} \in \mathcal{E}$ ,  $\tilde{e} \neq e$ :

$$\left. \begin{aligned} \sum_{v=0}^N [A]_{ev} [B]_{\tilde{e}v} &= [B]_{\tilde{e}, \tau(e)} - [B]_{\tilde{e}, \sigma(e)} = 0 \\ \sum_{v=0}^N [A]_{ev} [B]_{ev} &= [B]_{e, \tau(e)} - [B]_{e, \sigma(e)} = 1 \end{aligned} \right\} \Rightarrow AB^T = I_N \quad (6.11)$$

being  $A$  the incidence matrix defined in (2.6).

Let define the matrices:

$$\tilde{A} = \begin{bmatrix} A \\ \mathbf{1}_0^T \end{bmatrix} \quad \tilde{B} = \begin{bmatrix} B \\ \mathbf{1}^T \end{bmatrix},$$

so that:

$$\tilde{A}\tilde{B}^T = \begin{bmatrix} A \\ \mathbf{1}_0^T \end{bmatrix} \begin{bmatrix} B^T & \mathbf{1} \end{bmatrix} = \begin{bmatrix} AB^T & A\mathbf{1} \\ \mathbf{1}_0^T B & \mathbf{1}_0^T \mathbf{1} \end{bmatrix} = \begin{bmatrix} I_N & \mathbf{0} \\ \mathbf{0} & 1 \end{bmatrix} = I_{N+1}.$$

For the uniqueness of the inverse of a matrix:  $\tilde{A}^{-1} = \tilde{B}^T$  and so:

$$I_{N+1} = \tilde{B}^T \tilde{A} = \begin{bmatrix} B^T & \mathbf{1} \end{bmatrix} \begin{bmatrix} A \\ \mathbf{1}_0^T \end{bmatrix} = B^T A + \mathbf{1}\mathbf{1}_0^T.$$

It follows that:

$$B^T A = I_{N+1} - \mathbf{1}\mathbf{1}_0^T \quad \Rightarrow \quad A^T B = I_{N+1} - \mathbf{1}_0 \mathbf{1}^T. \quad (6.12)$$

Let now define the  $(N+1) \times (N+1)$  matrix:

$$Y = B^T Z B. \quad (6.13)$$

Then, by (6.11) and (6.12):

$$\begin{cases} LY = (A^T Z^{-1} A)(B^T Z B) = A^T B = I_{N+1} - \mathbf{1}_0 \mathbf{1}^T \\ Y \mathbf{1}_0 = B^T Z B \mathbf{1}_0 = 0. \end{cases}$$

## 6.2 Case studies

---

It results that the matrix  $Y$  defined in (6.13) satisfies the properties in Lemma 1, and so we have found a characterization for the matrix  $X$  (in the following we will indicate  $X = B^T Z B$ ).

By this result, we can directly obtain the elements of the matrix  $X$ . It is easy to verify that, given two nodes  $h$  and  $k$

$$X_{h,k} = [B^T Z B]_{h,k} = \sum_{e \in \mathcal{P}_{0,h} \cap \mathcal{P}_{0,k}} z(e) \quad (6.14)$$

where  $\mathcal{P}_{0,h}$  and  $\mathcal{P}_{0,k}$  are the paths connecting the PCC to the nodes  $h$  and  $k$  respectively. In particular,  $\mathcal{P}_{0,0}$  is empty and it confirms the fact that the first row and the first column of  $X$  are zero.

### Line structure

Consider the case of a 1-dimensional graph, i.e. an electrical network consisting in one single line with compensators equally distributed at unitary distances along the line ( $\mathbf{Z} = I$ ). We assume, without loss of generality:  $\mathcal{C} = \mathcal{V}$ . As said before, loads can be connected everywhere in the line because their presence does not influence the Hessian matrix  $M$ .

We start by calculating the matrix  $X$ ; being the line a special case of a tree, we can exploit (6.14):

$$X = B^T B = \begin{bmatrix} 0 & 0 & 0 & \cdots & 0 \\ 0 & 1 & 1 & \cdots & 1 \\ 0 & 1 & 2 & \cdots & 2 \\ \vdots & & & & \vdots \\ 0 & 1 & 2 & \cdots & N \end{bmatrix}. \quad (6.15)$$

Two different decompositions of the optimization problem are considered, corresponding to different clustering of the nodes into subsets. In all of them we assume that compensators are allowed to update their state in pairs, i.e.  $|\mathcal{C}_i| = 2$ ,  $1 \leq i \leq \ell$ ; for this particular structure, these subsets will be indicated as:

$$\mathcal{C}_{h,k} = \{h, k \mid h, k \in \mathcal{C}\}$$

and also the matrices  $F_i$  and  $\Omega_i$  introduced in the previous chapters will follow this notation.

We consider the following clustering choices (Figure 6.2):

- *nearest-neighbor* (or *1-step*) case: nodes able to communicate are the pairs of adjacent ones in the electric line:

$$\mathcal{C}_{h,k} = \{h, k \mid (h, k) = e \in \mathcal{E}\} = \{h, k \mid 0 \leq h \leq N-1, k = h+1\};$$

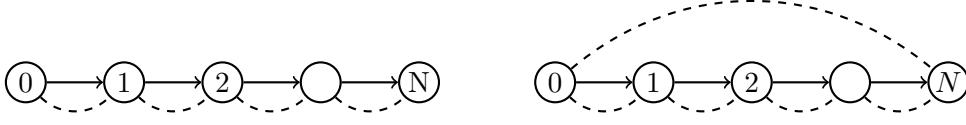


Figure 6.2: *nearest-neighbor* (or *1-step*) and *circle* clustering choices illustrated by the corresponding hypergraphs  $\mathcal{H}$  (dashed lines).

- *circle* case: nodes able to communicate are the pairs of adjacent ones in the electric line together with the pair constituted by the first and the last agent:

$$\mathcal{C}_{h,k} = \{h, k \mid 0 \leq h \leq N, k = (h+1) \bmod (N+1)\}.$$

For the *1-step* case, the  $h$ -th element of  $F_{h,k} \in \mathbb{R}^{(N+1) \times (N+1)}$  corresponds to the subproblem in which node  $h$  and node  $k = h+1$  are allowed to update their state.

As shown in (6.6), the matrix  $F_{h,k}$  may be expressed as follows, being  $|\mathcal{C}_{h,k}| = 2$  (notice we use the matrix  $X$  instead of  $M$  owing to the assumption  $\mathcal{C} = \mathcal{V}$ ):

$$F_{h,k} = I - \frac{(\mathbf{1}_h - \mathbf{1}_k)(\mathbf{1}_h - \mathbf{1}_k)^T X}{(\mathbf{1}_h - \mathbf{1}_k)^T X (\mathbf{1}_h - \mathbf{1}_k)} \quad (6.16)$$

where:

$$(\mathbf{1}_h - \mathbf{1}_k)^T X = [0 \cdots \underbrace{0}_h \underbrace{-1 \cdots -1}_k] \quad (\mathbf{1}_h - \mathbf{1}_k)^T X (\mathbf{1}_h - \mathbf{1}_k) = 1.$$

Then:

$$F_{h,k} = \begin{bmatrix} 1 & & & & & \\ & \ddots & & & & \\ & & 1 & \cdots & \cdots & \cdots & 1 \\ & & & 0 & -1 & \cdots & -1 \\ & & & & 1 & & \\ & & & & & \ddots & \\ & & & & & & 1 \end{bmatrix} \quad \begin{matrix} \leftarrow h \\ \leftarrow k \end{matrix} \quad (6.17)$$

By Assumption 14,  $p_i = p_{h,k} = \frac{1}{N}$  for all  $1 \leq i \leq \ell = N$  (or, equivalently:  $0 \leq h \leq N-1, k = h+1$ ) and:

$$\begin{aligned} \bar{F} = \mathbb{E}[F] &= \sum_{h=0}^{N-1} F_{h,k} p_{h,k} \quad \text{with } k = h+1 \\ &= \frac{1}{N} \begin{bmatrix} N & 1 & 1 & \cdots & 1 \\ 0 & N-1 & 0 & \cdots & 0 \\ \vdots & \ddots & \ddots & \ddots & \vdots \\ 0 & \cdots & 0 & N-1 & 0 \\ 0 & \cdots & \cdots & 0 & N-1 \end{bmatrix} \end{aligned}$$



## 6.2 Case studies

The matrix  $\bar{F}$  results to be a triangular matrix and so its eigenvalues are easily computed as they are the elements on the diagonal:

$$\Lambda_{\bar{F}} = \left[ 1, \frac{N-1}{N}, \dots, \frac{N-1}{N} \right]^T;$$

then:

$$\beta = \lambda_2(\bar{F}) = \frac{N-1}{N}.$$

In this specific case, it easy to analytically express the matrix  $\mathbf{F}$  associated with the linear transformation  $\mathcal{L}$ , because it results to be a triangular  $(N+1)^2 \times (N+1)^2$  matrix; its eigenvalues are:

$$\Lambda_{\mathcal{L}} = \left[ 1, \underbrace{\frac{N-1}{N}, \dots, \frac{N-1}{N}}_{3N}, \underbrace{\frac{N-2}{N}, \dots, \frac{N-2}{N}}_{N(N-1)} \right]^T.$$

For the analysis of the previous chapter, we can conclude:

$$\beta = R = 1 - \frac{1}{N}.$$

Consider now the case in which the hypergraph  $\mathcal{H}$  is a circle. In this case, as

$$\mathcal{C}_{h,k} = \{h, k \mid 0 \leq h \leq N, k = (h+1) \bmod(N+1)\},$$

the set of matrices  $\{F_{h,k}\}$ , includes the  $F_{h,k}$ 's of the *1-step* case ( $0 \leq h \leq N-1, k = h+1$ ), together with:

$$F_{N,0} = I - \frac{(\mathbf{1}_N - \mathbf{1}_0)(\mathbf{1}_N - \mathbf{1}_0)^T X}{(\mathbf{1}_N - \mathbf{1}_0)^T X (\mathbf{1}_N - \mathbf{1}_0)}$$

where:

$$(\mathbf{1}_N - \mathbf{1}_0)^T X = \begin{bmatrix} 0 & 1 & \dots & N \end{bmatrix} \quad (\mathbf{1}_N - \mathbf{1}_0)^T X (\mathbf{1}_N - \mathbf{1}_0) = N;$$

so:

$$F_{N,0} = \begin{bmatrix} 1 & \frac{1}{N} & \frac{2}{N} & \dots & \frac{N-1}{N} & 1 \\ 0 & 1 & 0 & \dots & \dots & 0 \\ \vdots & \ddots & \ddots & \ddots & & \\ \vdots & & \ddots & \ddots & \ddots & \\ 0 & \dots & \dots & 0 & 1 & 0 \\ 0 & -\frac{1}{N} & -\frac{2}{N} & \dots & -\frac{N-1}{N} & 0 \end{bmatrix} \quad (6.18)$$

By Assumption 14,  $p_i = p_{h,k} = \frac{1}{N+1}$  for all  $1 \leq i \leq \ell = N+1$  (or, equivalently:  $0 \leq h \leq N-1, k = (h+1) \bmod(N+1)$ ) and:

$$\bar{F} = \frac{1}{N+1} \begin{bmatrix} N+1 & \frac{1}{N}+1 & \frac{2}{N}+1 & \dots & \frac{N-1}{N}+1 & 2 \\ 0 & N & 0 & \dots & \dots & 0 \\ & & \ddots & & & \\ & & & \ddots & & \\ 0 & \dots & \dots & 0 & N & 0 \\ 0 & -\frac{1}{N} & -\frac{2}{N} & \dots & -\frac{N-1}{N} & N-1 \end{bmatrix} \quad (6.19)$$

where  $k = (h + 1) \bmod (N + 1)$ , and its eigenvalues can easily be calculated:

$$\Lambda(\bar{F}) = \left[ 1, \frac{N}{N+1}, \dots, \frac{N}{N+1}, \frac{N-1}{N+1} \right]^T \quad (6.20)$$

and therefore:

$$\beta = 1 - \frac{1}{N+1}.$$

In this case,  $\Lambda_{\mathcal{L}}$  cannot be easily expressed analytically as we did for the *1-step* case. However, we have computed  $R$  numerically and we have found that  $R \neq \beta$  in this case, but however  $\beta$  is a tight bound for  $R$  (see Section 7.2).

In both cases (*1-step* and *circle*) the parameter  $\beta$  does not depend on the length of the electric paths between adjacent compensators. In fact, if  $Z = \text{diag}(z(1), \dots, z(N))$ , with  $z(e) > 0$  (and at least an edge  $\tilde{e} \in \mathcal{E}$  such that  $z(\tilde{e}) \neq 1$ ):

$$X = B^T Z B = \begin{bmatrix} 0 & \cdots & \cdots & \cdots & \cdots & 0 \\ 0 & \psi_1 & \psi_1 & \psi_1 & \cdots & \psi_1 \\ 0 & \psi_1 & \psi_2 & \psi_2 & \cdots & \psi_2 \\ 0 & \psi_1 & \psi_2 & \psi_3 & \cdots & \psi_3 \\ \vdots & & & & & \vdots \\ 0 & \psi_N & \psi_N & \psi_N & \cdots & \psi_N \end{bmatrix} \quad (6.21)$$

where:

$$\psi_j = \sum_{e=1}^j z(e) \quad 1 \leq j \leq N.$$

Now:

$$(\mathbf{1}_h - \mathbf{1}_k)^T X = z(e) \cdot [0 \cdots \underbrace{0}_h \underbrace{-1}_k \cdots 1], \quad (\mathbf{1}_h - \mathbf{1}_k)^T X (\mathbf{1}_h - \mathbf{1}_k) = z(e),$$

for  $0 \leq h \leq N-1$ ,  $k = h+1$ ,  $(h, k) = e \in \mathcal{E}$ : they differ from the corresponding vectors in the case with  $\mathbf{Z} = I$  only for the factor  $z(e)$ ; then the matrices  $F_{h,k}$  are the same obtained in (6.17).

In the *circle* case, besides we need also  $F_{N,0}$ ; as:

$$(\mathbf{1}_N - \mathbf{1}_0)^T X = \begin{bmatrix} 0 & \psi_1 & \cdots & \psi_N \end{bmatrix} \quad (\mathbf{1}_N - \mathbf{1}_0)^T X (\mathbf{1}_N - \mathbf{1}_0) = \psi_N,$$

$$F_{N,0} = \begin{bmatrix} 1 & \frac{\psi_1}{\psi_N} & \frac{\psi_2}{\psi_N} & \cdots & \frac{\psi_{N-1}}{\psi_N} & 1 \\ 0 & 1 & 0 & \cdots & \cdots & 0 \\ \vdots & \ddots & \ddots & \ddots & \ddots & \vdots \\ \vdots & \ddots & \ddots & \ddots & \ddots & \vdots \\ 0 & \cdots & \cdots & 0 & 1 & 0 \\ 0 & -\frac{\psi_1}{\psi_N} & -\frac{\psi_2}{\psi_N} & \cdots & -\frac{\psi_{N-1}}{\psi_N} & 0 \end{bmatrix}.$$

## 6.2 Case studies

---

It is not equal to (6.18), but the resulting  $\bar{F}$  has a structure similar to (6.19):

$$\bar{F} = \frac{1}{N+1} \begin{bmatrix} N+1 & \frac{\psi_1}{\psi_N} + 1 & \frac{\psi_2}{\psi_N} + 1 & \cdots & \frac{\psi_{N-1}}{\psi_N} + 1 & 2 \\ 0 & N & 0 & \cdots & \cdots & 0 \\ & & \ddots & & & \\ & & & \ddots & & \\ 0 & \cdots & \cdots & 0 & N & 0 \\ 0 & -\frac{\psi_1}{\psi_N} & -\frac{\psi_2}{\psi_N} & \cdots & -\frac{\psi_{N-1}}{\psi_N} & N-1 \end{bmatrix}.$$

The eigenvalues are:

$$\Lambda(\bar{F}) = \left[ 1, \frac{N}{N+1}, \dots, \frac{N}{N+1}, \frac{N-1}{N+1} \right]^T$$

and:

$$\beta = \frac{N}{N+1}.$$

Thus, this paragraph has confirmed the results of Proposition 23: when the graph describing a microgrid is a line and a *nearest-neighbor clustering choice* has taken, then  $\beta$  assumes its smallest value:

$$R = \beta = 1 - \frac{1}{N}$$

and so we can conclude that this clustering strategy is the optimal one for the problem, at least with respect to  $\beta$ .

Other choices lead to worst results: this is the case of the *circle* strategy, which exhibits a larger value for  $\beta$ .

### 6.2.2 Circular structure

#### Resistance matrix

Consider an electrical network represented by a graph  $\mathcal{G} = (\mathcal{V}, \mathcal{E})$ , with  $|\mathcal{V}| = N+1$  and  $|\mathcal{E}| = N_{\mathcal{E}}$ . Assume that all the nodes in  $\mathcal{G}$  are connected to form a circular path.

The incidence matrix has the following form:

$$A = \begin{bmatrix} -1 & 1 & 0 & \cdots & 0 \\ 0 & \ddots & \ddots & \ddots & \vdots \\ \vdots & \ddots & \ddots & \ddots & 0 \\ \vdots & \ddots & \ddots & \ddots & 1 \\ 1 & \cdots & \cdots & 0 & -1 \end{bmatrix}$$

We assume that the nodes are equally distributed at unitary distances along the circle ( $\mathbf{Z} = I$ ).

The Laplacian matrix is:

$$L = A^T A = \begin{bmatrix} 2 & -1 & 0 & \cdots & 0 & -1 \\ -1 & 2 & -1 & 0 & \cdots & 0 \\ 0 & \ddots & \ddots & \ddots & \ddots & \vdots \\ \vdots & \ddots & \ddots & \ddots & \ddots & 0 \\ 0 & \cdots & 0 & -1 & 2 & -1 \\ -1 & 0 & \cdots & 0 & -1 & 2 \end{bmatrix} \quad (6.22)$$

For the calculus of the matrix  $X$ , we cannot exploit the results of the previous paragraph, because the graph is not a tree and properties of Definition 24 which allow to write  $X$  by (6.14) are not satisfied.

Here we will infer the matrix  $X$  by using the notion of *resistance distance*. Let consider a connected graph associated to an electrical network and replace each edge of it with a resistor of unit resistance. Then the resistance distance  $r_{h,k}$  between two vertices  $h$  and  $k$  of the graph is the effective electrical resistance between the corresponding two nodes of the associate network. By (2.13):

$$r_{h,k} = X_{h,h} + X_{k,k} - 2X_{h,k}. \quad (6.23)$$

As  $\mathcal{G}$  has a circular form, it results:

$$r_{h,k} = \frac{d_{h,k}(N+1-d_{h,k})}{N+1} \quad 0 \leq h, k \leq N \quad (6.24)$$

where  $d_{h,k}$  represents the length of the path between the nodes  $h$  and  $k$  in  $\mathcal{G}$ .

The resistance distance satisfies the following properties:

$$r_{h,k} = r_{k,h} \quad r_{h,k} = r_{(h+1) \bmod (N+1), (k+1) \bmod (N+1)} \quad 0 \leq h, k \leq N; \quad (6.25)$$

moreover, the elements along the main diagonal are equal to zero (as  $d_{h,h} = 0$ ).

A *resistance matrix*  $\mathcal{R}$  can be introduced, whose elements are  $r_{h,k}$ 's: owing to (6.25), the matrix  $\mathcal{R}$  is symmetric and circulant. For example, the resistance matrix related to a graph of 4 nodes (Figure 6.2.2) has the following form:

$$\mathcal{R} = \begin{bmatrix} 0 & a & b & a \\ a & 0 & a & b \\ b & a & 0 & a \\ a & b & a & 0 \end{bmatrix} = \begin{bmatrix} 0 & \frac{3}{4} & 1 & \frac{3}{4} \\ \frac{3}{4} & 0 & \frac{3}{4} & 1 \\ 1 & \frac{3}{4} & 0 & \frac{3}{4} \\ \frac{3}{4} & 1 & \frac{3}{4} & 0 \end{bmatrix}.$$

The following result allows to express the matrix  $X$  in terms of the resistance matrix, inspired by results in [26]:

**Theorem 25.** *The matrix  $X$  can be written as the sum of three terms as:*

$$X = -\frac{1}{2} (\mathcal{R}\Omega + \mathcal{R}Y - \mathbf{1}\mathbf{1}_0^T \mathcal{R}), \quad (6.26)$$

## 6.2 Case studies

where  $\Omega$  is the matrix defined in (5.15), whereas:

$$Y = \frac{1}{N} \begin{bmatrix} 1-N & \cdots & \cdots & 1-N \\ 1 & \cdots & \cdots & 1 \\ \vdots & & & \vdots \\ 1 & \cdots & \cdots & 1 \end{bmatrix}. \quad (6.27)$$

*Proof.* We first prove the following identity:

$$LRL = -2LXL : \quad (6.28)$$

$$\begin{aligned} [LRL]_{h,k} &= \sum_{m=0}^N \sum_{n=0}^N L_{h,m} r_{m,n} L_{n,k} \\ &= \sum_{m=0}^N \sum_{n=0}^N L_{h,m} (X_{m,m} + X_{n,n} - 2X_{n,m}) L_{n,k} \\ &= \sum_{m=0}^N L_{h,m} X_{m,m} \left( \sum_{n=0}^N L_{n,k} \right) + \sum_{n=0}^N L_{n,k} X_{n,n} \left( \sum_{m=0}^N L_{h,m} \right) - 2 \sum_{m,n=0}^N L_{h,m} X_{m,n} L_{n,k} \\ &= -2 \sum_{m=0}^N \sum_{n=0}^N L_{h,m} X_{m,n} X_{n,k} \end{aligned}$$

where we have used the fact that  $\mathbf{1} \in \ker L$  and so  $\sum_{n=0}^N L_{n,k} = \sum_{m=0}^N L_{h,m} = 0$ .

By Lemma 1

$$(XL)\mathcal{R}(LX) = (I - \mathbf{1}\mathbf{1}_0^T) \mathcal{R} (I - \mathbf{1}_0\mathbf{1}^T) = \mathcal{R} - \mathcal{R}\mathbf{1}_0\mathbf{1}^T - \mathbf{1}\mathbf{1}_0^T \mathcal{R} \quad (6.29)$$

as  $\mathbf{1}\mathbf{1}_0^T \mathcal{R}\mathbf{1}_0\mathbf{1}^T = r_{00}\mathbf{1}\mathbf{1}_0^T = 0$ .

By multiplying (6.28) by  $X$  from both left and right, it results:

$$\begin{aligned} X(LRL)X &= -2X(LXL)X \\ &= -2(XL)X(LX) \\ &= -2(I - \mathbf{1}\mathbf{1}_0^T)X(I - \mathbf{1}_0\mathbf{1}^T) \\ &= -2X \end{aligned} \quad (6.30)$$

and comparing (6.29) and (6.30):

$$X = -\frac{1}{2} [\mathcal{R} - \mathcal{R}\mathbf{1}_0\mathbf{1}^T - \mathbf{1}\mathbf{1}_0^T \mathcal{R}]. \quad (6.31)$$

In order to obtain (6.26), we express:

$$\mathbf{1}_0\mathbf{1}^T = \frac{\mathbf{1}\mathbf{1}^T}{N} - Y; \quad (6.32)$$

by remembering that  $\Omega = I - \mathbf{1}\mathbf{1}^T/N$  and by substituting (6.32) into (6.31):

$$X = -\frac{1}{2} \left[ \mathcal{R} \left( I - \frac{\mathbf{1}\mathbf{1}^T}{N} \right) + \mathcal{R}Y + \mathbf{1}\mathbf{1}_0^T \mathcal{R} \right] = -\frac{1}{2} (\mathcal{R}\Omega + \mathcal{R}Y - \mathbf{1}\mathbf{1}_0^T \mathcal{R}).$$

□

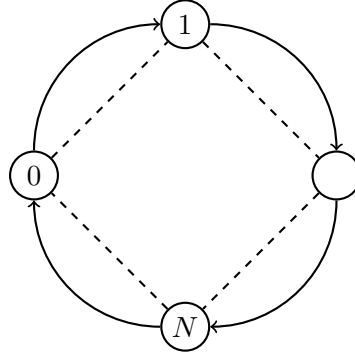


Figure 6.3: Electrical grid represented by a graph with a circular structure (continuous lines represent the electrical lines). All the nodes are assumed to be compensators; in dashed lines are represented the pairs of nodes allowed to communicate.

### Computation of $\beta$

Consider an electrical network represented by a graph  $\mathcal{G} = (\mathcal{V}, \mathcal{E})$ , with  $|\mathcal{V}| = N + 1$  and  $|\mathcal{E}| = N_{\mathcal{E}} = N + 1$  and suppose that  $\mathcal{C} = \mathcal{V}$ . Assume that all the compensators in  $\mathcal{G}$  are connected by one edge, in order to form a circular path and that they are equally distributed at unitary distances along the circle.

We consider the optimization problem where each cluster contains only two compensators, which are adjacent (*nearest-neighbor strategy*); here we will use the same notation of the previous paragraph:

$$\mathcal{C}_i = \mathcal{C}_{h,k} = \{h, k \mid 0 \leq h \leq N, \quad k = (h + 1) \bmod (N + 1)\},$$

and the same for the indices of the involved matrices.

As  $|\mathcal{C}_i| = 2$ ,  $1 \leq i \leq \ell = N + 1$ , then the expression (6.16) for  $F_{h,k}$  can be used and now we calculate the numerator and the denominator of its second addendum.

Notice that we will use the matrix  $X$  instead of the Hessian matrix  $M$  thanks to the assumption  $\mathcal{C} = \mathcal{V}$ .

By (6.26):

$$(\mathbf{1}_h - \mathbf{1}_k)^T X = -\frac{1}{2}(\mathbf{1}_h - \mathbf{1}_k)^T [\mathcal{R} \Omega + \mathcal{R} Y - \mathbf{1}\mathbf{1}_0^T \mathcal{R}] = -\frac{1}{2}(\mathbf{1}_h - \mathbf{1}_k)^T [\mathcal{R} \Omega + \mathcal{R} Y] \quad (6.33)$$

where we have used the fact that  $\mathbf{1}\mathbf{1}_0^T \mathcal{R}$  is a matrix in which each column contains elements of the same value, and so  $(\mathbf{1}_h - \mathbf{1}_k)^T (\mathbf{1}\mathbf{1}_0^T \mathcal{R}) = 0$ .

Let define  $X' = -\frac{1}{2}\mathcal{R} Y$ : this is a matrix in which each row contains elements of the same value given by:

$$X'_{i,j} = -\frac{1}{2}[\mathcal{R} Y]_{i,j} = -\frac{1}{2} \left( \frac{1-N}{N} r_{i,0} + \frac{1}{N} \sum_{n \neq 0} r_{i,n} \right) \quad 0 \leq i, j \leq N;$$

## 6.2 Case studies

then  $(\mathbf{1}_h - \mathbf{1}_k)^T X'$  is a vector whose elements are all equal to:

$$\begin{aligned} [(\mathbf{1}_h - \mathbf{1}_k)^T X']_j &= -\frac{1}{2} \frac{(1-N)(r_{h,0} - r_{k,0}) + (r_{h,N} - r_{h,0})}{N} \\ &= \frac{r_{h,0} - r_{k,0}}{2}, \quad 0 \leq j \leq N, \end{aligned}$$

where we have used (6.25).

The vector  $(\mathbf{1}_h - \mathbf{1}_k)^T \mathcal{R} \Omega$  can be calculated by exploiting the definition of  $\Omega$ , whose elements are:

$$[\Omega]_{i,j} = \begin{cases} \frac{N-1}{N} & i = j \\ -\frac{1}{N} & i \neq j \end{cases} \quad 0 \leq i, j \leq N.$$

It implies that  $X'' := -\frac{1}{2} \mathcal{R} \Omega$  has the same structure of  $\mathcal{R}$  (it is symmetric and circulant), and, by using again (6.25):

$$\begin{aligned} [(\mathbf{1}_h - \mathbf{1}_k)^T X'']_j &= X''_{h,j} - X''_{k,j} = -\frac{1}{2} ([\mathcal{R} \Omega]_{h,j} - [\mathcal{R} \Omega]_{k,j}) \\ &= -\frac{1}{2} \left[ \frac{N-1}{N} r_{h,j} + \left(-\frac{1}{N}\right) \sum_{m \neq j} r_{h,m} - \frac{N-1}{N} r_{k,j} - \left(-\frac{1}{N}\right) \sum_{m \neq j} r_{k,m} \right] \\ &= -\frac{1}{2} \left( \frac{N-1}{N} (r_{h,j} - r_{k,j}) + \frac{1}{N} (r_{h,j} - r_{k,j}) \right) \\ &= \frac{r_{k,j} - r_{h,j}}{2}. \end{aligned}$$

By (6.33):

$$\begin{aligned} (\mathbf{1}_h - \mathbf{1}_k)(\mathbf{1}_h - \mathbf{1}_k)^T X &= -\frac{1}{2} (\mathbf{1}_h - \mathbf{1}_k)(\mathbf{1}_h - \mathbf{1}_k)^T (\mathcal{R} \Omega + \mathcal{R} Y) \\ &= (\mathbf{1}_h - \mathbf{1}_k)(\mathbf{1}_h - \mathbf{1}_k)^T (X'' + X') \\ &= (\mathbf{1}_h - \mathbf{1}_k) \mathbf{1}^T \Gamma_{h,k} + \frac{r_{h,0} - r_{k,0}}{2} (\mathbf{1}_h - \mathbf{1}_k) \mathbf{1}^T \end{aligned}$$

where  $\Gamma_{h,k} = \frac{1}{2} \text{diag}\{r_{k,0} - r_{h,0}, \dots, r_{k,N} - r_{h,N}\}$ .

The denominator of the second addendum in (6.16) is given by:

$$\begin{aligned} (\mathbf{1}_h - \mathbf{1}_k)^T X (\mathbf{1}_h - \mathbf{1}_k) &= -\frac{1}{2} (\mathbf{1}_h - \mathbf{1}_k)^T [\mathcal{R} \Omega + \mathcal{R} Y] (\mathbf{1}_h - \mathbf{1}_k) \\ &= (\mathbf{1}_h - \mathbf{1}_k)^T [X' + X''] (\mathbf{1}_h - \mathbf{1}_k) \\ &= (\mathbf{1}_h - \mathbf{1}_k)^T X'' (\mathbf{1}_h - \mathbf{1}_k) \\ &= X''_{h,h} - X''_{k,h} - (X''_{h,k} - X''_{k,k}) \\ &= 2(X''_{h,h} - X''_{h,k}) \\ &= 2(X''_{0,0} - X''_{0,1}) = r_{0,1} = \frac{N}{N+1} \end{aligned} \tag{6.34}$$

where we have exploited the structure of the matrix  $\mathcal{R} Y$  described before (all rows are equal and so:  $\mathcal{R} Y(\mathbf{1}_h - \mathbf{1}_k) = \mathbf{0}$ ), the fact that  $\mathcal{R} \Omega$  is a symmetric and circulant matrix and the properties in (6.24) and (6.25).

We can now construct the matrices  $F_{h,k}$ 's as:

$$\begin{aligned} F_{h,k} &= I - \frac{(\mathbf{1}_h - \mathbf{1}_k)(\mathbf{1}_h - \mathbf{1}_k)^T X}{(\mathbf{1}_h - \mathbf{1}_k)^T X (\mathbf{1}_h - \mathbf{1}_k)} \\ &= I - \frac{1}{r_{0,1}} (\mathbf{1}_h - \mathbf{1}_k)(\mathbf{1}_h - \mathbf{1}_k)^T (X' + X'') \end{aligned} \quad (6.35)$$

and, by Assumption (14), which implies  $p_i = p_{h,k} = \frac{1}{N+1}$ ,  $1 \leq i \leq \ell = N+1$  (or, equivalently:  $0 \leq h \leq N$ ,  $k = (h+1) \bmod(N+1)$ ):

$$\begin{aligned} \bar{F} = \mathbb{E}[F] &= \frac{1}{N+1} \sum_{h=0}^N F_{h,k} \\ &= \frac{1}{N+1} \sum_{h=0}^N \left[ I - \frac{1}{r_{0,1}} (\mathbf{1}_h - \mathbf{1}_k)(\mathbf{1}_h - \mathbf{1}_k)^T (X' + X'') \right] \\ &= I - \frac{1}{N+1} \frac{1}{r_{0,1}} (\bar{F}' + \bar{F}''), \end{aligned} \quad (6.36)$$

where:

$$\bar{F}' = \sum_{h=0}^N (\mathbf{1}_h - \mathbf{1}_k)(\mathbf{1}_h - \mathbf{1}_k)^T X' \quad \bar{F}'' = \sum_{h=0}^N (\mathbf{1}_h - \mathbf{1}_k)(\mathbf{1}_h - \mathbf{1}_k)^T X''.$$

It can be noticed that:

$$\bar{F}'' = \frac{1}{2} \begin{bmatrix} r_{N,0} - 2r_{0,0} + r_{1,0} & r_{N,1} - 2r_{0,1} + r_{1,1} & \cdots & r_{N,N} - 2r_{0,N} + r_{1,N} \\ r_{0,0} - 2r_{1,0} + r_{2,0} & r_{0,1} - 2r_{1,1} + r_{2,1} & \cdots & r_{0,N} - 2r_{1,N} + r_{2,N} \\ \vdots & \vdots & \ddots & \vdots \\ r_{N-1,0} - 2r_{N,0} + r_{0,0} & r_{N-1,1} - 2r_{N,1} + r_{0,1} & \cdots & r_{N-1,N} - 2r_{N,N} + r_{0,N} \end{bmatrix} \quad (6.37)$$

while:

$$\bar{F}' = -\frac{1}{2} \begin{bmatrix} r_{N,0} - 2r_{0,0} + r_{1,0} & r_{N,0} - 2r_{0,0} + r_{1,0} & \cdots & r_{N,0} - 2r_{0,0} + r_{1,0} \\ r_{0,0} - 2r_{1,0} + r_{2,0} & r_{0,0} - 2r_{1,0} + r_{2,0} & \cdots & r_{0,0} - 2r_{1,0} + r_{2,0} \\ \vdots & \vdots & \ddots & \vdots \\ r_{N-1,0} - 2r_{N,0} + r_{0,0} & r_{N-1,0} - 2r_{N,0} + r_{0,0} & \cdots & r_{N-1,0} - 2r_{N,0} + r_{0,0} \end{bmatrix} \quad (6.38)$$

By exploiting the properties (6.24) and (6.25) of the resistance distance, we can write the elements of matrices  $\bar{F}'$  and  $\bar{F}''$  as combinations of elements of the only first row of  $\mathcal{R}$ , i.e. elements such as  $r_{0,j}$ ,  $0 \leq j \leq N$ .

Neglecting the factor  $\frac{1}{2}$ ,  $\bar{F}'$  and  $\bar{F}''$  contain elements:

$$\begin{aligned} r_{(i-1) \bmod(N+1),j} - 2r_{i,j} + r_{(i+1) \bmod(N+1),j} &= r_{j,(i-1) \bmod(N+1)} - 2r_{j,i} + r_{j,(i+1) \bmod(N+1)} \\ &= \begin{cases} r_{0,1} + r_{0,N} & i = j \\ r_{0,i-j-1} - 2r_{0,i-j} + r_{0,i-j+1} & j < i, j \neq 0 \vee i \neq N \\ r_{0,N+1(i-j)-1} - 2r_{0,N+1+(i-j)} + r_{0,N+1+(i-j)+1} & j > i+1 \\ r_{0,N-1} - 2r_{0,N} + r_{0,0} & \text{otherwise} \end{cases} \end{aligned}$$



## 6.2 Case studies

---

with  $0 \leq i, j \leq N$ .

By (6.24):

$$r_{(i-1) \bmod (N+1), j} - 2r_{i,j} + r_{(i+1) \bmod (N+1), j} = \begin{cases} -\frac{2}{N+1} & i \neq j \\ \frac{2N}{N+1} & i = j. \end{cases} \quad (6.39)$$

It means that matrix  $\bar{F}''$  has all elements equal to  $-\frac{1}{N+1}$ , except from the main diagonal, whose elements are  $\frac{N}{N+1}$ ; the matrix  $\bar{F}'$  has the elements in the first row equal to  $-\frac{N}{N+1}$  and all the others are  $\frac{1}{N+1}$ .

Thus, by (6.36), (6.37), (6.38) and (6.39):

$$\begin{aligned} \bar{F} &= I - \frac{1}{N+1} \frac{1}{r_{0,1}} (\bar{F}' + \bar{F}'') \\ &= I - \frac{1}{N} \begin{bmatrix} 0 & -1 & -1 & \cdots & -1 \\ 0 & 1 & 0 & \cdots & 0 \\ \vdots & \ddots & \ddots & \ddots & \vdots \\ \vdots & & \ddots & \ddots & 0 \\ 0 & \cdots & \cdots & 0 & 1 \end{bmatrix} = \frac{1}{N} \begin{bmatrix} N & 1 & 1 & \cdots & 1 \\ 0 & N-1 & 0 & \cdots & 0 \\ \vdots & \ddots & \ddots & \ddots & 0 \\ \vdots & & \ddots & \ddots & 0 \\ 0 & \cdots & \cdots & 0 & N-1 \end{bmatrix}. \end{aligned}$$

As the matrix  $\bar{F}$  is triangular, its eigenvalues can be easily deduced as the elements along its main diagonal:

$$\Lambda(\bar{F}) = \left[ 1, \frac{N-1}{N}, \dots, \frac{N-1}{N} \right]^T$$

and, according to (5.23):

$$\beta = \frac{N-1}{N}.$$

Summarizing, in this paragraph we have tried to extend the results of the Section 6.2.1 to a more complicated topology of the network: a graph consisting of a set of nodes distributed along a circle.

We have analytically shown that the results of Proposition 23 still hold, provided that the compensators are equally distributed at unitary distances along the circle (i.e. it must be  $\mathbf{Z} = I$ : in Section 7.2 we will show that this result does not hold if this assumption is not satisfied, differently from the case of the line topology):

$$\beta = 1 - \frac{1}{N},$$

like when nodes were distributed along the line.

It is a further confirmation that the *nearest-neighbor clustering choice* is the optimal strategy for our problem, at least with respect to  $\beta$ , which will be shown to be a tight bound of  $R$  in Section 7.2.

Moreover, we will consider more general topologies for the grid and we will see that the *nearest-neighbor strategy* is still a good choice for the problem by simulations.



# Simulations and numerical results

---

In this section we present numerical simulations to validate both the models presented in the previous chapters and the randomized algorithm proposed in Chapter 4.

## 7.1 Validation of the static model

We considered the microgrid sketched in Figure 7.1. We assumed the following parameter values:

- nominal voltage at the PCC node ( $v = 0$ ): 230 V;
- nominal operating frequency:  $f_0 = 50$  Hz;
- lines' characteristic resistance:  $0.16 \text{ m}\Omega/\text{m}$
- lines' characteristic inductance:  $1 \text{ }\mu\text{H}/\text{m}$ ;
- length of the lines: uniformly distributed between 50 m and 200 m;
- injected powers:  $s(v) = |s(v)|e^{j\phi(v)}$ , with  $s(v)$  uniformly distributed between  $-10$  kW and  $0$  kW, and  $\cos \phi$  uniformly distributed between  $0.7$  and  $1$ .

We estimated the quality of the linear approximate model proposed in Section 2.2, comparing the node voltages obtained by solving the nonlinear system (2.7) and the ones computed via (2.11) by using the approximation (2.28).

As shown in Figure 7.2, the approximation error results to be negligible, and it holds even in the case in which voltage drops get close to the maximum that is generally



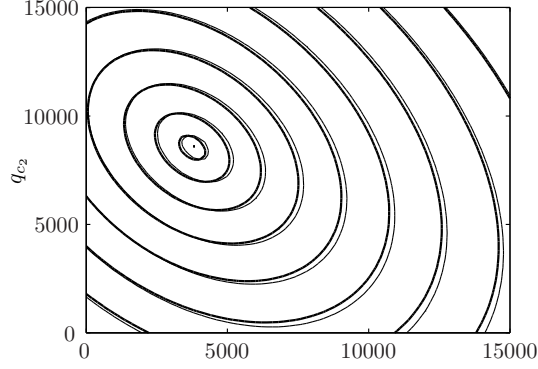


Figure 7.3: Contour plot of the exact distribution losses (thick line) and of the cost function whose gradient is given by the voltage measures, according to (3.11) (thin line).

## 7.2 Performance of the proposed algorithm

In this section, we simulate the behavior of the algorithm proposed in Chapter 4, and the performance of different clustering choices.

In particular, we confirm and extend numerically the results obtained in the previous chapter.

We considered a tree with 33 nodes and an average of 2.4 children for each internal node (not leaves), of height 6. We supposed that only nodes that are neighbors on the tree are allowed to communicate (*nearest neighbor clustering choice*).

We obtained numerically that Proposition 23 holds, being:

$$\beta = 1 - \frac{1}{32} = 0.9688,$$

and moreover:  $R = \beta$ .

If we make another clustering choice (*complete clustering choice*: each pair of nodes is allowed to communicate), then the results are different; for the aforementioned tree:

$$\beta = 0.9967 \quad R = 0.9937.$$

The same occurs when we consider a line topology for the grid: the *nearest-neighbor* strategy returns exactly the smallest possible value for  $\beta$  and so we can state that it is the optimal clustering choice for the problem.

In these cases, we can say that enabling communication among agents placed in distant points of the grid is detrimental for the convergence speed of the algorithm, whereas the optimal strategy consists in choosing a hypergraph  $\mathcal{H}$  which resembles the graph describing the physical interconnections of the network.

At the moment, we do not know if the result of Proposition 23 holds also when  $\mathcal{G}$  is not a tree. In Section 6.2.2, we have considered the case in which nodes are equally

	$N = 10$		$N = 50$		$N = 100$
	$\beta$	$R$	$\beta$	$R$	$\beta$
Line topology					
nearest-neighbor	0.8889	0.8889	0.9796	0.9796	0.9899
circle	0.9000	0.8943	0.9800	0.9798	0.9900
complete	0.9687	0.9480	0.9984	0.9972	0.9996
Circular topology					
nearest-neighbor	0.8889	0.8889	0.9796	0.9796	0.9899
star	0.9877	0.9760	0.9996	0.9992	0.9999
complete	0.9603	0.9336	0.9979	0.9960	0.9994

Table 7.1: Exact convergence rate  $R$  and bound  $\beta$  for different network lengths and different grid and communication topologies.

distributed at unitary distances along a circle. We have found that, if we assume a *nearest-neighbor clustering choice*, it still holds:

$$R = \beta = 1 - \frac{1}{N}.$$

Notice that it is true if we assume that  $\mathbf{Z} = I$ : the result does not hold if we choose a random diagonal matrix as  $\mathbf{Z}$ . For example, if:

$$\mathbf{Z} = \text{diag}(0.6432, 0.0501, 0.3064, 0.0586, 0.8447, 0.8683, 0.4044, 0.8980, 0.9415, 0.5731),$$

then:

$$\beta = 0.8990 \neq 1 - \frac{1}{N} = 0.9.$$

Table 7.1 contains the values of  $R$  and  $\beta$  for the topologies of the network analyzed in the previous chapter (line and circular topologies). It can be noticed that the values of  $R$  and  $\beta$  are very similar and so we can say that  $\beta$  is really a tight bound for  $R$ . This justifies the choice of including the case of a larger network, for which the problem of computing  $R$  could be numerically intractable.

Finally, we considered a network of 30 nodes, 11 of which are compensators (see the top part of Figure 7.5). We chose line impedances and loads similar to the ones in the previous section, and we considered the two following clustering choices:

- *nearest-neighbor gossip*: based on the result stated in Proposition 23, we enabled pairwise communication between nodes whose distance in the electric grid is lower than a given threshold; notice however that the hypotheses of Proposition 23 are not precisely verified, as the graph is not a tree;

## 7.2 Performance of the proposed algorithm

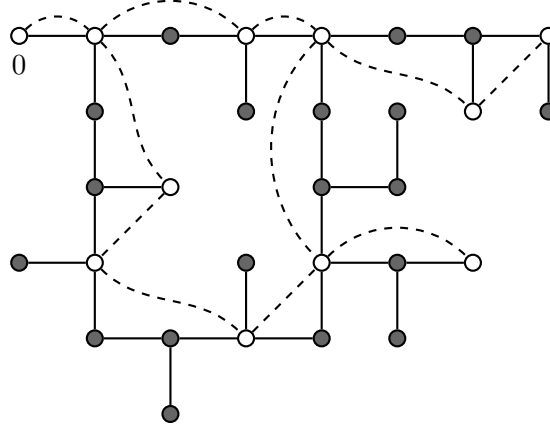


Figure 7.4: Graph of a network: compensators are in white, loads in gray. The dashed line represents the hypergraph  $\mathcal{H}$  when a *nearest-neighbor* clustering choice has taken.

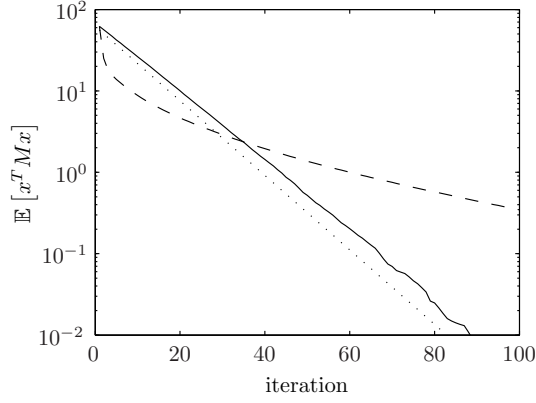


Figure 7.5: Simulation of the behavior of the algorithm, when applied to the network in Figure 7.4. The algorithm behavior (averaged over  $10^3$  realizations) has been plotted for two different clustering choices: *nearest-neighbor gossip* (solid line) and *star topology* (dashed). The dotted line represent the best possible performance.

- *star topology*: clusters are in the form  $\mathcal{C}_i = \{0, v\}$  for all  $v \in \mathcal{C}$ . The reason of this choice is that, as 0 is the PCC, the constraint  $\mathbf{1}^T q = 0$  is inherently satisfied: whatever variation in the injected reactive power is applied by  $v$ , it is automatically compensated by a variation in the demand from the transmission grid via the PCC.

The results of simulations are plotted in the bottom of Figure 7.5, together with the best achievable performance as given in Theorem 22.

The performance of the *nearest-neighbor gossip* algorithm still confirm to be better than the star topology, as Proposition 23 suggests.

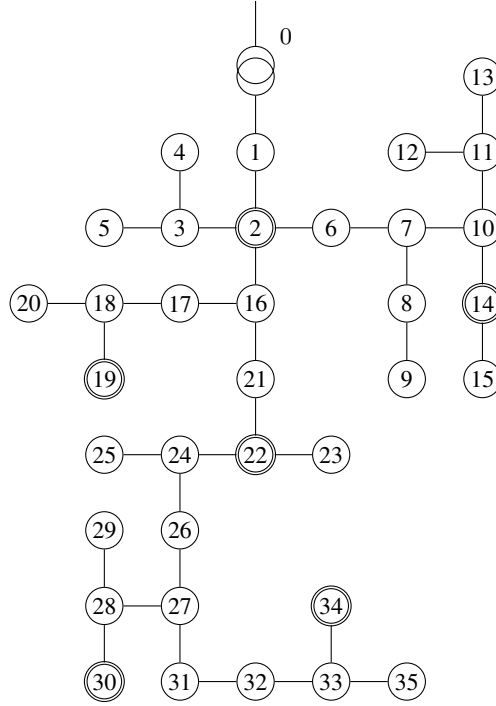


Figure 7.6: Graph describing a microgrid based on the IEEE37 test feeder. Circled nodes represent compensators, the others denote loads.

### 7.3 Dynamic model

In this section we validate the approximation that yielded to the linear dynamic model (4.13), by comparing its behavior with the nonlinear dynamics described by (4.9).

For this analysis, we used the microgrid in Figure 7.3: it is a 4.8 kV testbed inspired from the standard test feeder IEEE37 [28]. We however assumed that loads are balanced, and therefore all currents and signals can be described in a single-phase phasorial notation.

Following the modeling proposed in Section 4.3.1, we assumed that every node (but the PCC) behaves as a constant-power device with a first order dynamic. A quite short time constant of 1.6 ms has been chosen to describe the fast dynamic behavior of the compensators inverters, while the time constants of the loads have been distributed between 200 ms and 10 s.

A step change of 60 kVAR in the reference for the injected reactive power has been commanded to the compensator corresponding to node 30.

The first graph in Figure 7.7 shows how the voltage at the same node (30) exhibits a rich dynamic behavior, due to the coupling of many nonlinear systems. Indeed, even though the inverter dynamic response is very fast, the slower behavior of the loads affect the voltage response: after an initial quick rise, the voltage approaches its steady state value quite slowly.



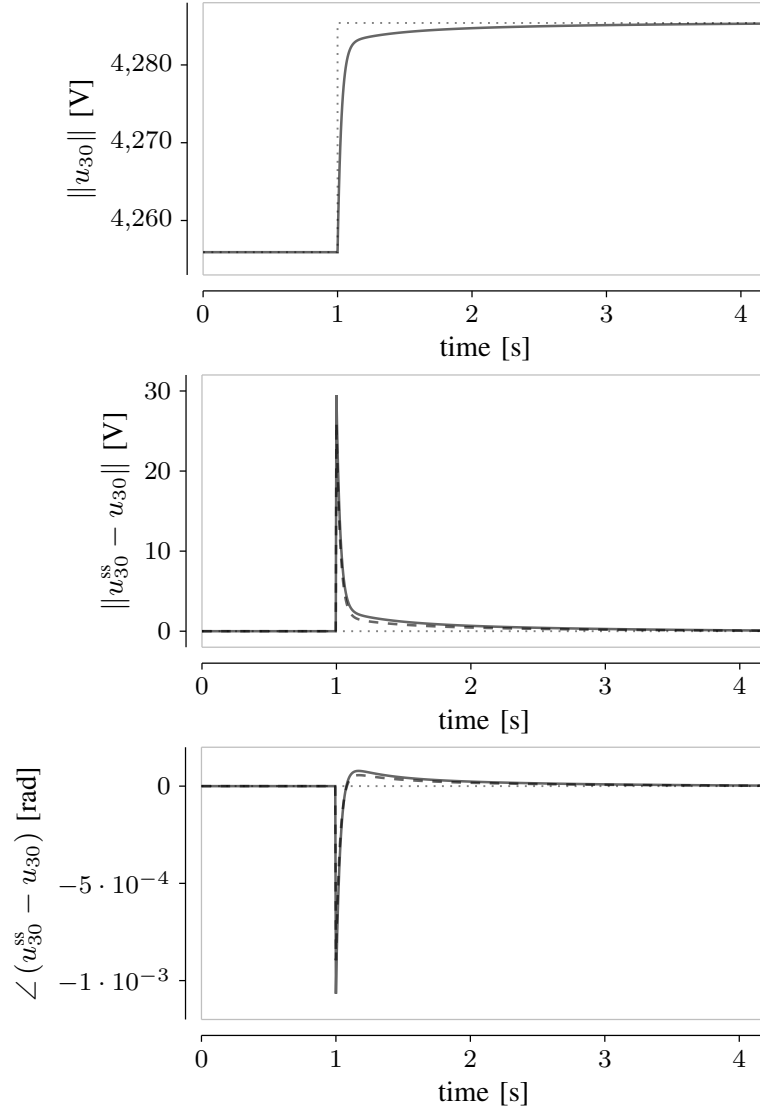


Figure 7.7: Voltage at node 30, after a step change in the reactive power injected by node 30. The dashed in the second and third panel is the output of the approximate linear model.

The dotted line in the same graph shows the value of the voltage  $u_{30}^{ss}$ , which is the voltage corresponding to the solution of the static power flow equations. The second and third panel in Figure 7.7 show the absolute value and the angle of the error between  $u_{30}$  and  $u_{30}^{ss}$ . The dashed line corresponds to the linear approximate model (4.13), which appears to be extremely close to the output of the nonlinear model.

In Figure 7.8, the same quantities have been plotted for another node (22), which kept its power reference constant while node 30 was actuating the system. This figure shows how the effect of actuation in one point of the microgrid propagates to other nodes, causing similar transients in the voltage measurements of other nodes. It also shows how the approximated linear model correctly describes this behavior.

Figure 7.9 shows how the same step change in the reactive power injected by node 30 affects the amount of reactive power flowing into the microgrid from the PCC.

### 7.3.1 Eigenvalue analysis

In this paragraph, we show the position of the eigenvalues of the linear model proposed, for the grid shown in Figure 7.3.

From Figure 7.10 we can state that the global system has a worse dynamic behaviour than each single node, in fact the position of the dominant eigenvalue of the state update matrix  $\Gamma$  in (4.13) lies at the right of all the eigenvalues  $-\frac{1}{\tau_v}$  (corresponding to the ideal case in which  $u_0 = \infty$ ).

In the same figure, the dominant eigenvalues of the system are shown when the nominal voltage has changed: obviously, decreasing the value of  $u_0$ , the dominant eigenvalues move towards the imaginary axis. It is possible that they become positive, because the nominal voltage is not sufficient to support the burden of the network. However, it does not necessarily mean that the system is unstable, in fact we are analyzing the eigenvalues of a linear approximate version of the exact model, even though it surely means that the system is "less stable".

In Figure 7.10 we analyze the position of the dominant eigenvalues of the system when increasing the number of the nodes of the network. Adding a little number of nodes does not affect the position of the eigenvalues; when the dimension of the grid becomes very different than the original network, then the scenario can deeply change, even though this fact is strongly dependent on the parameters of the grid.

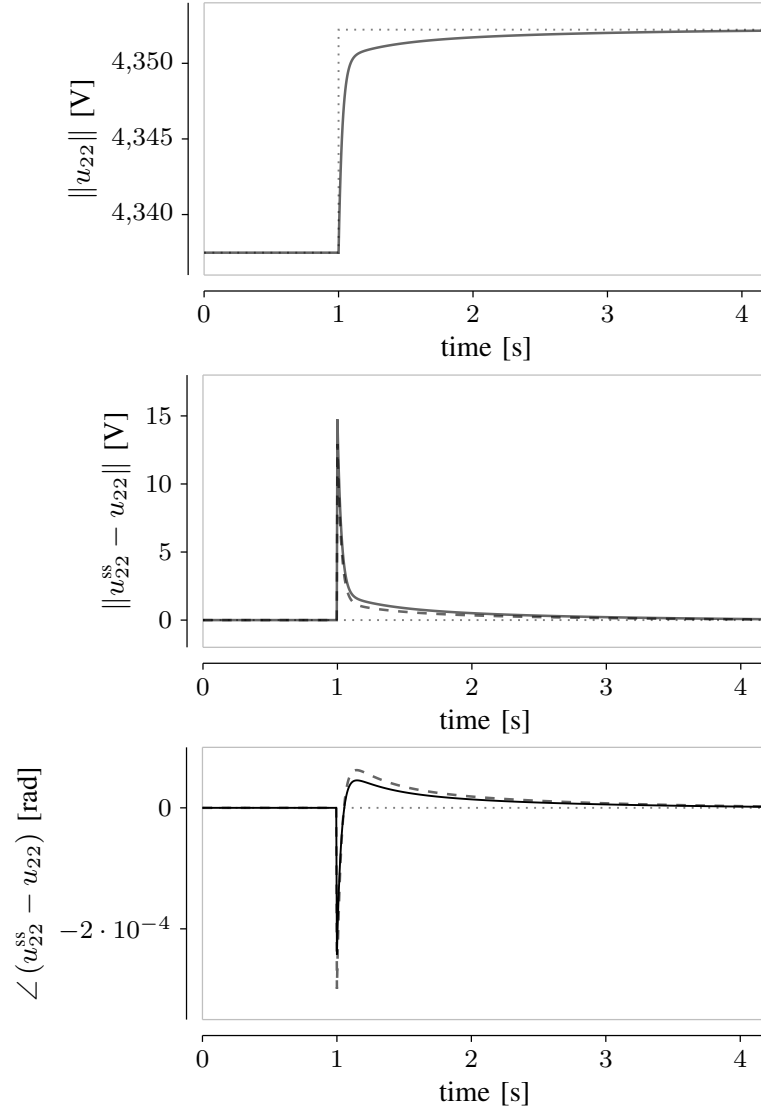


Figure 7.8: Voltage at node 22, after a step change in the reactive power injected by node 30. The dashed in the second and third panel is the output of the approximate linear model.

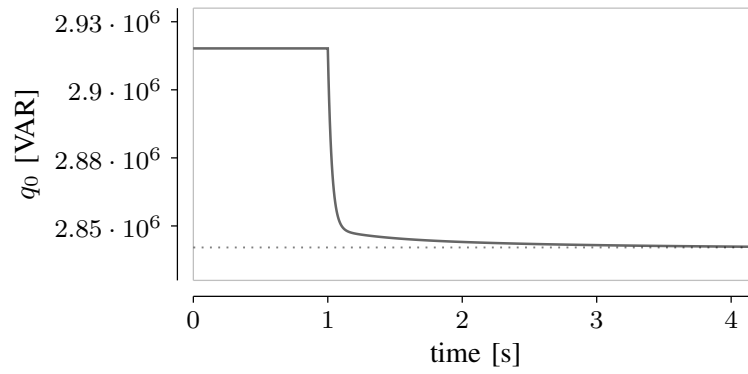


Figure 7.9: Reactive power flowing through the PCC, after a step change in the reactive power injected by node 30.

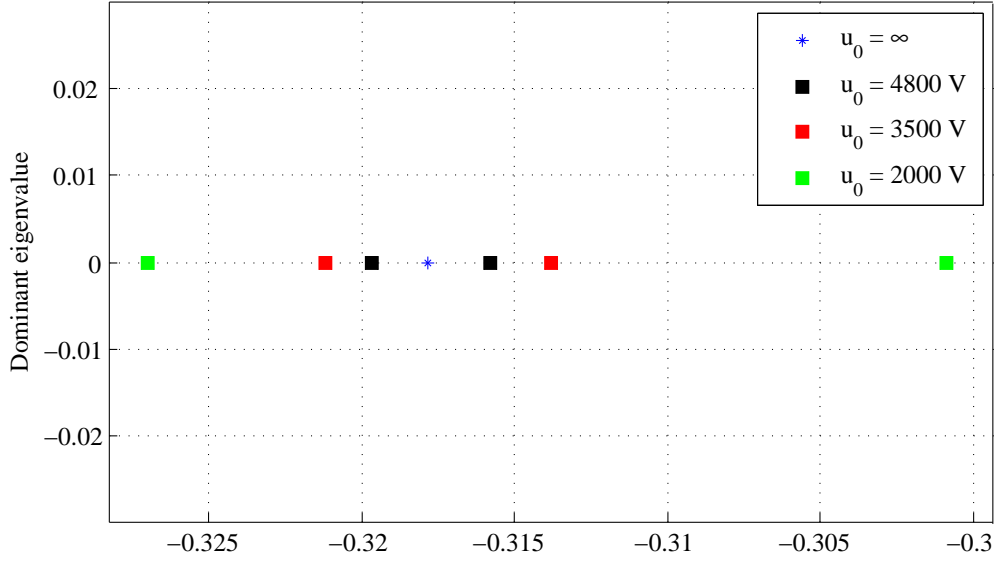


Figure 7.10: Positions of the dominant eigenvalue of the model (4.13) related to the network in Figure 7.3, for different values of  $u_0$ .

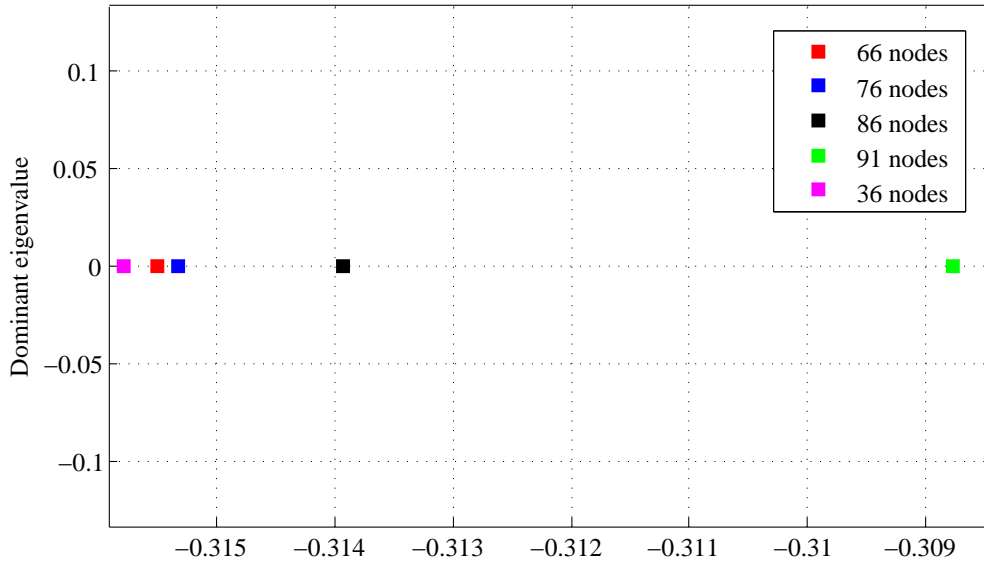


Figure 7.11: Positions of the dominant eigenvalue of the model (4.13) related to a network of different dimensions. In purple it is represented the dominant eigenvalue of the model related to the grid in Figure 7.3; the others have been obtained by adding nodes distributed along a line to the node 35.

# Conclusions

---

In this thesis we have considered the problem of optimal reactive power compensation in smart microgrids. It has been formulated as a quadratic optimization problem and this fact simplifies the studies: robust solvers are available for such problems and performance analysis becomes tractable.

In order to solve this problem, a randomized distributed algorithm, has been proposed: we have chosen such an algorithm owing to the typical characteristics that a smart microgrid could present.

The idea of the algorithm is the decomposition of the minimization problem into optimization subproblems, each one related to a subset of compensators (cluster); the agents belonging to a cluster are the ones able to communicate with each other: in fact we assume them to have only local knowledge of the system structure and the state (this is the reason we think a distributed algorithm is a preferable choice for our problem).

When a cluster is randomly selected, agents belonging to it solve their corresponding optimization subproblem by the Newton's method, which guarantees a fast (1-step) convergence to its optimum; the resolution of this subproblem allows these agents to update the amount of reactive power they inject, while the agents belonging to the other clusters keep their states constant.

Thus, each iteration of the algorithm make the state of the system change. This variation in the amount of reactive power injected at compensators affects the grid voltages, which are subject to a transient interval time. So we have proposed also a dynamic model of the microgrid: it allows an input-output relation between the complex power references commanded to compensators and their voltage measurements.

An approximation of this model has led to a linear system, which allows to employ tools such as eigenvalue analysis, transfer function, etc. In particular, by the position of the dominant eigenvalue of the system, it is possible to have an estimate of how long

after changing the vector  $q$  the grid voltages attain a new steady state, and so we obtain a lower bound on the interval time between consecutive iterations of the algorithm.

For the analysis of the designed algorithm, we have proposed a metric for the performance of the algorithm, for which we are able to provide a bound on the best achievable performance. We have found that, when the graph representing the microgrid is a tree, clustering agents which are close in the network is the optimal strategy for the speed of convergence of the algorithm.

Similar results (but in this case it is necessary taking some assumptions more) have been obtained when the agents are distributed to form a circular path and a short-range communication is imposed again.

However, simulations suggest the *nearest-neighbor* strategy is better than other choices also for other topologies of the network.

Future investigation could study other configurations of the grid, in order to confirm and extend analytically these issues.

Moreover, a next step could be validating the dynamic model with more detailed simulators or experimental testbeds, with loads having different steady-state characteristics and different dynamic behaviours.

# Convex optimization problems

---

An optimization problem is a problem of the form:

$$\begin{aligned} \min \quad & f(x) \\ \text{subject to} \quad & f_i(x) \leq 0, \quad i = 1, \dots, m \\ & h_i(x) = 0, \quad i = 1, \dots, p \end{aligned} \tag{A.1}$$

where  $x \in \mathbb{R}^n$  is the *optimization variable*,  $f: \mathbb{R}^n \rightarrow \mathbb{R}$  is the *objective function*,  $f_i: \mathbb{R}^n \rightarrow \mathbb{R}$  are the *inequality constraint functions* and  $h_i: \mathbb{R}^n \rightarrow \mathbb{R}$  are the *equality constraint functions*.

The goal is finding a  $x$  that minimizes  $f(x)$  among all  $x$  satisfying the  $m + p$  constraints.

The *optimal value* of the problem (A.1) is defined as:

$$p^{\text{opt}} = \inf\{f(x) \mid f_i(x) \leq 0, \ i = 1, \dots, m; \ h_i(x) = 0, \ i = 1, \dots, p\}$$

and it is achieved if the problem is solvable, i.e. there exists a (*globally*) *optimal point*  $x^{\text{opt}}$  such that  $x^{\text{opt}}$  is feasible (i.e.  $x^{\text{opt}}$  satisfies all the constraints in (A.1)) and  $f(x^{\text{opt}}) = p^{\text{opt}}$ .

It can be very hard to find optimal points; typically it is easier determining locally optimal points.

A point  $x^*$  is *locally optimal* if there exists a  $\epsilon > 0$  such that:

$$f(x^*) = \inf\{f(x) \mid f_i(x) \leq 0, \ i = 1, \dots, m; \ h_i(x) = 0, \ i = 1, \dots, p, \|x - x^*\|_2 \leq \epsilon\}.$$

Each global optimal point (if there exists) is also a locally optimal point, but the contrary is not generally true. However, there exist particular classes of optimization problems (i.e. convex optimization problems) in which each locally optimal point is also a globally optimal point.

A convex optimization problem is one of the form (A.1), where the functions  $f, f_1, \dots, f_m$  are convex and the equality constraint functions  $h_i(x) = a_i^T x - b_i$  are affine. An important property is that the feasible set, i.e. the set of all feasible points

$$\mathcal{X} = \{x \mid f_i(x) \leq 0, i = 1, \dots, m; h_i(x) = 0, i = 1, \dots, p\},$$

results to be convex.

Moreover, for convex optimization problems, any locally optimal point is also (globally) optimal.

So, we can state the following optimality criterion, whose proof can be found in [16].

**Proposition 26.** *Consider a convex optimization problem and let  $f$  be the objective function  $f$  differentiable. Then the point  $x$  is optimal if and only if:*

$$\begin{cases} x \in \mathcal{X} \\ \nabla f(x)^T(y - x) \geq 0 \quad \forall y \in \mathcal{X} \end{cases} \quad (\text{A.2})$$

## A.1 Convex optimization problems with equality constraints only

Let consider the convex optimization problem (A.1), where there are equality constraints but no inequality constraints; it can be expressed as follows:

$$\begin{aligned} \min \quad & f(x) \\ \text{subject to} \quad & Ax = b, \quad A \in \mathbb{R}^{p \times n} \end{aligned}$$

Let assume that the feasible set  $\mathcal{X}$  is nonempty (otherwise the problem is unfeasible). The optimality condition (A.2) for a feasible  $x$  can be expressed saying that

$$\nabla f(x)^T(y - x) \geq 0 \quad \forall y \in \mathcal{X} \quad (\text{A.3})$$

must hold for all  $y$  such that  $Ay = b$ .

If  $x$  is feasible, each feasible  $y$  has the form  $y = x + v$  with  $v \in \ker A$ . So (A.3) can be expressed as:

$$\nabla f(x)^T v \geq 0 \quad \forall v \in \ker A.$$

If a linear function is nonnegative on a subspace, then it must be zero on the subspace. So:

$$\nabla f(x) \perp \ker A.$$

As  $(\ker A)^\perp = \text{Im}(A^T)$ , then the (A.3) can be expressed as  $\nabla f(x) \in \text{Im } A^T$ , i.e. there exists a  $\rho \in \mathbb{R}^p$  such that:

$$\nabla f(x) + A^T \rho = 0.$$



## A.2 Descent methods

---

So, considering a convex optimization problem with equality constraints only like (A.3), the optimality condition (A.2) can be expressed by:

$$\begin{cases} Ax = b \\ \nabla f(x) + A^T \rho = 0, \exists \rho \in \mathbb{R}^p \end{cases} \quad (\text{A.4})$$

## A.2 Descent methods

In this section we will describe a numerical method for solving convex optimization problems, i.e. finding a solution of (A.2).

Solving this optimality system analytically can be very hard, so usually the optimization problems are solved by an iterative algorithm which computes a sequence of point  $x^{(0)}, x^{(1)}, \dots \in \text{dom} f$  with  $f(x^{(k)}) \rightarrow p^*$  as  $k \rightarrow \infty$ . The algorithm is terminated when  $f(x^{(k)}) - p^* \leq \epsilon$  where  $\epsilon > 0$  is a specified tolerance.

In particular, these algorithms produce a sequence  $x^{(k)}$  such that:

$$x^{(k+1)} = x^{(k)} + t^{(k)} \Delta x^{(k)},$$

where  $k$  denotes the iteration number,  $\Delta x$  is a vector called *step direction* and  $t^{(k)} \geq 0$  is a scalar called *step size*.

Here we present methods called *descent method*, i.e.:

$$f(x^{(k+1)}) < f(x^{(k)}),$$

except when  $x^{(k)}$  is optimal. They are characterized by the calculus of the step direction and step size. For example, there exist the *Newton's Method*, the *Gradient Method*, the *Steepest Descent Method* etc.

In the next paragraph we will present one of the most important algorithms for the optimization problems: *Newton's Method*. In particular, it is considered the *pure* Newton's Method, where a fixed step size  $t^{(k)} = t = 1$  is used.

### A.2.1 Newton's method for unconstrained problems

Consider a convex optimization problem:

$$\min f(x).$$

The vector

$$\Delta x = -[\nabla^2 f(x)]^{-1} \nabla f(x)$$

is called *Newton step* of  $f$  at  $x$ . It can be interpreted and motivated in several ways.

Consider the second-order Taylor approximation of  $f$  at  $x$ :

$$\hat{f}(x+v) = f(x) + \nabla f(x)^T v + \frac{1}{2} v^T \nabla^2 f(x) v;$$

it is a convex quadratic function of variable  $v$  and it is minimized by  $v = \Delta x$ .

Thus,  $\Delta x$  is what should be added to  $x$  in order to minimize the second-order approximation of  $f$  at  $x$ . So, if  $f$  is quadratic, then  $x + \Delta x$  is the exact minimizer of  $f$ , and, intuitively, if  $f$  is nearly quadratic, then  $x + \Delta x$  is a good estimate of the minimizer of  $f$ .

Newton's method presents many advantages over other Descent Methods, which makes it one of the most important algorithms for the optimization problems. In fact, Newton's Method presents a rapid convergence (in particular, a quadratic convergence near  $x^{\text{opt}}$ ); moreover it scales well with problem size.

The main disadvantage is the cost of forming and storing the Hessian and computing the Newton step, which requires solving a set of linear equations. However, in many cases it is possible to exploit the problem structure in order to reduce the cost of computing the Newton step.

### A.2.2 Newton's method for equality constrained problems

In order to derive the Newton step  $\Delta x$  for the equality constrained problem (A.3) at the feasible point  $x$ , we replace the objective function  $f$  with its second-order Taylor approximation near  $x$ ; the obtained problem is the following:

$$\begin{aligned} \min \quad & \hat{f}(x+v) = f(x) + \nabla f(x)^T v + \frac{1}{2} v^T \nabla^2 f(x) v \\ \text{subject to} \quad & A(x+v) = b. \end{aligned} \tag{A.5}$$

This is a convex quadratic optimization problem of variable  $v$  with equality constraints only, and can be solved analytically.

We define  $\Delta x$  as the solution of (A.5) (i.e.  $\Delta x$  minimizes  $\hat{f}$  under the constraint  $A(x+v) = b$ ): similarly to what said for the unconstrained case,  $\Delta x$  is what must be added to  $x$  to solve the problem when the quadratic approximation is used in place of  $f$ .

Remembering the optimality conditions (A.4),  $\Delta x$  is characterized by:

$$\begin{bmatrix} \nabla^2 f(x) & A^T \\ A & 0 \end{bmatrix} \begin{bmatrix} \Delta x \\ w \end{bmatrix} = \begin{bmatrix} -\nabla f(x) \\ 0 \end{bmatrix}.$$

Solving this system, we can define the Newton step as:

$$\Delta x = -(\nabla^2 f(x))^{-1} [\nabla f(x) + A^T w]$$

with the constraint  $A\Delta x = 0$ .

As in Newton's method for unconstrained problem, when  $f$  is exactly quadratic, the Newton update  $x + \Delta x$  exactly solves the equality constrained minimization problem; when  $f$  is nearly quadratic,  $x + \Delta x$  should be a very good estimate of the solution  $x^{\text{opt}}$ .

It can be shown that applying Newton's method with equality constraints is exactly the same as applying Newton's Method to the reduced problem obtained by eliminating

## A.2 Descent methods

---

the equality constraints. So the good properties of convergence of Newton's Method for unconstrained problems can be extended to Newton's Method for equality constrained problems.



# Kronecker product

---

## B.1 Definition

Consider two matrices  $A \in \mathbb{R}^{m \times n}$  and  $B \in \mathbb{R}^{p \times q}$ . The *Kronecker product* of  $A$  and  $B$  is defined as:

$$A \otimes B = \begin{bmatrix} a_{11}B & a_{12}B & \cdots & a_{1n}B \\ a_{21}B & \cdots & \cdots & a_{2n}B \\ \vdots & & & \\ a_{m1}B & \cdots & \cdots & a_{mn}B \end{bmatrix} \in \mathbb{R}^{mp \times nq}.$$

The same definition holds also if  $A$  and  $B$  are complex-valued matrices.

The Kronecker product of two vectors  $x \in \mathbb{R}^m$  and  $y \in \mathbb{R}^n$  is defined as follows:

$$x \otimes y = [x_1 y^T \cdots x_m y^T]^T = [x_1 y_1, \dots, x_1 y_n, x_2 y_1, \dots, x_m y_n]^T \in \mathbb{R}^{mn}$$

and

$$x \otimes y^T = [x_1 y \cdots x_m y]^T = xy^T \in \mathbb{R}^{m \times n}.$$

## B.2 Properties

An important result concerns the product of two matrices which are defined as the Kronecker product of matrices.

**Proposition 27.** *Given four matrices  $A \in \mathbb{R}^{m \times n}$ ,  $B \in \mathbb{R}^{r \times s}$ ,  $C \in \mathbb{R}^{n \times p}$  and  $D \in \mathbb{R}^{s \times t}$ , the product*

$$(A \otimes B)(C \otimes D) = AC \otimes BD \in \mathbb{R}^{mr \times pt}.$$

*Proof.* It easy to verify that:

$$\begin{aligned}
 (A \otimes B)(C \otimes D) &= \begin{bmatrix} a_{11}B & a_{12}B & \cdots & a_{1n}B \\ a_{21}B & \cdots & \cdots & a_{2n}B \\ \vdots & & & \\ a_{m1}B & \cdots & \cdots & a_{mn}B \end{bmatrix} \begin{bmatrix} c_{11}D & c_{12}D & \cdots & c_{1p}D \\ c_{21}D & \cdots & \cdots & c_{2p}D \\ \vdots & & & \\ c_{n1}D & \cdots & \cdots & c_{np}D \end{bmatrix} \\
 &= \begin{bmatrix} \sum_{k=1}^n a_{1k}c_{k1}BD & \cdots & \sum_{k=1}^n a_{1k}c_{kp}BD \\ \vdots & & \\ \sum_{k=1}^n a_{mk}c_{k1}BD & \cdots & \sum_{k=1}^n a_{mk}c_{kp}BD \end{bmatrix} \\
 &= AC \otimes BD.
 \end{aligned}$$

□

By exploiting the definition of Kronecker product and the result in Proposition 27, it easy to verify the following properties:

- $(A \otimes B)^T = A^T \otimes B^T$ ; it follows that, if  $A$  and  $B$  are symmetric square matrix, then  $A \otimes B$  is a symmetric matrix ;
- $(A \otimes B)(A^{-1} \otimes B^{-1}) = I \otimes I = I$ , provided that  $A$  and  $B$  are square nonsingular matrix; it follows that  $(A \otimes B)^{-1} = A^{-1} \otimes B^{-1}$ .

It can also be shown that:

$$\text{rank}(A \otimes B) = \text{rank}(A)\text{rank}(B) = \text{rank}(B \otimes A).$$

The following proposition states an important result about eigenvalues and eigenvectors of Kronecker product of two matrices.

**Proposition 28.** Consider two matrices  $A \in \mathbb{R}^{n \times n}$  and  $B \in \mathbb{R}^{m \times m}$ . Let be  $\lambda_i$ ,  $i = 1, \dots, n$  the eigenvalues of  $A$  and  $\mu_j$ ,  $j = 1, \dots, m$  the eigenvalues of  $B$ . Then the  $mn$  eigenvalues of  $A \otimes B$  are:  $\lambda_1\mu_1, \dots, \lambda_1\mu_m, \lambda_2\mu_1, \dots, \lambda_2\mu_m, \dots, \lambda_n\mu_m$ .

Moreover, let be  $x_1, \dots, x_p$  the linearly independent right eigenvectors of  $A$  corresponding to  $\lambda_1, \dots, \lambda_p$ ,  $p \leq n$ , and  $y_1, \dots, y_q$  the linearly independent right eigenvectors of  $B$  corresponding to  $\mu_1, \dots, \mu_q$ ,  $q \leq m$ . Then  $x_i \otimes y_j \in \mathbb{R}^{mn}$  are linearly independent right eigenvectors of  $A \otimes B$  corresponding to the eigenvalues  $\lambda_i\mu_j$ ,  $i = 1, \dots, p$ ;  $j = 1, \dots, q$ .

*Proof.* The basic idea of the proof is the following:

$$\begin{aligned}
 (A \otimes B)(x_i \otimes y_j) &= Ax_i \otimes By_j \\
 &= \lambda_i x_i \otimes \mu_j y_j \\
 &= \lambda_i \mu_j (x_i \otimes y_j).
 \end{aligned}$$

□

# Generalized inverse

---

Each nonsingular matrix  $A$  has a unique inverse  $A^{-1}$ , such that:

$$AA^{-1} = A^{-1}A = I.$$

In some recent years, numerous areas of applied mathematics required an expression for the "inverse" of matrices that are singular or rectangular.

It is possible via the concept of *generalized inverse* of a matrix  $A$ , i.e. a matrix  $B$  associated in some way to  $A$  such that:

- it exists for a class of matrices larger than the class of nonsingular matrices;
- it has some of the properties of the usual inverse;
- it reduces to the usual inverse when  $A$  is nonsingular.

**Definition 29.** Given a matrix  $(m \times n)$ -matrix  $A$ ,  $B$  is a *generalized inverse* of  $A$  if it is a  $(n \times m)$ -matrix such that:

$$ABA = A. \tag{C.1}$$

Typically, the generalized inverse exists for an arbitrary matrix. However, expression (C.1) does not characterize uniquely the matrix  $B$ : unlike the case of nonsingular matrices, there are many generalized inverses for different purposes.

For example, the matrix  $\mathbf{X}$  defined in Lemma 1, is a generalized inverse of the Laplacian matrix  $\mathbf{L}$ , because it satisfies (C.1), being:

$$\mathbf{LXL} = \mathbf{L}(I - \mathbf{1}\mathbf{1}_0^T) = \mathbf{L};$$

in addition, it satisfies another condition, which guarantees that also  $\mathbf{L}$  is a generalized inverse of  $\mathbf{X}$ , being:

$$\mathbf{XLX} = (I - \mathbf{1}\mathbf{1}_0^T)\mathbf{X} = \mathbf{X}.$$

## C.1 Moore-Penrose generalized inverse

As said before, it is possible to add conditions to the Definition 29 of a generalized inverse, in order to have always a unique generalized inverse (under the additional conditions).

**Definition 30.** Given a  $(m \times n)$ -matrix  $A$ , the matrix  $A^\sharp$  is the *Moore-Penrose generalized inverse* of  $A$  if it is the unique matrix such that:

- $A^\sharp A = A^\sharp$ ;
- $AA^\sharp A = A$ ;
- $(AA^\sharp)^T = AA^\sharp$ ;
- $(A^\sharp A)^T = A^\sharp A$ ;

More issues about the generalized inverses of a matrix can be found in [27].

Here we show a result, used in the proof of Proposition 8.

**Proposition 31.**

$$\ker(A^\sharp) = \ker(A^T) \quad \text{Im}(A^\sharp) = \text{Im } A \quad \forall A \quad (\text{C.2})$$

*Proof.* Let show the first relation before.

Let suppose  $y \in \ker(A^\sharp)$ ; then it also holds  $y \in \ker(A^T AA^\sharp)$ .

By using the properties of the Moore-Penrose pseudoinverse:

$$A^T AA^\sharp = A^T (AA^\sharp)^T = A^T (A^\sharp)^T A^T = (AA^\sharp A)^T = A^T$$

and so:

$$y \in \ker(A^\sharp) \Rightarrow y \in \ker(A^T AA^\sharp) = \ker(A^T).$$

Vice versa, if  $y \in \ker(A^T)$ , then  $y \in \ker(A^\sharp (A^\sharp)^T A^T)$ . As:

$$A^\sharp (A^\sharp)^T A^T = A^\sharp (AA^\sharp)^T = A^\sharp AA^\sharp = A^\sharp,$$

then:

$$y \in \ker(A^T) \Rightarrow y \in \ker(A^\sharp (A^\sharp)^T A^T) = \ker(A^\sharp).$$

By the relationship  $\ker A^\perp = \text{Im } A^T$ , it holds also:

$$\text{Im } A^\sharp = \text{Im } A^T \quad \forall A. \quad (\text{C.3})$$

□



## Quadratic forms

---

A quadratic form involving  $n$  real variables  $x_1, \dots, x_n$  is given by:

$$F(x_1, \dots, x_n) = \sum_{i,j=1}^n a_{i,j} x_i x_j, \quad a_{i,j} \in \mathbb{R}, \quad 1 \leq i, j \leq n. \quad (\text{D.1})$$

The quadratic form  $F(x_1, \dots, x_n)$  is said:

1. *positive definite* if  $F(x_1, \dots, x_n) > 0$  for all  $(x_1, \dots, x_n) \neq \mathbf{0}$ ;
2. *negative definite* if  $F(x_1, \dots, x_n) < 0$  for all  $(x_1, \dots, x_n) \neq \mathbf{0}$ ;
3. *positive semidefinite* if  $F(x_1, \dots, x_n) \geq 0$  for all  $(x_1, \dots, x_n) \in \mathbb{R}^n$  and exists a  $(x_1, \dots, x_n) \neq \mathbf{0}$  such that  $F(x_1, \dots, x_n) = 0$ ;
4. *negative semidefinite* if  $F(x_1, \dots, x_n) \leq 0$  for all  $(x_1, \dots, x_n) \in \mathbb{R}^n$  and exists a  $(x_1, \dots, x_n) \neq \mathbf{0}$  such that  $F(x_1, \dots, x_n) = 0$ ;
5. *indefinite* if  $F(x_1, \dots, x_n)$  is positive for some values of  $(x_1, \dots, x_n)$  and negative for other ones.

Given the quadratic form in (D.1), it can be expressed as:

$$F(x) = x^T A x,$$

where  $x = \begin{bmatrix} x_1 & \cdots & x_n \end{bmatrix}^T$  and  $A$  is a real symmetric matrix whose elements are  $a_{i,j}$ .

The matrix  $A$  associated to the quadratic form  $F$  is said positive definite (or positive semidefinite, etc) if the quadratic form  $F(x)$  is positive definite (or positive semidefinite, etc).

It can be shown that  $F$  is positive (negative) definite if and only if the eigenvalues of the associated matrix  $A$  are all positive (negative), whereas it is positive (negative)

semidefinite if and only if the corresponding matrix  $A$  has (at least) an eigenvalue in zero and all the others are positive (negative).

**Proposition 32.** *Let be  $A \in \mathbb{C}^{n \times n}$  a positive semidefinite matrix. Then:*

$$A > 0 \quad \Leftrightarrow \quad \ker A = \{0\}.$$

*Proof.* If there exists a vector  $v \in \ker A$ , then it is trivial:

$$Av = 0 \quad \Rightarrow \quad v^T Av = 0, \quad v \neq 0.$$

Vice versa, if  $\ker A = \{0\}$ , then

$$w = Av \neq 0, \quad \forall v \neq 0. \tag{D.2}$$

As each vector in  $\mathbb{C}^n$  can be written as the sum of a vector belonging to a subset of  $\mathbb{C}^n$  and a vector belonging to its orthogonal complement:  $w = \alpha v + w^\perp$ ,  $\alpha \neq 0$ . Then:

$$w^T w = w^T Av = \alpha v^T Av + (w^\perp)^T Av = \alpha v^T Av, \quad \alpha \neq 0;$$

as  $w^T w \neq 0$  by (D.2), then  $v^T Av \neq 0$  for all  $v \neq 0$ , i.e.  $A > 0$ . □

# Bibliography

---

- [1] D. P. Bertsekas and J. N. Tsitsiklis. *Parallel and Distributed Computation: Numerical Methods*. Athena Scientific, 1997.
- [2] S. Bolognani and S. Zampieri. Distributed quasi-Newton method and its application to the optimal reactive power flow problem. In *Proceedings NECSYS '10*, Annecy, France, 2010.
- [3] S. Bolognani, S. Zampieri. A gossip-like distributed optimization algorithm for reactive power flow control. In *Proc. IFAC World Congress 2011*. Milano, Italy, August 2011.
- [4] S. Bolognani, S. Zampieri. Distributed control for optimal reactive power compensation in smart microgrids. *50th IEEE Conference on Decision and Control and European Control Conference (CDC-ECC 2011)*. 2011.
- [5] F. Fagnani and S. Zampieri. Randomized consensus algorithms over large scale networks. *IEEE J. On Selected Areas in Comm.*, May 2008.
- [6] A. Ipakchi and F. Albuyeh. Grid of the future. Are we ready to transition to a smart grid? *IEEE Power Energy Magazine*, 2009.
- [7] M. Rotkowitz and S. Lall. A characterization of convex problems in decentralized control. *IEEE Transactions on Automatic Control*, February 2006.
- [8] E. Santacana, G. Rackliffe, L. Tang and X. Feng. Getting smart. With a clearer vision of the intelligent grid, control emerges from chaos. *IEEE Power Energy Mag.*, March 2010.
- [9] E. Tedeschi, P. Tenti and P. Mattavelli. Synergistic control and cooperative operation of distributed harmonic and reactive compensators. In *Proceedings of the IEEE Power Electronics Specialists Conference (PESC 2008)*, 2008.

- 
- [10] A. Cagnano, E. De Tuglie, M. Liserre and R. A. Mastromauro. Online optimal reactive power control strategy of PV inverters. *IEEE Transactions on Industrial Electronics*. October 2011.
- [11] J. N. Tsitsiklis, D. P. Bertsekas and M. Athans. Distributed asynchronus deterministic and stochastic gradient optimization algorithms. *IEEE Trans. automat. Contr.*, September 1986.
- [12] M. Prodanovic, K. De Brabandere, J. Van den Keybus, T. Green and J. Driesen. Harmonic and reactive power compensation as ancillary services in inverter-based distributed generation. *IET Generation, Transmission & Distribution*. 2007.
- [13] A. Rabiee, H. A. Shayanfar and N. Amjady. Reactive power pricing: Problems and a proposal for a competitive market. *IEEE Power Energy Magazine*, January 2009.
- [14] A. Gómez-Expósito, A. J. Conejo and C. Cañizares. *Electric energy system. Analysis and operation*. CRC Press. 2009.
- [15] A. Ghosh, S. Boyd and A. Saberi. Minimizing effective resistance of a graph. *SIAM Review*. February 2008.
- [16] S. Boyd and L. Vandenberghe. *Convex Optimization*. Cambridge University Press. 2008
- [17] A. van den Bos. Complex gradient and hessian. *IEE Proceedings on Vision, Image and Signal Process*. December 1994.
- [18] IEEE Task Force. Load Representation for dynamic performance analysis. *IEEE Transaction on Power Systems*. May 1993.
- [19] A. G. Phadke and B. Kasztenny. Synchronized phasor and frequency measurement under transient conditions. *IEEE Transactions on Power Delivery*. January 2009.
- [20] S. Bolognani, G. Cavraro, F. Cerruti, A. Costabeber. A linear dynamic model for microgrid voltages in presence of distributed generation. *First International Workshop on Smart Grid Modeling and Simulation (SmartGridComm 2011)*. Brussels, Belgium, 2011.
- [21] D. J. Hill. Nonlinear dynamic load models with recovery for voltage stability studies. *IEEE Transactions on Power Systems*. February 1993.
- [22] D. Karlsson and D. J. Hill. Modelling and identification of nonlinear dynamic loads in power systems. *IEEE Transactions on Power Systems*. February 1994.
- [23] W. Xu and Y. Mansour. Voltage stability analysis using generic dynamic load models. *IEEE Transactions on Power Systems*. February 1994.

- 
- [24] J. A. Lopes, C. L. Moreira and A. G. Madureira. Defining control strategies for microgrids islanded operation. *IEEE Transactions on Power Systems*. May 2006.
- [25] T. Green and M. Prodanovic. Control of inverter-based microgrids. *Electric Power Systems Research*. July 2007.
- [26] I. Gutman and W. Xiao. Generalized inverse of the Laplacian matrix and some applications. *Bulletin T. CXXIX de l'Académie serbe de sciences et des arts 2004. Classe des sciences mathématiques et naturelles sciences mathématiques*. Decembre 2003.
- [27] A. Ben-Israel and T. N. E. Greville. *Generalized inverses: theory and applications*. Wiley, New York. 1974.
- [28] W. H. Kersting. Radial distribution test feeders. *IEEE Transactions on Power Systems*. August 1991.